

VORTEX MOTION IN TRAPPED BOSE-EINSTEIN
CONDENSATES

ENIKO JULIANNA MARIA MADARASSY (FARKAS)

Thesis submitted for the degree of
Doctor of Philosophy



*School of Mathematics and Statistics
University of Newcastle upon Tyne
Newcastle upon Tyne
United Kingdom*

May 16, 2008

Dedicated to Mum, (Mami/Gyongyi) and Dad, (Feri) for all their love and support.

Acknowledgements

I am very grateful to my supervisor Carlo Barengi for all his help and guidance. He has always been ready to help and discuss my research with me.

Many thanks to my ex-groupmate, Anthony for his help and advice in programming from the real beginning of my PhD study until now.

Thanks to Andrew, for his permanent help and discussions both in programming and theory. Without his help my thesis wouldn't be as completed as it is.

Many thank to Brian for his scientific advice both in theory and programming, what has enriched the contents of my thesis.

Thanks to Louise and Demos for their useful advice.

Last but not least, I would like to say a big thanks to my sister Gyongyi (and her three daughters: Csengele, Kinga and Zselyke), to my brother Ferencz and his pair of lovers Gabi and finally to my ex-husband, Peter for their constant love and support.

Abstract

We have performed numerical simulations of various vortex configurations in a trapped Bose-Einstein condensate by solving the two-dimensional Gross-Pitaevskii equation in the presence of a simple model of interaction between the condensate and the finite temperature thermal cloud that surrounds it. In that interaction the non-condensed thermal cloud acts as a source of dissipation with a damping effect of excitations. In the case of a single vortex and a vortex - anti vortex pair, we have found that the path of the vortices depends on the initial position, the initial separation distance if the case of two vortices and dissipation.

This motion is periodic and it was found that sound waves are created by vortex motion; the intensity was stronger when the initial vortex separation distance was smaller. We have calculated the sound energy as the difference between the kinetic energy and the vortex energy.

With no dissipation the vortices followed the same path with a slight oscillation due to the sound waves. We found that the smaller the initial vortex separation distance d_0 is, the larger the sound production.

The period, frequency, translation speed, sound energy and vortex energy were measured for different initial separation distances d_0 and for different dissipation parameters γ . In the case of motion of one vortex, the connection between the dissipation γ and the friction coefficients, α and α' was studied as well.

To create a simple turbulent state, we put eight pairs of vortex - anti vortex at random positions in the condensate with initial separation distance $d_0 = 1.8$ between them. We have studied the decay rate of the total energy, kinetic energy, quantum energy, trap energy and the z - *component* of the angular momentum together with the increase rate of the internal energy. Finally, we finished our investigation by putting randomly vortex - anti vortex pairs and studied the decrease of the number of vortices with time t . We found that the decrease is exponential.

Contents

1	Introduction	1
1.1	Bose-Einstein Condensation and Superfluidity	1
1.1.1	Bose-Einstein Condensates	1
1.1.2	Vortices	2
1.2	Gross-Pitaevskii Equation	4
1.2.1	Harmonic Oscillator Units	5
1.2.2	Trapped and Dissipative Condensate	6
1.2.3	Hydrodynamic Equation	9
1.2.4	Thomas-Fermi Solution	10
1.3	Energies	11
1.4	Numerical Simulations	12
2	Motion of a Single Vortex	15
2.1	Introduction	15
2.2	Single Vortex Motion with Different γ 's	15
3	Connection Between γ and the Friction Coefficients, α and α'	24
3.1	Introduction	24
3.2	Schwarz Equation	24
3.3	Motion of Single Vortices with no Dissipation and with Different Dissipations	26
3.4	Motion of Single Vortices Having Different Initial Positions for $\gamma = 0.003$	29
3.5	Motion of Single Vortices with Different γ 's	34
3.5.1	Radial Position of Single Vortices as a Function of Time	35
4	Motion of Vortex - Anti Vortex Pair in a Trapped BEC	46
4.1	Introduction	46
4.2	Motion without Dissipation	46
4.3	Motion with Small Dissipation	58
4.4	Motion with $d_0 = 1.8$ and Different γ 's	64
4.4.1	Energy Balance	67
4.5	Motion of a Single Vortex and Vortex - Anti Vortex Pair with Different Dissipations	67
4.5.1	Additional Vortices	72

5	Motion of Random Vortex - Anti Vortex Pairs and Vortex Lattice Formation	75
5.1	Introduction	75
5.2	Motion of an Array of Vortices	75
5.3	Randomly Placed Vortex - Anti Vortex Pairs	77
5.4	Motion of Vortex - Anti Vortex Pairs and Formation of a Mini Turbulent System	81
5.5	Vortex Lattice Formation in a Rotating Bose-Einstein Condensate	81
6	Summary - Future Work	90
6.1	Conclusions	90
6.2	Decay of Soliton - like Perturbations into Vortices. Creation of a Mini Turbulent Vortex System	92
A	Connection Between the Precession Frequency of a Single Vortex and Vortex Pair	97
B	Detailed Calculations of the Hydrodynamic Equations	101
C	Tables	105
C.1	Tables Relating Connections Between $\alpha, \alpha', \gamma, x_0, \omega, \tau$ and the Exponential Constant of the Radial Position of the Vortex, F_1	105
C.2	Tables Relating Different Energies, L_z , the Initial Positions of Eight Vortex Pairs and the Decay Rate of the Number of Vortices	105
D	Parts of the Numerical Code	112

List of Figures

1.1	(a):Trajectory of a single vortex initially located at: $(x_0, y_0) = (1, 0)$. (b): Trajectory of the left vortex of vortex-antivortex pair initially located at $(x_0, y_0) = (\pm 1, 0)$.	13
2.1	(a): The 3D density plot of the condensate without vortices ($\gamma = 0$). (b): Equilibrium condensate for $C = 2000$. The density contours correspond respectively to 17%, 33%, 50%, 60% and 83% of the maximum density at the centre..	16
2.2	(a): Trajectories, (b): x -components vs. time and (c): y - components vs. time corresponding to Figure 2.2 (a) of a single vortex initially located at $(x_0, y_0) = (0.9, 0)$ for $\gamma = 0$ (purple/dotted line); $\gamma = 0.01$ (red/solid line); $\gamma = 0.07$ (green/dashed line) and $\gamma = 0.1$ (blue/small dashed line)..	17
2.3	(a): Trajectories, (b): x -components vs. time and (c): y - components vs. time corresponding to Figure 2.3 (a) of a single vortex initially located at $(x_0, y_0) = (1.3, 0)$ and for $\gamma = 0$ (purple/dotted line); $\gamma = 0.01$ (red/solid line); $\gamma = 0.07$ (green/dashed line) and $\gamma = 0.1$ (blue/small dashed line)	18
2.4	For a single vortex with $(x_0, y_0) = (0.9, 0)$: (a,b): total energy and kinetic energy for $\gamma = 0$ (green/upper horizontal line); $\gamma = 0.01$ (red line); $\gamma = 0.07$ (blue line) and $\gamma = 0.1$ (purple/shortest line). For (left): $\gamma = 0$ and for (right): $\gamma = 0.01$ (red/solid line); $\gamma = 0.07$ (green/dashed line) and $\gamma = 0.1$ (blue/small dashed line) for (c,d): internal energy, (e,f): quantum energy, (g,h): trap energy and (i,j): z -component of the angular momentum.	19
2.5	(a): Total energy and (b): kinetic energy corresponding to Figure 2.4 for $\gamma = 0.003$ (red/upper line) and for $\gamma = 0.01$ (green/lower line).	20
2.6	Kinetic energy for a single vortex with (a): $(x_0, y_0) = (0.9, 0)$ and for $\gamma = 0.01$ (green/lower line) and $=0.003$ (red/upper line) and with (b): $(x_0, y_0) = (0.7, 0)$ (blue/lower line); $= (0.9, 0)$ (red/middle line) and $= (1.1, 0)$ (green/upper line) for the same $\gamma = 0.003$	20
2.7	Trajectories for a single vortex with $(x_0, y_0) = (-0.9, 0)$ for (a,b): (left): $\gamma = 0.03$ and for (right): $\gamma = 0.01$ for (c,d): (left): $\gamma = 0.003$ and for (right): $\gamma = 0.001$. . .	21
2.8	Trajectories for a single vortex with $x_0 = -2.0$ (a): for $\gamma = 0$ (red line/solid line) and $\gamma = 0.003$ (green line/dashed line) and for (b): $\gamma = 0.03$ (green line/dashed line. We can see that the vortex have left the condensate.) and $\gamma = 0.01$ (red line/solid line).	21

2.9 (left): x -component and (right): y -component of trajectories for a single vortex with (a,b): $(x_0, y_0) = (-0.9, 0)$ and for $\gamma = 0.03$ (red line/shortest time scale); $\gamma = 0.01$ (green line) and $\gamma = 0.001$ (blue line/longest time scale) and for (c,d): $\gamma = 0.003$ and with $(x_0, y_0) = -0.9, 0)$ (red line/longest time scale) and $= (-2, 0)$ (green line/shortest time scale) and with (e,f): $(x_0, y_0) = (-2, 0)$ and $\gamma = 0.03$ (green line/shortest time scale); $\gamma = 0.01$ (purple line); $\gamma = 0.003$ (blue line); $\gamma = 0.001$ (aquamarine line/longest time scale); $\gamma = 0$ (red line/same amplitude). 22

2.10 Radius of trajectory for a single vortex with (a): $(x_0, y_0) = (-0.9, 0)$ and for $\gamma = 0.03$ (red/last vertical wavy line); $\gamma = 0.01$ (purple line); $\gamma = 0.003$ (blue line) and $\gamma = 0.001$ (green/first horizontal wavy line) and with (b): $(x_0, y_0) = (-2, 0)$ and for $\gamma = 0.03$ (green/last vertical wavy line); $\gamma = 0.01$ (purple line); $\gamma = 0.003$ (blue line); $\gamma = 0.001$ (aquamarine line) and $\gamma = 0$ (red/first horizontal wavy line). 23

3.1 (Position (\mathbf{s}), tangent (\mathbf{s}'), normal (\mathbf{s}'') and binormal ($\mathbf{s}' \times \mathbf{s}''$) vectors for a vortex line. Here, $\mathbf{s} = \mathbf{s}(\xi, t)$, represent a space curve, which describe a quantised vortex filament and ξ is arc length and t is time. Prime denotes derivative with respect to ξ . 25

3.2 If a body moves in a fluid (or vice versa) circulation around the body forms. On one side of the body the total velocity is higher (hence the pressure is lower/ Bernoulli's Theorem) than the other side. The pressure difference causes the force transverse to the motion. So, for a body with circulation, the direction of motion is changed by the Magnus force. 25

3.3 A single vortex rotation and the self-induced velocity of the line due to its own curvature. 27

3.4 Friction coefficient α (circles) and α' (triangles) as a function of initial position $(x_0, y_0 = 0)$ for $\gamma = 0.003$ 28

3.5 Friction coefficient α as a function of time for a single vortex for $\gamma = 0.003$ and for $x_0 = 0.9$ (a); 1.5 (b); 1.8 (c); 2.4 (d); 3.9 (e) and 4.5 (f). 30

3.6 Friction coefficient α' as a function of time for a single vortex for $\gamma = 0.003$ and for $x_0 = 0.6$ (a); 0.9 (b) and 1.5 (c). 31

3.7 (a): Precession frequency, ω_0 as a function of initial positions, $(x_0, 0)$ for a vortex, which orbits the trap in absence of dissipation for $C = 2000$. (b,c): (left): period and (right): frequency of the first circle of motion as a function of initial positions, $(x_0, 0)$ for a single vortex for $\gamma = 0.003$ 32

3.8 Vortex precession frequency, ω_0 for a single vortex with $(x_0, y_0) = (0.9, 0)$ (circle) and $(1.45, 0)$ (triangle) as a function of γ 33

3.9 Friction coefficients α' for a single vortex vs initial positions $x_0 = 0.6$ (0.1098); 2.4 (0.132); 3.6 (0.2038); 4.2 (0.226); 4.8 (0.25); 5.4 (0.2855). (We have the frequency of motion in the bracket), $(y_0 = 0)$ and for $\gamma = 0.003$. Here, we compare the values of α' for different initial positions but for almost the same times, (which vary between 313.61 and 401.63). 34

3.10 Friction coefficient α as a function of time for a single vortex for (left): $(x_0, y_0) = (0.9, 0)$ and (right): $(x_0, y_0) = (1.45, 0)$. for (a,b): $\gamma = 0$ and for (c,d): $\gamma = 0.016$ and for (e): $\gamma = 0.032$ and for $(x_0, y_0) = (1.45, 0)$ 36

3.11	Friction coefficient α' as a function of time for (left): $(x_0, y_0) = (0.9, 0)$ and for (right): $(x_0, y_0) = (1.45, 0)$ for (a,b): $\gamma = 0$, for (c,d): $\gamma = 0.016$ and for (e,f): $\gamma = 0.032$	37
3.12	(a): Friction coefficient α for a single vortex with initial position $(x_0, y_0) = (0.9, 0)$ (triangles) and $(x_0, y_0) = (2, 0)$ (circles) as a function of γ . The linear fit for α is: $\alpha = c_1 + c_2\gamma$, where $c_1=0.007$ and $c_2=5.092$. (b): Friction coefficient α' corresponding to Figure. 3.11(a).	38
3.13	Friction coefficients α as a function of γ for a single vortex with initial positions, $(x_0, y_0) = (0.9, 0)$ and $(1.45, 0)$. Triangles represent the case when $(x_0, y_0) = (1.45, 0)$ and circles represent the case for $(x_0, y_0) = (0.9, 0)$. The linear fit for α is: $\alpha = c_1 + c_2\gamma$, where $c_1=0.007$ and $c_2=4.44$	38
3.14	Friction coefficients α' for a single vortex with $(x_0, y_0) = (0.9, 0)$ and for dissipations, $\gamma = 0.008$ (0.1459); 0.012 (0.1459); 0.016 (0.1465); 0.02 (0.1416); 0.024 (0.1453); 0.028 (0.1413).The numbers in the paranthesis are the frequencies of motion, ω	38
3.15	(a): Period, τ and (b): frequency, ω of the first circle like trajectory of motion for a single vortex with initial positions, $(x_0, y_0) = 0.9$ (circles) and with $(x_0, y_0) = 1.45$ (triangles).	39
3.16	Trajectory for a single vortex with $(x_0, y_0) = (0.9, 0)$ and for $\gamma = 0.032$. We can see that in the end of its motion the vortex moves out to the border of the condensate.	39
3.17	Radius of the trajectories as a function of time for a single vortex with initial positions, from bottom to top $x_0 = 0.6; 0.9; 1.2; 1.5; 1.8; 2.1; 2.4; 2.7; 3.0; 3.3; 3.6; 3.9; 4.2; 4.5; 4.8; 5.1; 5.4; 5.7; 6.0$, $y_0 = 0$ and for $\gamma = 0.003$	40
3.18	Radius of trajectories for a single vortex as a function of time with (a,b): $(x_0, y_0) = (0.9, 0)$ and with (c,d): $(x_0, y_0) = (1.45, 0)$ for dissipations (left): from the green(a)/red(c) horizontal line to the green curved line $\gamma = 0; 0.004; 0.008; 0.012; 0.016; 0.02; 0.024; 0.028; 0.032; 0.036; 0.04$ and (right): from the right red curved line to the left red curved line $\gamma = 0.044; 0.048; 0.052; 0.056; 0.06; 0.064; 0.068; 0.072; 0.076; 0.08$	41
3.19	Log of radius of trajectories as a function of time for a single vortex with $(x_0, y_0) = (0.9, 0)$ and for dissipations from bottom red to top: (a): $\gamma = 0; 0.004; 0.008; 0.012$ and 0.016 and (b): $\gamma = 0.02; 0.028; 0.032$ and 0.04 and (c): $\gamma = 0.044; 0.048; 0.052; 0.056$ and 0.06 and (d): $\gamma = 0.068; 0.072$ and 0.076	42
3.20	Log of radius of trajectories as a function of time for a single vortex with $(x_0, y_0) = (1.45, 0)$ and for dissipations from bottom red to top: (a): $\gamma = 0; 0.004; 0.008$ and 0.012 and (b): $\gamma = 0.028; 0.032$ and 0.036 and (c) $\gamma = 0.044; 0.048; 0.056$ and 0.06 and (d): $\gamma = 0.068; 0.072$ and 0.076	43
3.21	Log of radius of trajectories as a function of time for a single vortex for $\gamma = 0.003$ and with initial positions x_0 , from bottom red to top: (a): $0.6; 0.9; 1.2; 1.5; 1.8$ and (b): $2.1; 2.4; 2.7; 3.0; 3.3; 3.6$ and (c): $3.9; 4.2; 4.5; 4.8$ and (d): $5.1; 5.4; 5.7; 6.0$. ($y_0 = 0$ in every cases).	44
3.22	Exponential constant, Γ_1 of the radius of vortex trajectory as a function of γ for a single vortex with (a,b): (left): $(x_0, y_0) = (0.9, 0)$ and (right): $(x_0, y_0) = (1.45, 0)$ and (c) as a function of x_0 for $\gamma = 0.003$	45

4.1	Contourplot of the density for a vortex - antivortex pair for $d_0 = 0.8$, $\rho_{max} = 0.012$, and with levels: 0.01, 0.008, 0.006, 0.004, 0.002, (the levels decrease as you move outwards) at times: (a): $t = 87.2$, (b): $t = 93$, (c): $t = 98.8$, (d): $t = 104.4$, (e): $t = 110.2$ and (f): $t = 116$	48
4.2	Contourplot of the density for a vortex - antivortex pair for $d_0 = 2.86$, $\rho_{max} = 0.012$, and with levels: 0.01, 0.008, 0.006, 0.004, 0.002, (the levels decrease as you move outwards) at times: (a): $t = 50$, (b): $t = 1334$, (c): $t = 750$ and (d): $t = 2034$	49
4.3	Contourplot of the density for the vortex - antivortex pair corresponding to Figure 4.2 at time (a): $t = 0.2$ and at time (b): $t = 29$	49
4.4	(a): x -component and (b) y -component of the trajectory as a function of time for one of the vortices in the vortex pair for $d_0 = 1.8$	50
4.5	(a): Trajectories of one of the vortices from the vortex pair with $d_0 = 1.8$, (b): x -components and (c): y - components of trajectories vs. time corresponding to Figure 2.9(a) for $\gamma = 0$ (purple/dotted line); $\gamma = 0.01$ (red/solid line); $\gamma = 0.07$ (green/dashed line) and $\gamma = 0.1$ (blue/small dashed line).	50
4.6	(left): x -component and (right): y -component of the trajectories as a function of time for one of the vortices in the vortex pair for d_0 (a,b): $= 1$ and (c,d): $= 1.43$	51
4.7	Correlation between vortex energy and sound energy for the vortex - anti vortex pair when $d_0 = 2.86$ and $\gamma = 0$. The correlation coefficient is $cc = -0.844$	53
4.8	For a vortex - anti vortex pair with $d_0 = 2.86$ and $\gamma = 0$ (a): Internal energy, (b): Trap energy, (c): Quantum energy, (d): Total energy, (e): Kinetic energy, (f): Sound energy and (g): Vortex energy.	54
4.9	Sound waves on the density plot for the vortex - anti vortex pair for $d_0 = 2$ at $t = 2.6$ (for $\gamma = 0$).	55
4.10	Vortex pair velocity as a function of d_0 (circle) measured at the centre of the condensate and compared to vortex pair velocity, v_∞ in homogeneous condensate (green/dashed line), for $\gamma = 0$	55
4.11	Period of motion for one of the vortices in the vortex - anti vortex pair for $\gamma = 0$	56
4.12	Frequency of one vortex in the vortex pair calculated with two methods. Triangle symbols represent the value obtained from $\omega_{pair} = 1/\tau_{pair}$ and circle symbols represent the value which was calculated with the help of the corresponding single vortex frequency $\omega'_{pair} \sim \sqrt{2}\omega_{single}$	57
4.13	Kinetic energy for the vortex - anti vortex pair for $\gamma = 0.003$ with (a): $d_0 = 2.86$ and with (b): $d_0 = 1.5$	58
4.14	Total energy corresponding to Figure(4.13(a) - 4.13(b)). In (b) We can see that about $t = 220$, the vortex leave the condensate.	58
4.15	Internal energy corresponding to Figure(4.13(a) - 4.13(b)).	59
4.16	Quantum energy corresponding to Figure(4.13(a) - 4.13(b)).	59
4.17	Trap energy corresponding to Figure(4.13(a) - 4.13(b)).	59

4.18	Energies corresponding to Figure(4.13(a) - 4.13(b)): (a,b): Sound energy for shorter time (compare with Figure 4.19(a) and Figure 4.19(b)), (c,d): Vortex energy for shorter time (compare with Figure 4.20(a) and Figure 4.20(b)), (e,f): Kinetic energy for shorter time (compare with Figure 4.13(a) and Figure 4.13(b)) and (g,h): Total energy for shorter time (compare with Figure 4.14(a) and Figure 4.14(b)).	61
4.19	Sound energy corresponding to Figure(4.13(a) - 4.13(b)).	62
4.20	Vortex energy corresponding to Figure(4.13(a) - 4.13(b)).	62
4.21	Correlation between vortex energy and sound energy for the vortex - anti vortex pair with $d_0 = 2.86$ and $\gamma = 0.003$. The correlation coefficient is $cc = -0.841$	62
4.22	Internal energy corresponding to Figure(4.13(a) - 4.13(b)) for shorter time (compare with Figure 4.15(a) and Figure 4.15(b)).	63
4.23	Trap energy corresponding to Figure(4.13(a) - 4.13(b)) for shorter time (compare with Figure 4.17(a) and Figure 4.17(b)).	63
4.24	Quantum energy corresponding to Figure(4.13(a) - 4.13(b)) for shorter time (compare with Figure 4.16(a) and Figure 4.16(b)).	64
4.25	Sound waves on the density plot for the vortex - anti vortex pair with $d_0 = 1$ and $\gamma = 0.01$ at time, $t = 2.4$	65
4.26	(a): Total energies and (b): Kinetic energies for the vortex - anti vortex pair with $d_0 = 1.8$ and $\gamma = 0$ (red line/solid line); $\gamma = 0.01$ (green line/dashed line); $\gamma = 0.07$ (purple line/dotted line); $\gamma = 0.1$ (blue line/small dashed line)	65
4.27	(a): Quantum energies for the vortex - anti vortex pair with $d_0 = 1.8$ for (a): $\gamma = 0$ (red line/solid line) and $\gamma = 0.01$ (green line/dashed line) and for (b): $\gamma = 0.07$ (green line/dashed line) and $\gamma = 0.1$ (red line/solid line).	66
4.28	Internal energies for the vortex - anti vortex pair with $d_0 = 1.8$ for (a): $\gamma = 0$ (red line/solid line) and $\gamma = 0.01$ (green line/dashed line) and for (b): $\gamma = 0.07$ (green line/dashed line) and $\gamma = 0.1$ (red line/solid line).	66
4.29	Trap energies for the vortex - anti vortex pair with $d_0 = 1.8$ for (a): $\gamma = 0$ (red line/solid line) and $\gamma = 0.01$ (green line/dashed line) and for (b): $\gamma = 0.07$ (green line/dashed line) and $\gamma = 0.1$ (red line/solid line).	66
4.30	Decay rate of the total energy, $\beta = dE/dt$ as a function of γ (a,b): (left): for a single vortex with $(x_0, y_0) = (0.9, 0)$ and (right): for a vortex - anti vortex pair with $d_0 = 1.8$ and (c): for a single vortex with $(x_0, y_0) = (2.86, 0)$	69
4.31	For a vortex - anti vortex pair with $d_0 = 5.98$ and $\gamma = 0.03$ the decrease of (a,b): (left): the total energy and (right): of the kinetic energy and the (c,d): (left): the increase of the internal energy and (right): the decrease of the trap energy.	70
4.32	For $\gamma = 0$, the <i>red/solid</i> line stands for the function, $f(t) = a/t$ and (a): (+) represents the fluid velocity, $v_1 = \sqrt{v_x^2 + v_y^2}$, at the position, where the first vortex from the vortex - anti vortex pair was placed originally, $(x_0, y_0) = (2.99, 0)$ and (b) (+) represents the fluid velocity, $v_2 = \sqrt{v_x^2 + v_y^2}$, at the position, where the second vortex from the vortex - anti vortex pair was placed originally, $(x_0, y_0) = (-2.99, 0)$	71
4.33	3D plot of the density for two vortex - antivortex pairs with $d_0 = 1.3$ and 5.98 ($x_0 = \pm 2.99$ and ± 0.65) for no dissipation at $t = 0$	72

4.34	For a vortex - anti vortex pair with initial positions, $x_0 = \pm 2.99$; $y_0 = 0$ and for $\gamma = 0.03$, the fluid velocity at position where (a): the vortex of the vortex -anti vortex pair was placed originally, $x_0 = 2.99$; $y_0 = 0$ and where (b): the anti vortex of the vortex -anti vortex pair was placed originally, $x_0 = -2.99$; ($y_0 = 0$). For two vortex - anti vortex pairs with initial positions, $x_0 = \pm 0.65$; ± 2.99 ($y_0 = 0$) and for $\gamma = 0$, the fluid velocity at position where (a): the vortex of the vortex -anti vortex pair was placed originally, $x_0 = 2.99$; $y_0 = 0$ and where (b): the anti vortex of the vortex -anti vortex pair was placed originally, $x_0 = -2.99$; ($y_0 = 0$).	73
4.35	For two vortex - antivortex pairs with $d_0 = 1.3$ and 5.98 ($x_0 = \pm 2.99$ and ± 0.65), and for $\gamma = 0$ (a,b): (left): the total energy and (right): the kinetic energy and (c,d): (left): the internal energy and (right): the trap energy.	74
5.1	Contour plot of density with an array of vortices in case of $\gamma = 0.03$ and for $\Omega = 0.75$	76
5.2	For an array of vortices with $\gamma = 0.003$ and for $\Omega = 0.75$ (a): the total energy as a function of time and b): the z -component of the angular momentum as a function of time. (With small dissipation the decay of the saturated values due to γ is not so significant.	76
5.3	For an array of vortices with $\gamma = 0.003$ the increase of the total energy until its saturated value for (a): $\Omega = 0.7$ and (b): $\Omega = 0.85$	77
5.4	For an array of vortices with $\gamma = 0.07$ and $\Omega = 0.75$ (a,b): (left): the total energy as a function of time and (right): the z -component of the angular momentum as a function of time and the (c): \log (base e) of the total energy as a function of time compared with $f(x) = a + bx$, where $a = 3.1211$ and $b = -0.002084$. We can see that with dissipation the total energy decreases. For larger values of γ , this decrease is more significant.	78
5.5	For an array of vortices with $\gamma = 0.03$ and $\Omega = 0.75$, (left): the different energies/ L_z of the (a): total energy, (c): kinetic energy, (e): trap energy, (g): internal energy, (i): quantum energy, (k): L_z and (right): the corresponding \log (base e) values as a function of time (compared with $f(x) = a + bx$), where (b): $a = 2.5832$ and $b = 0.016962$, (d): $a = -3.9922$ and $b = 0.179224$, (f): $a = 1.7665$ and $b = 0.025185$, (h): $a = 2.6821$ and $b = -0.027926$, (j): $a = -13.0613$ and $b = 0.126919$ and (l): $a = -2.7013$ and $b = 0.192771$	79
5.6	For an array of vortices for $\Omega = 0.75$ (a,b): (left): the increase rate of the total energy (red circles/lower circles) and kinetic energy (green circles/upper circles) and (right): the increase rate of the trap energy (blue circles/upper circles) and the decay rate of the internal energy (purple circles/lower circles) and (c): the increase rate of the quantum energy (blue circles/lower circles) and the z -component of the angular momentum (purple circles/upper circles) as a function of γ	80

5.7	For randomly placed vortex - anti vortex pairs and for dissipations: $\gamma = 0.03; 0.032; 0.036; 0.04; 0.048; 0.056; 0.07; 0.072; 0.076$ and 0.084 (from the red upper line to the red lower line) (a,b): (left): the total energy and (right): the kinetic energy and (c,d): (left): the quantum energy and (right): the internal energy and (e,f): (left): the trap energy and (right): the z-component of the angular momentum as a function of time.	82
5.8	For random vortex - anti vortex pairs with $d_0 = 1.8$ (a,b): (left): the decay/increase rate, β of the total energy (purple filled circles/middle filled circles), of the trap energy (blue circles/lower circles) and of the internal energy (red filled squares/upper filled squares) and (right): the increase rate, β of the kinetic energy (purple circles/upper circles) and of the z-component of the angular momentum (blue circles/lower circles) and (c): the increase rate, β of the quantum energy (purple circles) as a function of γ	83
5.9	Number of vortices divided by the number of vortices at $t = 0$ as a function of time, for random vortex - anti vortex pairs with $d_0 = 1.8$ compared with $f(x) = \exp(\beta t)$ for (a): $\gamma = 0.003$ and $\beta = -0.0089$, (b): $\gamma = 0.048$ and $\beta = -0.0837$, (c): $\gamma = 0.07$ and $\beta = -0.1437$, (d): $\gamma = 0.1$ and $\beta = -0.184$, (e): $\gamma = 0.003; 0.048; 0.07; 0.1$ (from top to bottom) and the corresponding β 's: $-0.0089; -0.0837; -0.1437; -0.184$, (f): Decay rate, β of the number of vortices as a function of γ , corresponding to Figure(5.9(a) - 5.9(d))	84
5.10	Density profile of the condensate for a vortex-anti vortex pair at (a): $t_1 = 15$ and (b) $t_2 = 21$. (A vortex-anti vortex pair begins to move together.) and at (c): $t_1 = 25$ and (d) $t_2 = 33$. (The pair stops to move together.) and at (e): $t_1 = 175$ and (f) $t_2 = 176$. (A vortex-anti vortex pair begins to destroy each other).	85
5.11	Density profile of the condensate for a vortex-anti vortex pair at (a): $t_1 = 182$ and (b) $t_2 = 185$. (We can see the annihilation and the sound wave production.) and at (c): $t_1 = 208$ and (d) $t_2 = 212$. (Two vortices annihilate each other.) and at (e): $t_1 = 215$ and (f) $t_2 = 222$. (Two big sound waves cross the condensate (e) and the system becomes turbulent (f)).	86
5.12	Density profile (left) and phase profile (right) of the condensate for $\Omega = 0.85$ at (a,b) $t = 0.2$, (c,d) $t = 11$, (e,f) $t = 16.4$, (g,h) $t = 20$	88
5.13	Density profile (left) and phase profile (right) of the condensate for $\Omega = 0.85$ at (a,b) $t = 22.4$, (c,d) $t = 26.8$, (e,f) $t = 54.8$	89
6.1	(a): Density of the condensate at the beginning without perturbations/vortices. (b): Perturbation created from the phase change. An original sound wave forms and propagates.	93
6.2	(a): Perturbation decays into vortex pairs and simultaneously sound waves appear. (b): From originally five pairs of vortices, only two pairs have survived.	93
6.3	(a): Phase of the condensate for Case I. At the edge of the condensate both $Imag(\psi)$ and $Real(\psi) \rightarrow 0$. Clearly, the phase, which is: $Phase = \tan^{-1}(Imag\psi/Real\psi) \rightarrow 0$. We note the large fluctuations of the phase on the outer part of the condensate. (b): We can see the different phase in the two regions: $y > 0$ and $y < 0$	93

6.4	Stable condensate with $N = 20$ vortices for $\Omega = 0.85$ (a): at $t = 199.8$ before the phase imprinting. The vortices are visible as holes in the density profile or (b): as discontinuities from 0 to 2π of the phase profile at $t = 200$	95
6.5	(a): Density and (b): phase profiles at $t = 200.4$ corresponding to Figure 6.4.	95
6.6	(a): Density and (b): phase profiles at $t = 201.95$ corresponding to Figure 6.4. (<i>mini turbulence</i>).	95
6.7	Kinetic energy (solid curve, top), vortex energy (dashed curve, middle) and sound energy (dotted curve, bottom).	96
A.1	.The velocities acting on both vortex and anti-vortex. Here, we choose one of them. Upper plot: The velocity induced by the neighbour vortex being on a distance of \mathbf{r} . Lower plot: The vortex-anti vortex move parallelly on the y -direction (because of their initial positions) with a tangential velocity, \mathbf{v}_t . We can see the relation between \mathbf{v}_t and \mathbf{v}_i	98

List of Tables

3.1	Friction coefficient α' as a function of dissipation, γ corresponding to Figure 3.8. . .	33
4.1	The y -component of the velocity calculated with $v'_y = tg\alpha = \Delta y/\Delta t$ and with the form $v_y \sim 1/d_0$	55
4.2	Translation speed, v_∞ for the vortex pair.	56
4.3	Period, τ of motion of the vortex pair.	57
4.4	This table presents the initial position (x_0, y_0) of one vortex in the vortex pair, the initial separation distance between the vortices, d_0 , the initial position for the single vortex, which was placed in the centre of the trajectory of the vortex/anti-vortex, x_{0s} , the period and frequency of motion for the pair of vortices, τ_{pair} and ω_{pair} , the period and frequency of motion for the single vortex, τ_{single} and ω_{single} , the frequency of motion of the vortex pair (calculated with the help of ω_{single}) ω'_{pair} and the difference between the two frequencies ω_{pair} and ω'_{pair}	57
4.5	Energy balance for the case of vortex - anti vortex pairs with initial separation distance, $d_0 = 2.86, 1.5$ and 1.8 and for the case of a single vortex with initial position, $x_0 = 0.9$	68
4.6	Decay rate of the total energy for a single vortex with initial positions, $x_0 = 0.9$ (β_1); 2.86 (β_2), $y_0 = 0$ and for vortex - anti vortex pair with initial separation distance, $d_0 = 1.8$ (β_3) as a function of γ	68
4.7	Fluid initial velocity at the same position, where the first vortex - antivortex pair were placed originally as a function of γ for two and four vortices.	73
C.1	Friction coefficients, α and α' as a function of γ for initial positions: $(x_0, y_0) = 0.9$ and 2	105
C.2	Friction coefficients, α and α' as a function of initial position, $(x_0, 0)$ for a single vortex ($\gamma = 0.003$).	106
C.3	Friction coefficient α as a function of initial position $(x_0, 0)$ for a single vortex ($\gamma = 0.003$).	106
C.4	Friction coefficient α' as a function of ω and $(x_0, 0)$ for a single vortex ($\gamma = 0.003$).	106
C.5	Period τ and frequency ω of motion for a single vortex as a function of $(x_0, 0)$ ($\gamma = 0.003$).	107
C.6	Period τ and frequency ω of motion for a single vortex as a function of γ for $(x_0, y_0) = (0.9, 0)$	107

C.7	Period, τ and frequency, ω of motion for one vortex as a function of γ for $(x_0, y_0) = (1.45, 0)$	108
C.8	Exponential constant, Γ_1 of the radius of vortex trajectory as a function of γ for a single vortex with $(x_0, y_0) = (0.9, 0)$	108
C.9	Exponential constant, Γ_1 of the radius of vortex trajectory as a function of γ for a single vortex with $(x_0, y_0) = (1.45, 0)$	109
C.10	Exponential constant, Γ_1 of the radius of vortex trajectory as a function of x_0 for a single vortex with $\gamma = 0.003$	109
C.11	Maximum values, saturated values and difference between them for E_{tot} , E_{kin} , E_{trap} , E_{int} , E_q and L_z for an array of vortices with $\gamma = 0.03$ and $\Omega = 0.75$	109
C.12	Maximum values, saturated values and difference between them for E_{tot} , E_{kin} , E_{trap} , E_{int} , E_q and L_z for an array of vortices with $\gamma = 0.07$ and $\Omega = 0.75$	110
C.13	Increase rate of E_{tot} , E_{kin} , E_{trap} , E_{int} (decay rate), E_q and L_z (when the vortices come in in the condensate) as a function of $\gamma = 0.003$; 0.03 and 0.07 for $\Omega = 0.75$	110
C.14	Initial positions of eight pairs of vortex - anti vortex (totally 16) with a proper sign.	110
C.15	Decay rate of total energy, trap energy and quantum energy and increase rate of internal energy for different γ 's.	110
C.16	Decay rate of kinetic energy and z -component of the angular momentum for different γ 's.	111
C.17	Decay rate β of number of vortices and the corresponding γ when the random vortex - anti vortex pairs were placed in the condensate with $d_0 = 1.8$	111

Chapter 1

Introduction

1.1 Bose-Einstein Condensation and Superfluidity

Below $T_\lambda = 2.17\text{K}$, ^4He is known as He II. In that case the superfluid part of Helium has no thermal resistance and viscosity. London (London, 1938) connected these superfluid properties with Bose and Einstein's works on the quantum statistics of bosons.

Atoms at ultralow temperatures behave as indistinguishable particles. At low temperatures, bosons prefer to occupy the same quantum mechanical state. This behaviour is governed by the laws of quantum mechanics. For $T < T_c$, bosons have a tendency to be together in a single state forming a BEC. This theory was later expanded by Tisza (Tisza, 1938) and Landau (Landau, 1941) in the two-fluid model containing *non – condensed* or *normal* fluid of quasi-particle excitations. According to Landau, the elementary excitations are sources of viscosity in a quantum fluid.

The phenomenon of BEC has been studied in different domains like astrophysics, particle physics, condensed matter, atomic physics together with two and one dimensional systems, multicondensates, non-linear and linear atom optics, superfluidity and vortices (discovery of vortices in JILA and Paris, solitons in Hannover and NIST, Freschbach resonances at MIT, JILA, Orsay and Texas.)

1.1.1 Bose-Einstein Condensates

A Bose-Einstein condensate (BEC) is a state of matter of a system of bosons confined in an external potential. The atoms are cooled to temperatures very near to absolute zero. Under this condition quantum effects become evident on a macroscopic scale. This follows from the fact that a large fraction of the atoms collapse into the lowest quantum state of the external potential. The history of BEC has its origin in Satyendra Nath Bose's (Bose, 1924) and Albert Einstein's (Einstein, 1925) works in the 1920s on the quantum statistics of particles with integer spin.

The first weakly-interacting atomic Bose-Einstein condensate was produced by Eric Cornell and Carl Wieman in 1995, at the University of Colorado at Boulder NIST-JILA lab, (Cornell & Wieman, 1995, 1998). They used a gas of rubidium atoms cooled to 170 nanokelvin (nK). A dilute

weakly-interacting Bose-Einstein condensate (BEC) was also obtained in a confined ultracold gas of sodium and lithium atoms (Davis *et al.*, 1995; Bradley *et al.*, 1995) with the help of cooling and trapping techniques (Chu *et al.*, 2003). Cornell, Wieman and Wolfgang Ketterle were awarded the 2001 Nobel Prize in Physics for this achievement. One can create a cloud of dilute BEC by confining in a magneto-optical trap about 10^9 atoms with the help of laser beams and magnetic fields. In that state, the temperature is $T \approx 10^{-5}K$ and the number density is $n \approx 10^{10}cm^{-3}$. To obtain BEC, the temperature of the cloud is reduced ($T \approx 10^{-6}K$ and $n \approx 10^{14}cm^{-3}$) by radio-frequency pulses to evaporate higher energy atoms in magnetic trap with a harmonic confinement (Hess, 1986). The particle interactions are low-energy, two-body collisions described by the atomic s-wave scattering length, a . More than 99% of atoms are condensed at zero temperature. The interactions are weak due to the scattering cross-section is much less than the mean space between particles ($n^{1/3}a \ll 1$).

Dilute BECs, regulated and managed by electromagnetic and optical means, have been produced with Rubidium (Anderson *et al.*, 1995), Lithium (Bradley *et al.*, 1995), Sodium (Davis *et al.*, 1995), spin-polarised Hydrogen (Fried, 1998), meta-stable Helium (Santos, 2001), Potassium (Modugno, 2001), Caesium (Weber *et al.*, 2003) and Ytterbium (Takasu, 2003). Combination of experimental and theoretical informations of BEC give us a good insight in fundamental concepts of condensed matter physics.

There are various envisaged applications of the BEC theory. The stimulated transfer of bosonic atoms into a given state of an optical or magnetic trap was demonstrated in (Holland *et al.*, 1996). This is a model for an atom laser, which are beams of coherent atoms, (Anderson & Kasevich, 2003; Hansch & Esslinger, 1999; Hagley, 1999). Atom chips (Ott *et al.*, 2001; Hansel *et al.*, 2001) enable coherent atom optics with reduced dimensionality (one dimension) by suitable trap geometries.

1.1.2 Vortices

The most striking properties of superfluids are the creation and observation of quantum vortices. Solving an equation, which describes the bosons at very low temperatures (the Gross-Pitaevskii equation), we can see that it allows solutions which are topologically non-trivial e.g. vortices with zero density and non-zero fluid circulation. A vortex is manifested as a density hole within the condensate. In superfluids, vortices are characterised by quantised circulations. They can decay under collision, at the boundary of the condensate or due to other dissipative mechanism.

The conditions for vortex creation depend upon the shape of the condensate and the form of the trapping potential. The standard method of generating quantised vortices in a superfluid is by rotation about a fixed axis when quantised vortex lines appear aligned with the axis of rotation. At low rotation frequencies the superfluid remains stationary. Provided that the rotation is greater than a critical value, one or more vortices form (Baym & Pethick, 1996) at the edge and enter the condensate. Their presence reduces the free energy of the system, and they become energetically favourable, above a certain critical rotation frequency (Fetter & Svidzinsky, 2001).

Experiments with Vortices in Cold Gases

JILA researchers have observed vortices in *BEC* of Rubidium atoms due to the developments of new methods of generation and control of macroscopic matter waves. As the system rotates, the condensate surface modes become excited. These modes transfer energy and angular momentum to vortex structures, which enter from the edge of the condensate.

So, in dilute *BECs* creation of quantised vortices can be achieved in many ways: by rotation of the cloud applying an anisotropic perturbation in single-component condensate (Madison *et al.*, 2000; Haljan *et al.*, 2001), by optical phase-imprinting (Leanhardt, 2002), by a dynamical phase-imprinting method in a two-component *BEC* (Matthews, 1999) et cetera. Vortex structures have been observed in different forms like single vortices (Matthews, 1999; Madison *et al.*, 2000; Anderson *et al.*, 2000), vortex lattices (Madison *et al.*, 2000; Abo-Shaeer *et al.*, 2001; Hodby *et al.*, 2003) and vortex rings (Anderson *et al.*, 2001). Regular vortex lattices have been investigated from a few vortices (Madison *et al.*, 2000) to several vortices (Abo-Shaeer *et al.*, 2001). Also, numerous vortices tend to form a vortex lattice.

The dynamics of a vortex line have been studied experimentally in precessional motion in trap (Anderson *et al.*, 2000), by bending (Rosenbusch *et al.*, 2002), by Kelvin wave excitation (Bretin *et al.*, 2003), gyroscopic oscillations (Hodby *et al.*, 2003) and splitting of multi-charged vortices (Shin, 2004).

Quantisation of Circulation

Any rotation of the fluid must be in the form of vortex lines, which introduce quantum circulation. The macroscopic wavefunction can be represented in terms of the fluid density and the macroscopic phase: $\psi(\mathbf{r}, t) = \sqrt{\rho(\mathbf{r}, t)}e^{iS(\mathbf{r}, t)}$ The phase around any closed contour, K_1 is $2\pi q$, where $q = 0, \pm 1, \pm 2, \dots$

$$\int_{K_1} \nabla S \cdot d\mathbf{l} = 2\pi q. \quad (1.1)$$

We know that the gradient of the phase describes the local velocity flow, $\mathbf{v}_s = (\hbar/m)\nabla S$. The superfluid velocity around the vortex line has a fixed circulation. So, the superfluid rotation induced by a vortex line can be expressed in terms of circulation about a contour, K , which is an arbitrary closed loop in the superfluid:

$$\Gamma = \oint_K \mathbf{v}_s \cdot d\mathbf{l} = q \left(\frac{h}{m} \right) = \kappa, \quad (1.2)$$

where, Γ is the circulation, h is Planck's constant and m is the mass of the BEC atom. The circulation of the fluid possesses multiple values of h/m , which shows that is quantised in units of $\kappa = q(h/m)$. For $q > 1$ the system is unstable.

Also from Eq. (1.2) it follows that the velocity around a single vortex is:

$$\mathbf{v}_s = \frac{\Gamma}{2\pi r} \hat{\psi}, \quad (1.3)$$

where, \mathbf{v}_s is the superfluid velocity around a single vortex at a point r , and $\hat{\psi}$ is the unit of angle. There is an energy barrier between non-vortex and vortex states. The superfluid has 0 vorticity ($\nabla S = 0$) in every place excluding singular points in 2D or lines in 3D, which are the centre of point vortices or vortex lines. These leads to the expression of the tangential velocity:

$$v_t = \frac{n\hbar}{mr_{\perp}}, \quad (1.4)$$

here, r_{\perp} is the distance from the vortex axis. The minimum density grows to the bulk value over a length-scale of order the healing length (Baym & Pethick, 1996). As we move away from the vortex the velocity slowly decreases. If we move towards the vortices then the superfluid density tends to zero.

Let us finish this section with the definition of the *healing length*, ξ . This is the distance over which the density changes from its bulk value to zero and is the vortex core parameter. So, ξ is the distance over which the fluid density can react to perturbations.

1.2 Gross-Pitaevskii Equation

Due to the low temperature of the BECs, many of the physical properties of the system are understood within the so called mean-field approximation. A characteristic feature of the mean-field approach comes from the dilute nature of the bose gases.

We can write the Bose field operator as a sum of the condensate wavefunction and an operator describing the non-condensed bosons:

$$\hat{\Psi}(\mathbf{r}, t) = \Psi(\mathbf{r}, t) + \hat{\Psi}'(\mathbf{r}, t), \quad (1.5)$$

where $\Psi(\mathbf{r}, t) \equiv \langle \hat{\Psi}(\mathbf{r}, t) \rangle$ is the average value of $\hat{\Psi}(\mathbf{r}, t)$ and $\hat{\Psi}'(\mathbf{r}, t)$ represents fluctuations. \mathbf{r} and t are position and time respectively. The single-particle density matrix is written as:

$$\rho_1(\mathbf{r}, \mathbf{r}') = \langle \hat{\Psi}^{\dagger}(\mathbf{r})\hat{\Psi}(\mathbf{r}') \rangle, \quad (1.6)$$

where $\hat{\Psi}^{\dagger}(\mathbf{r})$ is the field operator creating a particle at a point r and $\hat{\Psi}(\mathbf{r}')$ is the field operator annihilating a particle at r' . In dilute Bose gases close to $T = 0$ temperatures, we can neglect the non-condensed bosons $\hat{\Psi}'(\mathbf{r}, t)$. In that case the mean-field order parameter precisely coincides with the classical field $\Psi(\mathbf{r}, t)$ with well defined phase.

If we treat the system like a classical object, the wave function of the condensate behaves like a complex order parameter with a modulus and a phase and contains all relevant information about the system and satisfies a nonlinear Schroedinger equation (*NLSE*), called the Gross-Pitaevskii equation (*GPE*), which was obtained independently by Gross (Gross, 1957) and Pitaevskii (Ginzburg & Pitaevskii, 1958).

So, the zero temperature dynamics of weakly interacting particles of confined and dilute BECs are described by a mean-field macroscopic wavefunction, Ψ . Note, that the condensate density is

$\rho(\mathbf{r}, t) = |\Psi(\mathbf{r}, t)|^2$ and its phase is defined by $S = \tan^{-1}(Im(\Psi)/Re(\Psi))$. With the help of them we can define the *Madelung transformation*:

$$\Psi(\mathbf{r}, t) = \sqrt{\rho(\mathbf{r}, t)}e^{iS(\mathbf{r}, t)} = |\Psi(\mathbf{r}, t)|e^{iS(\mathbf{r}, t)}, \quad (1.7)$$

The inter-atomic collisions are described by the s-wave scattering length, a . Since the condensate is dilute, the atomic interactions are binary collisions and are expressed by a *contact potential*

$$V_{int}(\mathbf{r}, \mathbf{r}') = g\delta(\mathbf{r} - \mathbf{r}'), \quad (1.8)$$

where, g is the scattering coefficient, \mathbf{r} and \mathbf{r}' are positions. The coupling constant, g is given by

$$g = \frac{4\pi\hbar^2 Na}{m}, \quad (1.9)$$

where, m is the atomic mass, N is the number of atoms and \hbar is the reduced Planck constant $\hbar \equiv h/2\pi$. If $g < 0$, we have effectively attractive interactions and for $g > 0$, we have effectively repulsive interactions. Heisenberg's relation $i\hbar\partial\hat{\Psi}/\partial t = [\hat{\Psi}, \hat{H}]$ for the field operator yields the equation of motion of the macroscopic mean-field wave function:

$$i\hbar\frac{\partial\Psi(\mathbf{r}, t)}{\partial t} = \left(-\frac{\hbar^2}{2m}\nabla^2 + V_{tr}(\mathbf{r}, t) + g|\Psi(\mathbf{r}, t)|^2 \right) \Psi(\mathbf{r}, t), \quad (1.10)$$

which is the time-dependent equation, known as the Gross-Pitaevskii equation. This is a non-linear time dependent Schroedinger equation (NLSE) because of the nonlinear term $|\Psi(\mathbf{r}, t)|^2$. We normalise $\Psi(\mathbf{r}, t)$ by:

$$\int |\Psi(\mathbf{r}, t)|^2 d^3\mathbf{r} = N. \quad (1.11)$$

For a thermodynamic system, the chemical potential is defined as the amount by which the energy of the system would change by introducing an additional particle, assuming that, the entropy and volume are held fixed. The chemical potential is an important parameter and is defined as the partial derivative, $\mu = \partial E/\partial N$, where, E is the internal energy.

The GPE is a zero temperature model and describes numerous static and dynamic properties at temperatures much less than the transition temperature. In a frame of reference rotating with angular velocity Ω and for $\Psi(\mathbf{r}, t) = e^{-i\mu t/\hbar}\psi(\mathbf{r})$, the GPE has the form:

$$i\hbar\frac{\partial\psi(\mathbf{r}, t)}{\partial t} = \left[-\frac{\hbar^2}{2m}\nabla^2 + V_{tr} + g|\psi(\mathbf{r}, t)|^2 - \mu - \Omega L_z \right] \psi(\mathbf{r}, t), \quad (1.12)$$

So, the term $-\Omega L_z = i\hbar\Omega(x\partial_y - y\partial_x)$ is due to the rotation of the system about z axis with a frequency Ω .

1.2.1 Harmonic Oscillator Units

It is suitable to use the GPE in dimensionless form. Associated with harmonically-confined BEC, we use harmonic oscillator units (h.o.u) in the whole thesis, (Ruprecht *et al.*, 1995). That means that in our case the units of length, time and energy are: $\sqrt{\frac{\hbar}{2m\omega_\perp}}$, ω_\perp^{-1} and $\hbar\omega_\perp$. Here, ω_\perp is the

radial trapping frequency. So,

$$\tilde{x}_{HO} = \frac{x}{\sqrt{\frac{\hbar}{2m\omega_{\perp}}}}, \quad \tilde{t}_{HO} = t\omega_{\perp}, \quad \tilde{\varepsilon}_{HO} = \frac{\varepsilon}{(\hbar\omega_{\perp})} \quad (1.13)$$

where, $\tilde{\varepsilon}_{HO}$, \tilde{x}_{HO} and \tilde{t}_{HO} stand for energy, length and time. The normalisation of the wavefunction is changed via:

$$\int_{-\infty}^{\infty} |\psi(\mathbf{r}, t)|^2 d^3\mathbf{r} = \int_{-\infty}^{\infty} |\tilde{\psi}_{HO}(\tilde{\mathbf{r}}_{HO}, \tilde{t}_{HO})|^2 d^3\tilde{\mathbf{r}}_{HO} = 1, \quad (1.14)$$

where, $\tilde{\psi}_{HO}(\tilde{\mathbf{r}}_{HO}, \tilde{t}_{HO}) = l^{1/2}\psi(\mathbf{r}, t)$ and $l = \sqrt{\hbar/2m\omega_{\perp}}$.

1.2.2 Trapped and Dissipative Condensate

Harmonic Trap

The achievement and studies of BECs require cooling of metastable atomic samples. In a trapped gas, the BEC can be regarded as a coherent standing matter wave. The harmonic confinement of the 2D BECs is described by the trapping potential, V_{tr} . Let us begin with the dimensional geometry in 3D, which has a cylindrical symmetry about the z-axis:

$$V_{tr}(z, r) = \frac{m}{2}(\omega_z^2 z^2 + \omega_r^2 r^2). \quad (1.15)$$

Under a transverse confinement, the dynamics of the system become quasi-2D and the vortex line becomes rectilinear (Aftalion & Jerrard, 2002). In this system, the 2D GPE yields a good description of the condensate. In our simulation, we use a 2D dimensionless form:

$$V_{tr}(r) = \frac{1}{2}(\omega_r^2 r^2), \quad (1.16)$$

where, $r = \sqrt{(1 + \epsilon_x)x^2 + (1 + \epsilon_y)y^2}$, with $\epsilon_x = 0.03$, $\epsilon_y = 0.09$ and $\omega_r = 2\pi \times 219$ Hz, corresponding to the *ENS* experiment, see (Madison *et al.*, 2000). Here, ϵ_x and ϵ_y , describe small deviations of the trap from the axi-symmetry. So, the condensate is elongated along the x -axis due to this small anisotropy and the boundary surface of the condensate becomes unstable. This phenomenon plays a key role in the formation of the vortices.

Dissipative Regime

To understand several experiments with vortices (Rosenbusch *et al.*, 2002; Abo-Shaeer *et al.*, 2002) and solitons, it is helpful to include the dynamical coupling of the condensate to the thermal cloud, the effect of dimensionality and the role of quantum fluctuations (Proutkakis, 2007).

In superfluid helium the problem of quantised vortices and mutual friction force on the vortex were well described at finite temperature (Barenghi *et al.*, 2001), when on account of the presence of a thermal cloud, dissipation arises. This non-condensed part acts as a source of dissipation, having as a result, the damping of excitations like collective modes (Jin *et al.*, 1997; Chevy *et al.*, 2002).

The mean-field (Fedichev & Shlyapnikov, 1999) and collisional (Duine *et al.*, 2004) damping with uniform densities were well understood. Mean field coupling between the condensate and thermal cloud leads to a lower frequency oscillation. In that case for example, a soliton loses energy (Burger *et al.*, 1999) to the thermal cloud (Jackson *et al.*, 2007). At non-zero temperature, the evolution and dissipation of vortex rings in a condensate was studied in the relation of the classical field approximation (Berloff & Youd, 2007a).

The decay of a vortex at finite temperatures was investigated with the help of the GPE and a Boltzmann kinetic equation for the thermal cloud (Zaremba *et al.*, 1999). In a trapped Bose gas, the two-fluid hydrodynamics of the condensate and non-condensate was described by including the dissipation, associated with viscosity and thermal conduction, see (Zaremba *et al.*, 1999).

Inclusion of a damping term γ into the GPE (Choi *et al.*, 1998), models dissipative losses that occur in real environments. Collective damped oscillations was noticed due to some dissipative mechanism (Ensher *et al.*, 1996). We can state that the dynamical dissipation factor γ , plays a significant role in condensates, which in our equation:

$$(i - \gamma) \hbar \frac{\partial \psi(\mathbf{r}, t)}{\partial t} = \left[-\frac{\hbar^2}{2m} \nabla^2 + V_{tr}(\mathbf{r}, t) + g|\psi(\mathbf{r}, t)|^2 - \mu - \Omega L_z \right] \psi(\mathbf{r}, t), \quad (1.17)$$

is the γ -term.

Pitaevskii developed a method of phenomenological damping (Pitaevskii, 1958, 1959) for superfluidity near the λ point. The added phenomenological dissipation parameter, γ , models the interaction of the condensate with the thermal cloud (Tsubota *et al.*, 2002; Abo-Shaeer *et al.*, 2002). We can compare its microscopic justification with the help of (Penckwitt *et al.*, 2002; Gardiner *et al.*, 2002) and (Choi *et al.*, 1998; Tsubota *et al.*, 2002).

In accordance with Penckwitt et al (Penckwitt *et al.*, 2002) and Gardiner et al (Gardiner *et al.*, 2002) in a simple unified theory of vortex nucleation and vortex lattice formation the condensate grows due to a rotating thermal cloud. This was derived from a growth equation by using a simple form for the transition probability:

$$W^+(N) \approx g \frac{4m(akT)^2}{\pi \hbar^3}, \quad (1.18)$$

which originally comes from (Gardiner *et al.*, 1997) having a form as:

$$W^+(N) = \frac{4m(akT)^2}{\pi \hbar^3 e^{2\mu/kT}} \left[\frac{\mu_N}{kT} K_1 \left(\frac{\mu_N}{kT} \right) \right], \quad (1.19)$$

and which describes the net rate of atom transfer, where k is the Boltzmanns constant, T is the temperature of the noncondensate, a is the s-wave scattering length, N is the number of atoms each of mass m , K_1 is a modified Bessel function and the correction factor, $g \approx 3$ (is different from the parameter g used throughout this thesis, which describes interatomic collisions). The chemical potential of the Thomas-Fermi approximation is described by:

$$\mu_N = \left(15Ng\omega_x\omega_y\omega_z m^{3/2} / 16\pi\sqrt{2} \right)^{2/5}, \quad (1.20)$$

So, their final equation, which is the vortex growth equation becomes:

$$(i - \gamma)\hbar \frac{\partial \psi(\mathbf{r}, t)}{\partial t} = -\frac{\hbar^2}{2m} \nabla^2 \psi(\mathbf{r}, t) + V_{tr}(\mathbf{r}, t) \psi(\mathbf{r}, t) + g|\psi(\mathbf{r}, t)|^2 \psi(\mathbf{r}, t) - \Omega L_z \psi(\mathbf{r}, t) + i\gamma \mu_{NC} \psi(\mathbf{r}, t), \quad (1.21)$$

where, $\psi(\mathbf{r}, t)$ is the field operator, the nonlinear interaction term is $g = 4\pi a \hbar^2 / m$, V_{tr} is the harmonic trap potential, Ω is the angular velocity, μ_{NC} is the noncondensate chemical potential, L_z is the angular momentum operator. A microscopic expression for the phenomenological dissipation parameter γ is given in terms of temperature and scattering length:

$$\gamma \equiv \frac{4mga^2kT}{\pi\hbar^2} \equiv \frac{\hbar W^+}{kT} \approx 0.01, \quad (1.22)$$

The physics described here is the growth of a condensate in a frame rotating with angular velocity Ω about the z-axis from a vapour cloud, which is itself stationary in the rotating frame.

This is analogous with vortex nucleation from a rotating vapour cloud performed by the *JILA* group (Haljan *et al.*, 2001). For $a \approx 10^{-8}m$ and $g = 3$, they find, $\gamma \approx 0.01$.

Our dimensionless equation:

$$(i - \gamma) \frac{\partial \psi(\mathbf{r}, t)}{\partial t} = \left(-\frac{1}{2} \nabla^2 + V_{tr} + C|\psi|^2 - \mu - \Omega L_z \right) \psi(\mathbf{r}, t), \quad (1.23)$$

is the same as presented by (Choi *et al.*, 1998) and (Tsubota *et al.*, 2002), where a phenomenological model of the process of vortex lattice formation was suggested. To deduce this equation one begins with the standard *GPE*, which describes the motion of the mean field, $\psi(\mathbf{r}, t)$:

$$i\hbar \frac{\partial \psi(\mathbf{r}, t)}{\partial t} = -\frac{\hbar^2}{2m} \nabla^2 \psi(\mathbf{r}, t) + V_{tr}(\mathbf{r}, t) \psi(\mathbf{r}, t) + g|\psi(\mathbf{r}, t)|^2 \psi(\mathbf{r}, t), \quad (1.24)$$

where, $g = 4\pi \hbar^2 a / m$. The *GPE* contains no term which describes damping. A relaxation process can be described by:

$$i\hbar \frac{\partial \psi(\mathbf{r}, t)}{\partial t} = \hat{L} \psi(\mathbf{r}, t), \quad (1.25)$$

The operator \hat{L} cannot be Hermitian. The anti-Hermitian part of \hat{L} is associated with the processes by which equilibrium is approached and have the form:

$$i\gamma \left(\frac{\hbar^2}{2m} \nabla^2 \psi(\mathbf{r}, t) + V_{tr}(\mathbf{r}, t) \psi(\mathbf{r}, t) + g|\psi(\mathbf{r}, t)|^2 \psi(\mathbf{r}, t) - \mu \psi(\mathbf{r}, t) \right), \quad (1.26)$$

where γ is a dimensionless factor and is inversely proportional to the relaxation time. The final equation including relaxation to equilibrium is:

$$i\hbar \frac{\partial \psi(\mathbf{r}, t)}{\partial t} = (1 + i\gamma) \left\{ -\frac{\hbar^2}{2m} \nabla^2 + V_{tr}(\mathbf{r}, t) + g|\psi(\mathbf{r}, t)|^2 - \mu \right\} \psi(\mathbf{r}, t), \quad (1.27)$$

This equation is the same as our equation, see Eq. 1.17. As a consequence, γ leads to a dissipation of energy from the system in such a way that it transforms towards the ground state, preserving particle number. Unlike Eq. 1.21-Eq. 1.22, here $\gamma < 0$ for damping to take place due to the

different way the equation is written. Now, consider the mean field, $\psi(\mathbf{r}, t)$ to be expressed by two components:

$$\psi = e^{-i\mu t} (\psi_g + \delta). \quad (1.28)$$

Evolution in Eq. 1.27 results in the damping of δ toward zero.

Physically, γ represents the rate at which the excited components turn into the condensate and is approximated by the transition probability $W^+(N)$ estimated in (Gardiner *et al.*, 1997). Using the quantum kinetic theory, $W^+(N)$ gives the rate at which the thermal particles above the condensate band enter the condensate due to collisions. The condensate does not act back on the thermal component to change its temperature. This assumption is valid in quasiequilibrium situations.

According to *MIT* experiment (Mewes *et al.*, 1996) and using their reported values together with the expression of Eq. 1.19 for γ , it was found:

$$|\gamma| \approx \left| \frac{W^+(N)}{\omega} \right| \approx 0.03, \quad (1.29)$$

for $T \approx T_c/10$ and $a \approx 3.45\text{nm}$. Here, ω is the trap frequency and $\omega = 2\pi \times 19\text{ Hz}$. The corresponding damping time is $\approx 200\text{ ms}$ and is of the same order of magnitude as the experimental damping time of 250 ms (of the *MIT* experiment).

1.2.3 Hydrodynamic Equation

For a homogeneous system with $\Omega = 0$, is valid:

$$(i - \gamma)\hbar \frac{\partial \psi(\mathbf{r}, t)}{\partial t} = \left(-\frac{\hbar^2}{2m} \nabla^2 + g|\psi(\mathbf{r}, t)|^2 - \mu \right) \psi(\mathbf{r}, t). \quad (1.30)$$

Now, we introduce the fundamental connection between the GPE and the equations of classical fluid mechanics. For this purpose, we recast the GPE by the Madelung transformation, which is defined by Eq. 1.7. The phase ($S(\mathbf{r}, t)$) can be related to the velocity by:

$$\mathbf{v}(\mathbf{r}, t) = \frac{\hbar}{m} \nabla S(\mathbf{r}, t). \quad (1.31)$$

Substituting (1.7) and (1.31) into the (1.30), we obtain the real part and the imaginary part of the GPE. So, the real part is:

$$-\hbar \left(R \frac{\partial S}{\partial t} + \gamma R \frac{\partial R}{\partial t} \right) = -\frac{\hbar^2}{2m} (\nabla^2 R - R(\nabla S)^2) + gR^3 - \mu R \quad (1.32)$$

and then the imaginary part becomes:

$$\hbar \left(\frac{\partial R}{\partial t} - \gamma R \frac{\partial S}{\partial t} \right) = -\frac{\hbar^2}{2m} (2\nabla S \cdot \nabla R + R\nabla^2 S). \quad (1.33)$$

Also, we put the GPE in fluid dynamics form with the help of the real and imaginary parts of the GPE. After some arrangements, (see *Appendix B* for more details), we obtain two equations:

$$\frac{\partial \rho}{\partial t}(1 + \gamma^2) + \nabla \cdot (\rho \mathbf{v}) + \frac{2\gamma\rho}{\hbar} \left(\frac{mv^2}{2} + \frac{g\rho}{m} - \mu \right) - \gamma\hbar \sqrt{\frac{\rho}{m}} \frac{\partial^2 \sqrt{\frac{\rho}{m}}}{\partial x_j \partial x_j} = 0. \quad (1.34)$$

The first one is similar to the *Classical Equation of Continuity* or *Equation of Mass Conservation* plus some extra terms due to the dissipation γ . For $\gamma = 0$, this equation becomes the *Classical Equation of Continuity*. In our notation, x_i is the i^{th} Cartesian component ($i = 1, 2, 3$) of the position and

$$p = \frac{g\rho^2}{2m^2}, \sigma_{ij} = \frac{\hbar^2}{2m^2} \left[\rho^{1/2} \frac{\partial^2 \rho^{1/2}}{\partial x_i \partial x_j} - \frac{\partial \rho^{1/2}}{\partial x_i} \frac{\partial \rho^{1/2}}{\partial x_j} \right], \quad (1.35)$$

where, p is a pressure and σ_{ij} are the quantum stresses. Furthermore,

$$\sigma_{ij} = \frac{\hbar^2}{2m} \rho \left(\frac{\partial^2 \ln \rho^{1/2}}{\partial x_i \partial x_j} \right) = \frac{\hbar^2}{4m^2} \rho \frac{\partial^2 \ln \rho}{\partial x_i \partial x_j}. \quad (1.36)$$

Finally, we obtain our second equation:

$$\rho \left(\frac{\partial v_i}{\partial t} + v_j \frac{\partial v_j}{\partial x_i} \right) = -\frac{\partial p}{\partial x_i} + \frac{\partial \sigma_{ij}}{\partial x_j} - \frac{\gamma\hbar}{2m} \left(-\frac{1}{\rho} \frac{\partial \rho}{\partial x_i} \frac{\partial \rho}{\partial t} + \frac{\partial^2 \rho}{\partial x_i \partial t} \right), \quad (1.37)$$

which is similar to the *Classical Euler Equation* plus some extra terms due to the dissipation γ . This is the unintegrated form of the *Momentum Equation*. For $\gamma = 0$, this equation becomes the classical *Conservation of Momentum*. We interpret every term, which involves γ as being to do with the exchange of momentum and atoms between the normal fluid and the superfluid. For example, for the exchange of momentum, the terms involving gamma and velocity and for the exchange of atoms the terms including gamma and density.

1.2.4 Thomas-Fermi Solution

The Thomas-Fermi (TF) solution represents an approximation of the density profile. In the case of comparatively strong interactions, we can neglect the kinetic energy term (∇^2 terms) in the GPE. In that situation, we have a dominant interaction and potential. Assuming a steady state ($\partial/\partial t = 0$), the solution of Eq. 1.17 and Eq. 1.30 is Eq. 1.38. The dimensionless form of the density for the Thomas-Fermi approximation (TFA) (Baym & Pethick, 1996) becomes:

$$\rho(\mathbf{r}) = \frac{\mu - V_{tr}(\mathbf{r}, t)}{C} \quad \text{for} \quad \mu \geq V(\mathbf{r}) \quad (1.38)$$

and

$$\rho(\mathbf{r}) = 0, \quad \text{elsewhere}, \quad (1.39)$$

where $C = 4\pi Na/L$ is the dimensionless form of the coupling constant g , N is the number of atoms, a is the scattering length and L is the extension of the condensate in the z - direction. The Thomas-Fermi radius, is limited as $0 \leq r_{TF} \leq \sqrt{2\mu}$.

1.3 Energies

Introduction of the γ parameter changes the nature of GPE, so the total energy now is not conserved. The vortex is thermodynamically unstable (Rokhsar, 1997; Svidzinsky & Fetter, 2000a; Jackson *et al.*, 2000). At the centre of the trap, a vortex has maximum energy, because of the locally homogeneous density. In order to perform our analysis, we decompose the total energy, E_{tot} , into kinetic, internal, quantum and trap contributions,

$$E_{tot} = E_{kin} + E_{int} + E_q + E_{trap}, \quad (1.40)$$

where

$$E_{kin}(t) = \int \frac{\hbar^2}{2m} \left(\sqrt{\rho(\mathbf{x}, t)} \mathbf{v}(\mathbf{x}, t) \right)^2 d^2\mathbf{r}, \quad (1.41)$$

$$E_{int}(t) = \int g (\rho(\mathbf{x}, t))^2 d^2\mathbf{r}, \quad (1.42)$$

$$E_q(t) = \int \frac{\hbar^2}{2m} \left(\nabla \sqrt{\rho(\mathbf{x}, t)} \right)^2 d^2\mathbf{r}, \quad (1.43)$$

$$E_{trap}(t) = \int \rho(\mathbf{x}, t) V_{tr} d^2\mathbf{r}. \quad (1.44)$$

Notice that, the kinetic energy (E_{kin}) is related with the velocity field. The internal energy (E_{int}) represents the internal energy of the fluid. The quantum energy (E_q) comes from the gradient of the condensate and the trap energy (E_{trap}) has its origin from the applied trap potential.

Furthermore, we decompose the kinetic energy, E_{kin} , into a part due to the sound field, E_{sound} , and a part due to vortices, E_{vortex} (Ogawa *et al.*, 2001; Parker & Adams, 2005):

$$E_{kin} = E_{sound} + E_{vortex}. \quad (1.45)$$

The compressible part of the kinetic energy is concerned with the acoustic emission, (Ogawa *et al.*, 2001). To approximate E_{vortex} , firstly, we take the real-time vortex distribution. At a given time t , the vortex energy, E_{vortex} , is obtained by propagating the *GPE* in imaginary time, which yields the lowest energy state for a given vortex configuration (with the same potential and number of particles), but without sound, (Parker & Adams, 2005). At this point the sound energy is recovered from $E_{sound} = E_{kin} - E_{vortex}$. The excited sound has a propagation speed $c_s = \sqrt{0.5C|\psi|^2} = 3.8124$ at the peak density of an unperturbed condensate, where C is the dimensionless form of the coupling constant g .

The imaginary time propagation minimises the chemical potential, μ , because in that case we obtain the lowest energy state of the system. It can be initially estimated as $\mu = 2\hbar\sqrt{a/m}$ and in dimensionless form as:

$$\mu = \frac{1}{2} \sqrt{\frac{4C}{\pi}}, \quad (1.46)$$

from the Thomas-Fermi solution. By the single-step integration is found:

$$\mu = -\frac{\ln \frac{\langle |\psi(t)|^2 \rangle}{\langle |\psi(t+\Delta t)|^2 \rangle}}{2\Delta t}, \quad (1.47)$$

after the initial Thomas-Fermi solution has relaxed to a time - independent solution in the harmonic trap, where $\langle \dots \rangle$ denotes spatial average. The dimensionless form of the energy contributors are:

$$E_{kin}(t) = \int \frac{1}{2} \left(\sqrt{\rho(\mathbf{x}, t)} \mathbf{v}(\mathbf{x}, t) \right)^2 d^2\mathbf{r}, \quad (1.48)$$

$$E_{int}(t) = \int C (\rho(\mathbf{x}, t))^2 d^2\mathbf{r}, \quad (1.49)$$

$$E_q = (t) \int \frac{1}{2} \left(\nabla \sqrt{\rho(\mathbf{x}, t)} \right)^2 d^2\mathbf{r}, \quad (1.50)$$

and

$$E_{trap}(t) = \int \rho(\mathbf{x}, t) V_{tr} d^2\mathbf{r}. \quad (1.51)$$

1.4 Numerical Simulations

To explore the dynamical instabilities and the relaxation to the equilibrium of the system, we perform numerical simulations using the time-dependent Gross-Pitaevskii equation. We describe in Appendix E a technique for creating a single vortex and vortex - anti vortex pairs. We solve the GPE numerically due to the non-linear term, $C|\psi(\mathbf{r})|^2$. In our case, this is performed using the *Crank - Nicholson* numerical method.

In imaginary time, excitations are damped exponentially. Also, μ and ψ converge to a stationary solution. In a frame rotating about the z -axis with angular velocity Ω , the dimensionless $2D$ GPE becomes:

$$(i - \gamma) \frac{\partial \psi}{\partial t} = \left(-\frac{1}{2} \nabla^2 + V_{tr} + C|\psi|^2 - \mu - \Omega L_z \right) \psi, \quad (1.52)$$

where, the angular momentum operator is given by $L_z = i(x\partial_y - y\partial_x)$. The trapping potential is expressed by Eq. 1.16. The *dissipation* is represented by γ . Unless stated otherwise, we set $C = 2000$ in the whole thesis. So, C corresponds to a large number of particles and μ is almost constant for the vortex initial positions close to the centre of the condensate. Positive C corresponds to repulsive interactions and for large C , the interaction term in the chemical potential dominates. To model the thermal cloud in our simulation, we use generally $\gamma = 0.03$ or different values.

The calculation is performed in a square box of size D , divided into a grid of 300×300 points. We choose D so that it is larger than the trapped condensate, and impose boundary conditions $\psi = 0$ at $x = \pm D/2$ and $y = \pm D/2$. Typically, $D = 13$, see our discussion of a typical condensate without any vortices in Chapter 4. The error in locating the vortex is of the order of ± 0.01 .

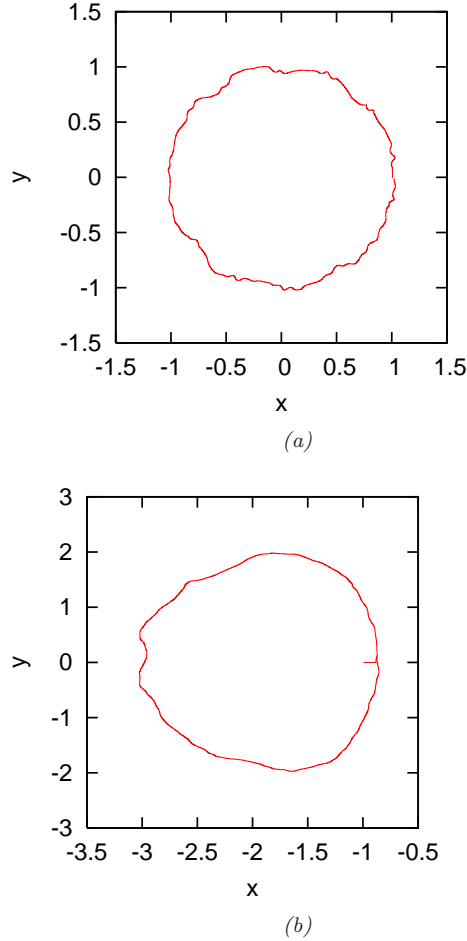


Figure 1.1: (a):Trajectory of a single vortex initially located at: $(x_0, y_0) = (1, 0)$. (b): Trajectory of the left vortex of vortex-antivortex pair initially located at $(x_0, y_0) = (\pm 1, 0)$.

During an orbit, the relative size of the oscillations are respectively: $\Delta E_{kin}/E_{kin} \simeq 0.125$, $\Delta E_q/E_q \simeq 0.097$, $\Delta E_{int}/E_{int} \simeq 0.029$ and $\Delta E_{trap}/E_{trap} \simeq 0.031$, where ΔE_{kin} , ΔE_q , ΔE_{int} and ΔE_{trap} are the amplitudes of these oscillations, see (Madarassy & Barenghi, 2008a). The reason of these oscillations is that, as the vortex precesses, it generates sound waves, which, unable to escape the trap, are reabsorbed by the vortex and explains the orbital wiggles apparent in Figure 1.1(a) and in Figure 1.1(b) (the other reason is that the centre of mass of a condensate containing a relative large vortex hole oscillates).

Let us denote by U , the quantity:

$$U = C|\psi|^2 + V_{tr} - \mu \quad (1.53)$$

and by f , the fraction

$$f = \frac{\gamma + i}{\gamma^2 + 1} \quad (1.54)$$

Then, we solve the simple equation:

$$\frac{\partial\psi}{\partial t} = f \left(-\frac{1}{2}\nabla^2 + U - \Omega L_z \right) \psi \quad (1.55)$$

To avoid the formation of vortices due to the rotation of the trapping potential, in the case of a single vortex, vortex - anti vortex pairs and selection of randomly placed vortex - anti vortex pairs, in this thesis, $\Omega = 0$. In Chapter 5 its value is different from zero.

In order to imprint a vortex at location (x_0, y_0) , we take for initial condition ψ , the Thomas-Fermi approximation, multiplied times a suitable function which is proportional to $(x - x_0) + i(y - y_0)$ and vanishes at (x_0, y_0) . So, in these cases due to our method of creation of vortices the vortex/vortices have a determined position/positions (see for more details the *Appendix D*). Their presence and origin do not depend on the trap rotating frequency, Ω .

In this thesis the simulation of vortex motion is performed in two-dimensions (2D).

Chapter 2

Motion of a Single Vortex

2.1 Introduction

In the trapped, dilute BEC, an off-centre vortex follows a trajectory of constant potential: in other words, it displays precession about the trap centre (Rokhsar, 1997; Svidzinsky & Fetter, 2000*a*). A straight-line vortex moving through the thermal cloud causes dissipation via scattering of thermal excitations of the vortex core. The result is a movement towards a local minimum of the energy; a motion from the trap centre to the edge of the condensate. The vortex spirals outward (Rokhsar, 1997). In the centre, a vortex line is stationary. Because of the thermal and quantum fluctuations, a vortex positioned off-centre is made to spiral outwards and has a finite lifetime (Duine *et al.*, 2004).

We made our simulations with special emphasis on comparing the case of no dissipation with the case of dissipation. In this chapter, we are concerned with the dynamics of a single vortex. At finite temperatures the vortex loses energy and moves radially towards the condensate edge. The radial position of the vortex as a function of time is an exponential function. We give more description about this behaviour in the next chapter. Our off-centre vortex accelerates from its initial condition, gaining an almost constant angular velocity around the trap centre. Single vortices with one quantum of circulation have been produced (Matthews, 1999; Madison *et al.*, 2000) and observed (Matthews, 1999; Madison *et al.*, 2000; Anderson *et al.*, 2000; Hodby *et al.*, 2003).

2.2 Single Vortex Motion with Different γ 's

Without dissipation the vortex has a circle-like trajectory with an almost constant radius and with more fluctuations, see the centre trajectory in Figure 2.2(a) and Figure 2.3(a). The difference between these two figures is the vortex initial position.

In this chapter, we present the dissipative dynamics of single vortices with $(x_0, y_0) = (0.9, 0)$ in a BEC. First, we put for γ the following values: 0; 0.01; 0.07 and 0.1 and later 0; 0.001; 0.003; 0.01 and 0.03. First, we prepare a condensate without vortices. From Figure(2.1(a) - 2.1(b)),

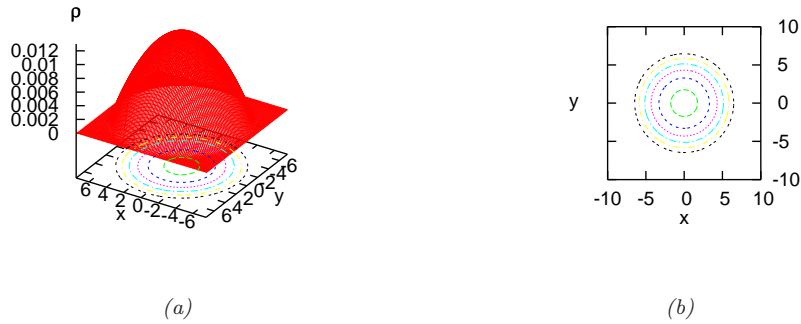


Figure 2.1: (a): The 3D density plot of the condensate without vortices ($\gamma = 0$). (b): Equilibrium condensate for $C = 2000$. The density contours correspond respectively to 17%, 33%, 50%, 60% and 83% of the maximum density at the centre..

we can see that the maximum level of density is equal to 0.012. Later, we put vortices in the condensate, (see Appendix D) at different initial positions on the line $y_0 = 0$.

We consider a vortex motion according to a phenomenological dissipative model of a *BEC*. Since, the vortex is a stationary solution, it will remain at the centre. At that place, the vortex arrangement is unstable to infinitesimal displacements (Jackson *et al.*, 2000). Experimentally, one has observed the precession of the vortex around the trap centre (Madison *et al.*, 2000). This tell us that an off-centre vortex follows a path of constant potential. Dissipation transfers energy from a moving vortex to the sound (thermal cloud). This decay causes the vortex to move towards a local minimum (lower densities and larger radii). As a result of the cyclical motion and the inhomogeneity of the condensate the compressibility changes, so the moving vortex pair produce acoustic emission.

An off-axis vortex will follow a path of constant energy being equivalent to precession around the trap centre. With dissipation ($\gamma \neq 0$), the vortex will spiral out of the condensate (Fedichev & Shlyapnikov, 1999) and this is due to the dissipative drift towards lower energies.

With dissipation the total energy decreases, (see Figure 2.4(a)). There are similarities between the kinetic energy and the total energy (see Figure 2.5(b) and Figure 2.5(a)). In Figure 2.4(j), Figure 2.5(b) , Figure 2.6(a) and Figure 2.6(b) the final values of L_z and kinetic energy are zero because the vortex left the condensate. Figure 2.6(b) shows the variation of the kinetic energy as a function of time for a single vortex with different initial positions for the same dissipation, $\gamma = 0.003$

Without dissipation, the average values of these energies are *constant*. On the other hand, with dissipation the small fluctuations become damped as we can see from Figure 2.4. For small dissipations the energy functions follow a modulation from the vortex cyclical motions. With larger values of γ these fluctuations disappear. The decrease/increase of different energies and L_z with time for different γ 's is presented in Figure 2.4, where, we compare the case of no dissipation with the case of different dissipations.

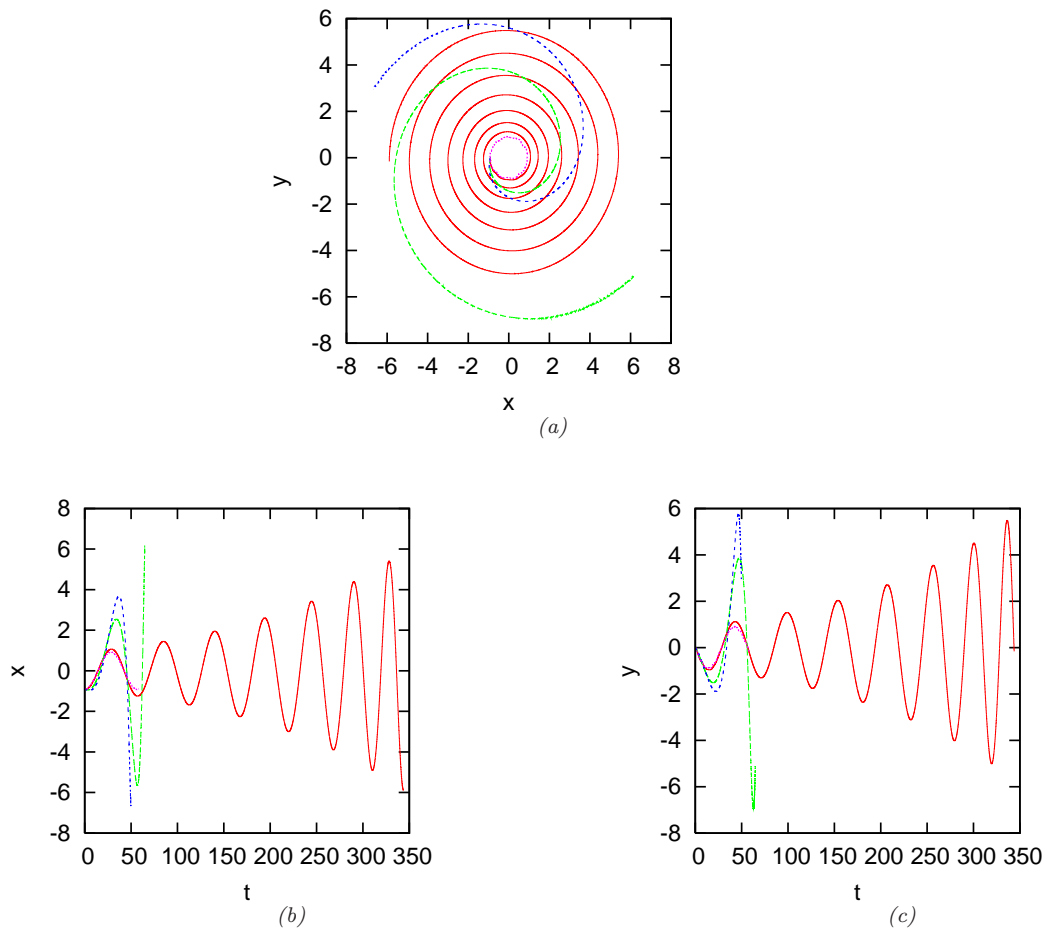


Figure 2.2: (a): Trajectories, (b): x -components vs. time and (c): y - components vs. time corresponding to Figure 2.2 (a) of a single vortex initially located at $(x_0, y_0) = (0.9, 0)$ for $\gamma = 0$ (purple/dotted line); $\gamma = 0.01$ (red/solid line); $\gamma = 0.07$ (green/dashed line) and $\gamma = 0.1$ (blue/small dashed line).

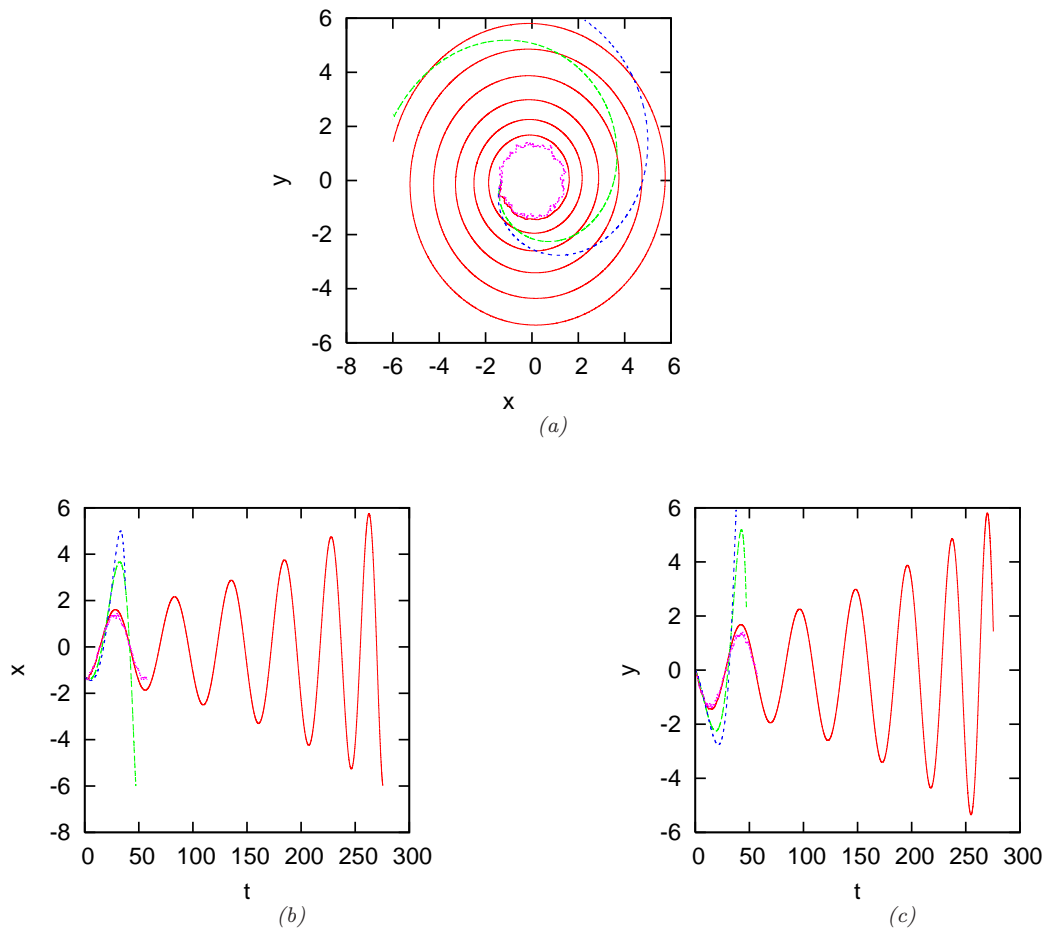


Figure 2.3: (a): Trajectories, (b): x -components vs. time and (c): y - components vs. time corresponding to Figure 2.3 (a) of a single vortex initially located at $(x_0, y_0) = (1.3, 0)$ and for $\gamma = 0$ (purple/dotted line); $\gamma = 0.01$ (red/solid line); $\gamma = 0.07$ (green/dashed line) and $\gamma = 0.1$ (blue/small dashed line)

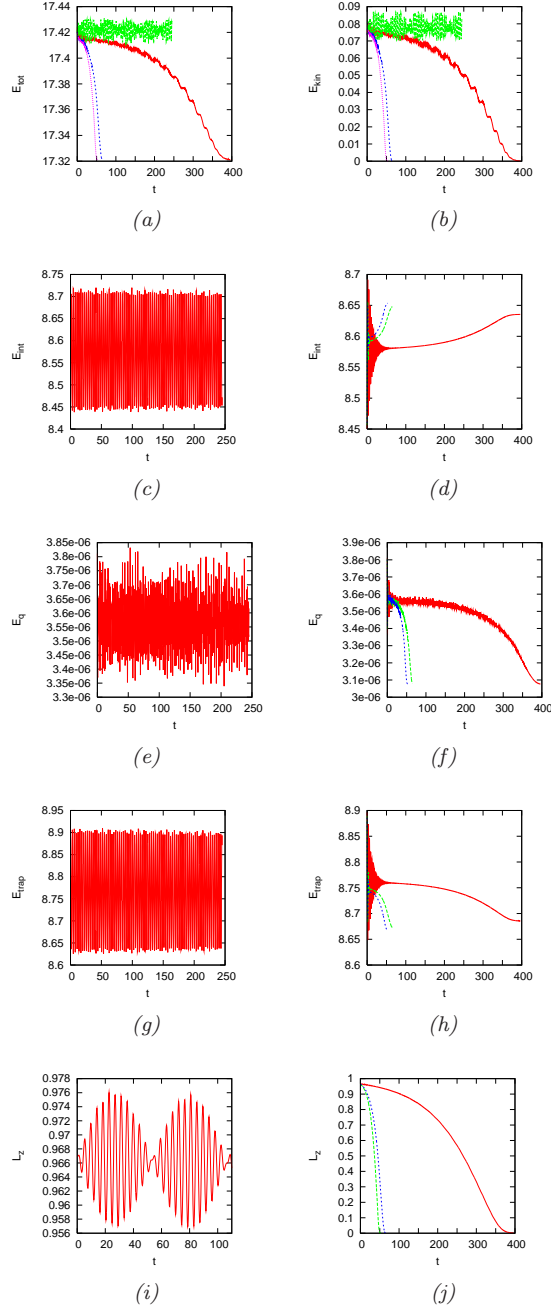


Figure 2.4: For a single vortex with $(x_0, y_0) = (0.9, 0)$: (a,b): total energy and kinetic energy for $\gamma = 0$ (green/upper horizontal line); $\gamma = 0.01$ (red line); $\gamma = 0.07$ (blue line) and $\gamma = 0.1$ (purple/shortest line). For (left): $\gamma = 0$ and for (right): $\gamma = 0.01$ (red/solid line); $\gamma = 0.07$ (green/dashed line) and $\gamma = 0.1$ (blue/small dashed line) for (c,d): internal energy, (e,f): quantum energy, (g,h): trap energy and (i,j): z -component of the angular momentum.

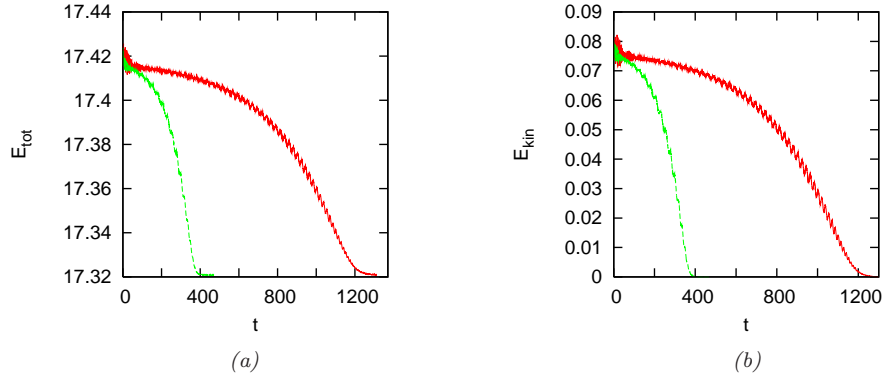


Figure 2.5: (a): Total energy and (b): kinetic energy corresponding to Figure 2.4 for $\gamma = 0.003$ (red/upper line) and for $\gamma = 0.01$ (green/lower line).

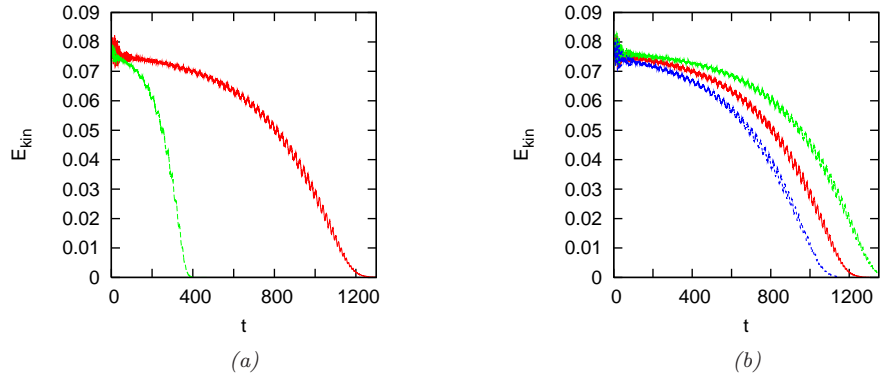


Figure 2.6: Kinetic energy for a single vortex with (a): $(x_0, y_0) = (0.9, 0)$ and for $\gamma = 0.01$ (green/lower line) and $=0.003$ (red/upper line) and with (b): $(x_0, y_0) = (0.7, 0)$ (blue/lower line); $= (0.9, 0)$ (red/middle line) and $= (1.1, 0)$ (green/upper line) for the same $\gamma = 0.003$.

Our single vortex in this section has $(x_0, y_0) = (0.9, 0)$ and $(x_0, y_0) = (2, 0)$. Let us continue this section with some plots of different energies and also of different trajectories with dissipations. Larger dissipation means shorter trajectory and shorter time, that the vortex needs to leave the condensate. As we increase γ , the paths become shorter and shorter, see Figure(2.7(a) - 2.7(d)), Figure(2.9(a) - 2.9(f)) and Figure(2.8(a) - 2.8(b)).

We sum up our conclusions with the help of Figure 2.10(a) and Figure 2.10(b), where, we see that with larger γ , the radius of trajectory becomes larger more quickly than with small γ , when r is almost unchanged.

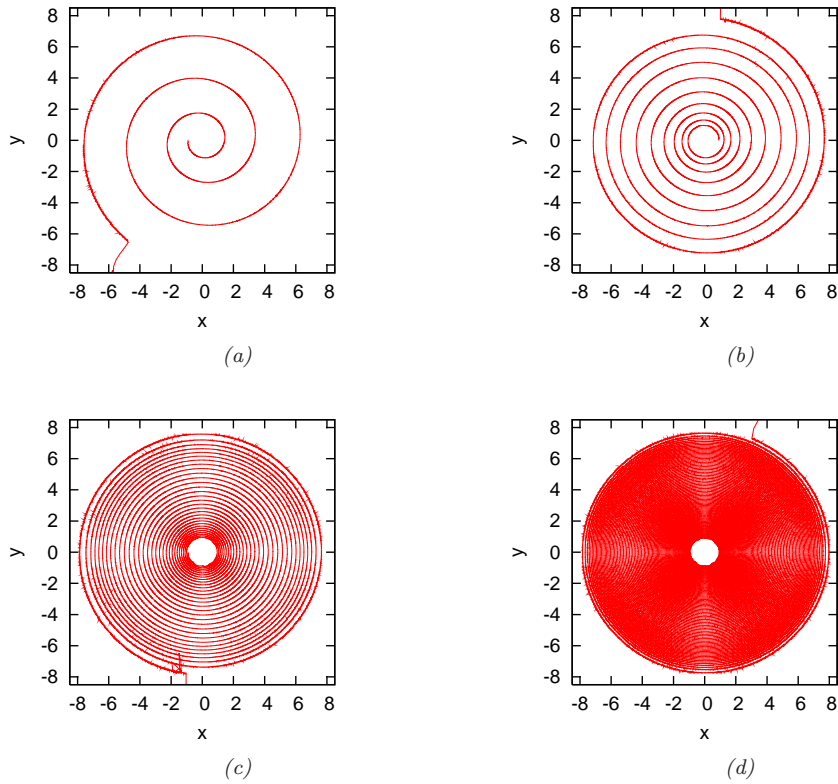


Figure 2.7: Trajectories for a single vortex with $(x_0, y_0) = (-0.9, 0)$ for (a,b): (left): $\gamma = 0.03$ and for (right): $\gamma = 0.01$ for (c,d): (left): $\gamma = 0.003$ and for (right): $\gamma = 0.001$.

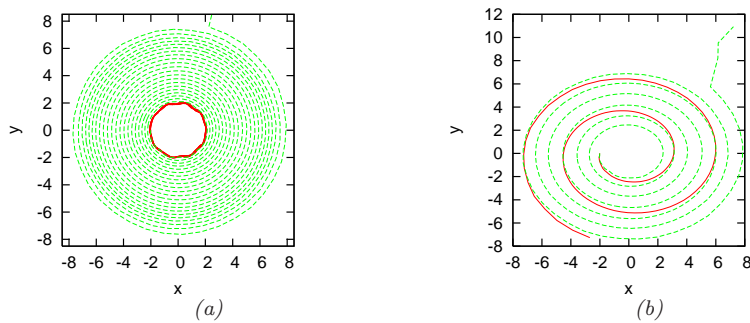


Figure 2.8: Trajectories for a single vortex with $x_0 = -2.0$ (a): for $\gamma = 0$ (red line/solid line) and $\gamma = 0.003$ (green line/dashed line) and for (b): $\gamma = 0.03$ (green line/dashed line). We can see that the vortex have left the condensate.) and $\gamma = 0.01$ (red line/solid line).

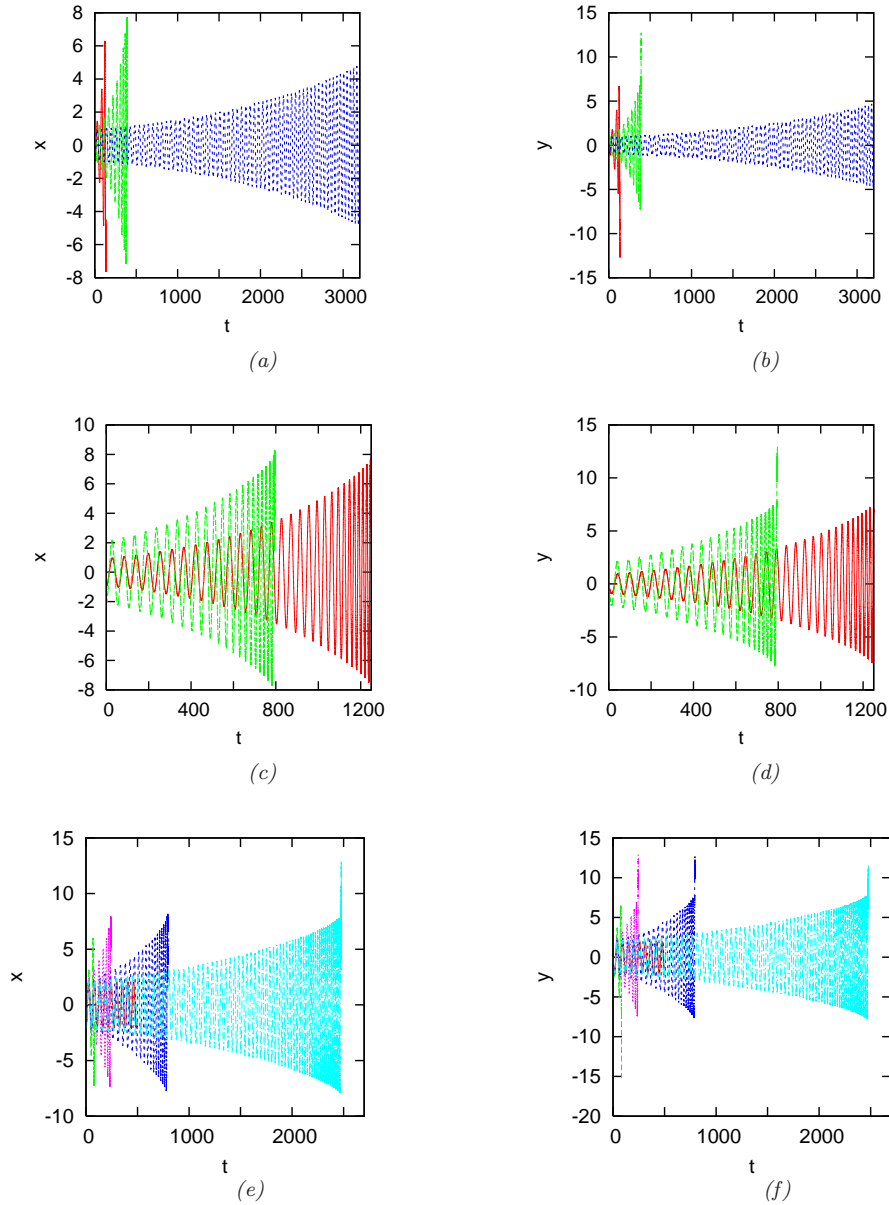


Figure 2.9: (left): x -component and (right): y -component of trajectories for a single vortex with (a,b): $(x_0, y_0) = (-0.9, 0)$ and for $\gamma = 0.03$ (red line/shortest time scale); $\gamma = 0.01$ (green line) and $\gamma = 0.001$ (blue line/longest time scale) and for (c,d): $\gamma = 0.003$ and with $(x_0, y_0) = -0.9, 0$ (red line/longest time scale) and $= (-2, 0)$ (green line/shortest time scale) and with (e,f): $(x_0, y_0) = (-2, 0)$ and $\gamma = 0.03$ (green line/shortest time scale); $\gamma = 0.01$ (purple line); $\gamma = 0.003$ (blue line); $\gamma = 0.001$ (aquamarine line/longest time scale); $\gamma = 0$ (red line/same amplitude).

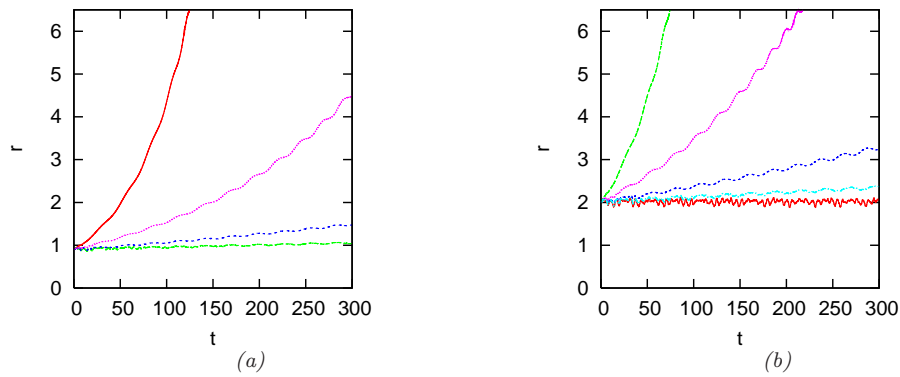


Figure 2.10: Radius of trajectory for a single vortex with (a): $(x_0, y_0) = (-0.9, 0)$ and for $\gamma = 0.03$ (red/last vertical wavy line); $\gamma = 0.01$ (purple line); $\gamma = 0.003$ (blue line) and $\gamma = 0.001$ (green/first horizontal wavy line) and with (b): $(x_0, y_0) = (-2, 0)$ and for $\gamma = 0.03$ (green/last vertical wavy line); $\gamma = 0.01$ (purple line); $\gamma = 0.003$ (blue line); $\gamma = 0.001$ (aquamarine line) and $\gamma = 0$ (red/first horizontal wavy line).

Chapter 3

Connection Between γ and the Friction Coefficients, α and α'

3.1 Introduction

In this chapter by fitting the finite-temperature trajectories, we found connections between the phenomenological damping parameter γ and friction coefficients α and α' . We present these friction coefficients as a function of the vortex initial position together with the vortex precession frequency and period as a function of dissipation and the vortex initial position.

3.2 Schwarz Equation

A mathematical model for the motion of a quantised vortex line was presented by Schwarz (Schwarz, 1982, 1988). To obtain the Schwarz equation, we have to define the Magnus force together with a drag force. They play a key part in describing the motion of a line vortex.

Magnus Force and Drag Force

In Figure 3.1 a quantised vortex filament is represented as $\mathbf{s} = \mathbf{s}(\xi, t)$, where ξ is the arc length and t is the time. The vectors \mathbf{s}' , \mathbf{s}'' and $\mathbf{s}' \times \mathbf{s}''$, are perpendicular to each other and have tangent, normal and binormal directions. In this notation, prime denotes derivative with respect to ξ .

Using the Magnus force, which is a lift force, we derive the velocity, \mathbf{v}_L of the curve of vortex line at the point \mathbf{s} . When the vortex line moves in the flow on one side of the filament, the circulation creates an increased velocity, which causes the pressure to decrease. On the other side of the filament, the velocity decreases and the pressure increases, which corresponds to the opposite situation. As a consequence of the Magnus force, the direction of motion is reversed. This force per unit length on a vortex filament is

$$\mathbf{F}_M = \rho_s \Gamma \mathbf{s}' \times (\mathbf{v}_L - \mathbf{v}_s), \quad (3.1)$$

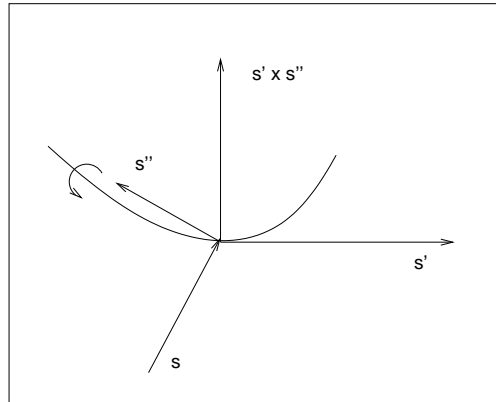


Figure 3.1: (Position (\mathbf{s}), tangent (\mathbf{s}'), normal (\mathbf{s}'') and binormal ($\mathbf{s}' \times \mathbf{s}''$) vectors for a vortex line. Here, $\mathbf{s} = \mathbf{s}(\xi, t)$, represent a space curve, which describe a quantised vortex filament and ξ is arc length and t is time. Prime denotes derivative with respect to ξ .

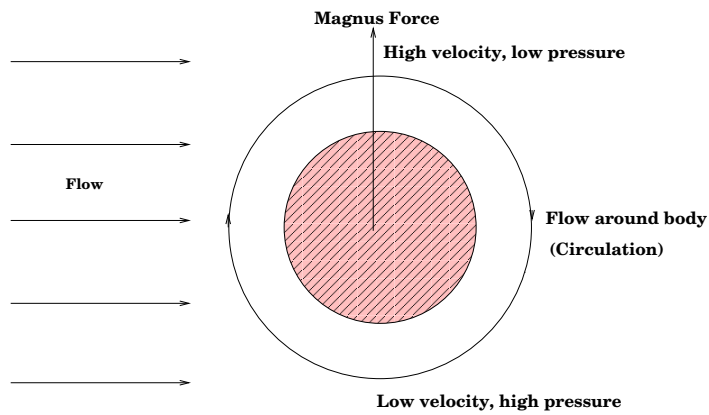


Figure 3.2: If a body moves in a fluid (or vice versa) circulation around the body forms. On one side of the body the total velocity is higher (hence the pressure is lower/ Bernoulli's Theorem) than the other side. The pressure difference causes the force transverse to the motion. So, for a body with circulation, the direction of motion is changed by the Magnus force.

where, the *circulation* Γ is defined by Eq. (1.2). If a vortex line moves through a normal fluid the absorption and scattering of phonons and rotons appears as a drag force

$$\mathbf{F}_D = -\alpha\rho_s\Gamma\mathbf{s}' \times \left[\mathbf{s}' \times (\mathbf{v}_n - \mathbf{v}_s) \right] - \alpha'\rho_s\Gamma\mathbf{s}' \times (\mathbf{v}_n - \mathbf{v}_s), \quad (3.2)$$

where α and α' are known (Hall & Vinen, 1956; Barenghi *et al.*, 1983) as temperature dependent mutual friction coefficients.

Equation of Motion

To develop the equation of motion, we use Newton's second law: $\mathbf{F} = m\mathbf{a}$. The vortex mass is zero, due to its very small core size. So,

$$\mathbf{F} = \mathbf{F}_M + \mathbf{F}_D = \rho_s\Gamma\mathbf{s}' \times (\mathbf{v}_L - \mathbf{v}_s) - \alpha\rho_s\Gamma\mathbf{s}' \times \left[\mathbf{s}' \times (\mathbf{v}_n - \mathbf{v}_s) \right] + \alpha'\rho_s\Gamma\mathbf{s}' \times (\mathbf{v}_n - \mathbf{v}_s), \quad (3.3)$$

$$\mathbf{F} = \rho_s\Gamma\mathbf{s}' \times \left[(\mathbf{v}_L - \mathbf{v}_s) - \alpha\mathbf{s}' \times (\mathbf{v}_n - \mathbf{v}_s) + \alpha'(\mathbf{v}_n - \mathbf{v}_s) \right] = 0. \quad (3.4)$$

The term in the square brackets, has the direction of \mathbf{s}' or is zero, then

$$\mathbf{v}_L = \frac{d\mathbf{s}}{dt} = \mathbf{v}_s + \alpha\mathbf{s}' \times (\mathbf{v}_n - \mathbf{v}_s) - \alpha'\mathbf{s}' \times \left[\mathbf{s}' \times (\mathbf{v}_n - \mathbf{v}_s) \right]. \quad (3.5)$$

3.3 Motion of Single Vortices with no Dissipation and with Different Dissipations

Our aim is to find a connection between the dissipation, γ and the friction coefficients α and α' . From the motion of single vortices (in our case, with initial positions: $(x_0, y_0) = (0.9, 0)$ and $(2, 0)$, where, x_0 is the distance from the centre) and their interactions with the normal fluid component, dissipation develops. The condensate is a quantum fluid and can absorb energy in quantised units corresponding to the excitations of the system.

Dissipation and viscosity/friction can arise just as a consequence of the creation of phonons. Let us, introduce our studied subject with the corresponding theory. The velocity of a vortex line at position \mathbf{S} is $\mathbf{v}_L = d\mathbf{S}/dt$. In the vortex filament model of Schwarz (Schwarz, 1982, 1988) the motion of a quantised vortex in superfluid helium is determined by the balance of Magnus and drag forces. The resulting equation for the vortex position, $\mathbf{s} = \mathbf{s}(t)$, is the Schwarz's equation:

$$\mathbf{v}_L = \mathbf{v}_s + \mathbf{v}_{si} + \alpha\mathbf{s}' \times (\mathbf{v}_N - \mathbf{v}_s - \mathbf{v}_{si}) - \alpha'\mathbf{s}' \times \left[\mathbf{s}' \times (\mathbf{v}_N - \mathbf{v}_s - \mathbf{v}_{si}) \right]. \quad (3.6)$$

where, \mathbf{v}_N is the externally applied normal fluid velocity, \mathbf{v}_s is the externally applied superfluid velocity, \mathbf{v}_{si} is the self-induced velocity of the vortex line due to its own curvature and \mathbf{s}' is the unit vector along the vortex line at \mathbf{s} .

Let, $\mathbf{v}_N = \mathbf{v}_s = 0$, and consider a point vortex on the plane (x, y) . Let $\mathbf{v}_{si} = \omega r \hat{\theta}$, where, ω is measured in a trap at temperature, $T = 0$ for $\gamma = 0$. So we have:

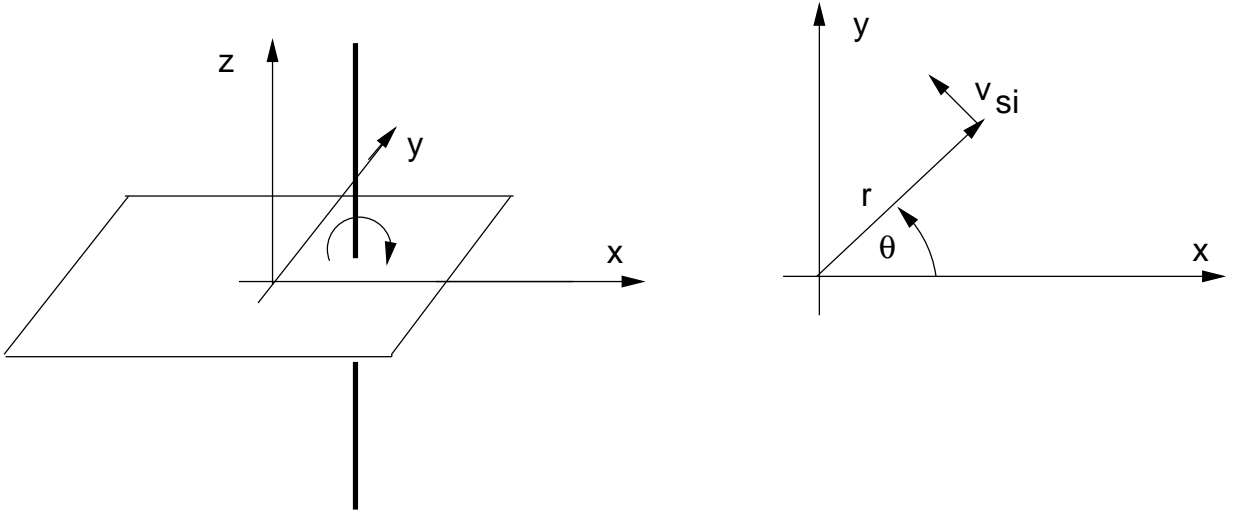


Figure 3.3: A single vortex rotation and the self-induced velocity of the line due to its own curvature.

$$\mathbf{v}_L = \mathbf{v}_{si} + \alpha \hat{\mathbf{z}} \times (-\mathbf{v}_{si}) - \alpha' \hat{\mathbf{z}} \times [\hat{\mathbf{z}} \times (-\mathbf{v}_{si})]. \quad (3.7)$$

To obtain the vortex line velocity, we use cylindrical coordinates, $\mathbf{s} = (r, \theta, z = 0)$ and due to the fact that the vortex spins around with angular velocity, ω , our final formula becomes:

$$\mathbf{v}_L = \omega r \hat{\theta} + \alpha \omega r \hat{\mathbf{z}} \times \hat{\theta} - \alpha' \omega r \hat{\mathbf{z}} \times [\hat{\mathbf{z}} \times \hat{\theta}]. \quad (3.8)$$

Rearranging, we find:

$$\mathbf{v}_L = \omega r \hat{\theta} + \alpha \omega r \hat{\mathbf{r}} - \alpha' \omega r \hat{\theta}. \quad (3.9)$$

or

$$\mathbf{v}_L = \omega r (1 - \alpha') \hat{\theta} + \alpha \omega r \hat{\mathbf{r}}. \quad (3.10)$$

Since

$$\mathbf{v}_L = (\dot{r}, r\dot{\theta}, 0) = \left(\frac{d\mathbf{r}}{dt}, \mathbf{r} \frac{d\theta}{dt}, 0 \right), \quad (3.11)$$

we obtain:

$$\frac{d\mathbf{r}}{dt} = \alpha \omega \mathbf{r}, \quad \mathbf{r} \frac{d\theta}{dt} = \omega r (1 - \alpha') \Rightarrow \frac{d\theta}{dt} = \omega (1 - \alpha'). \quad (3.12)$$

So the exact solutions are:

$$\mathbf{r}(t) = \mathbf{r}(0) e^{-\alpha \omega t}, \quad \theta(t) = \theta(0) + \omega (1 - \alpha') t. \quad (3.13)$$

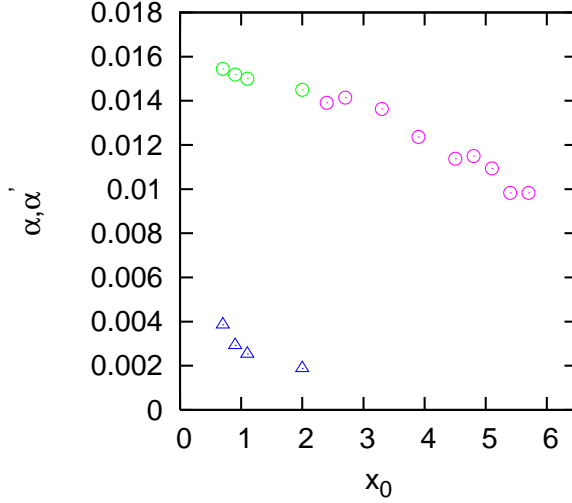


Figure 3.4: Friction coefficient α (circles) and α' (triangles) as a function of initial position ($x_0, y_0 = 0$) for $\gamma = 0.003$.

In two - dimensions, $\mathbf{s} = (x, y)$ and $\mathbf{s}' = \hat{\mathbf{z}}$, where $\hat{\mathbf{z}}$ is the unit vector along the z axes. In our case, \mathbf{v}_{self} is the precessing velocity of the vortex in trap in the absence of thermal cloud.

So, assuming $\mathbf{v}_s = 0$ and $\mathbf{v}_n = 0$ (stationary thermal cloud) and using cylindrical coordinates (r, θ) , the solution to the Schwarz's equation becomes:

$$r(t) = r(0)e^{-\alpha\omega t}, \quad \theta(t) = \theta(0) + \omega(1 - \alpha')t. \quad (3.14)$$

By fitting the calculated vortex position (at given value of γ) to Eqs. 3.14, we deduce the friction coefficients α and α' . The results slightly depends on the initial position of the vortex because the condensate is not homogeneous near the edge.

Figure 3.4, see also the values of α in Appendix C (Table C.2 and Table C.3), show that the deduced values of α is approximately constant for $x_0 < 2$ (centre part of the condensate) and decreases more rapidly for $x_0 > 2$ (outer part of the condensate).

For initial condition sufficiently close to the centre of the condensate, we find that α is proportional to the dissipation parameter γ , as shown in Figure 3.12(a).

The transverse friction coefficient, α' , is much smaller than α , thus more difficult to determine. Figure 3.12(b) shows that α' is approximately proportional to γ only for small values of γ .

3.4 Motion of Single Vortices Having Different Initial Positions for $\gamma = 0.003$

With the help of a numerical Condor software development (*Condor method*), we run simultaneously many programs; here 20. Actually, we use this method, when we calculate the sound and vortex energy for the case of no dissipation and with dissipation as well. However, at that time, there are 4340 programs running simultaneously. The utility of this method can be explained with the fact that we can study how α and α' vary with different x_0 for a chosen γ .

We can do different combinations as well with these data to understand more factors describing α , α' , γ , x_0 , τ and ω . These are discussed in more detail in Appendix C. (See for example Table C.3, Table C.4, Table C.5, Table C.6 and Table C.7).

So, now let us begin with a study about the time variation of α and α' for different x_0 . The system is unstable in the beginning with large fluctuations, so it needs some relaxation time, up to about $t = 50$. (In Chapter 1., we pointed out that, the reason of these oscillations is that, when the vortex precesses, it generates sound waves, which, unable to escape the trap, are reabsorbed by the vortex). After that, the α and α' functions follow the modulation of the vortex cyclical motion, (see Figure 3.5(a)-Figure 3.5(f), and for the case of α' , see Figure 3.6(a)-Figure 3.6(c)).

As we increase x_0 , the fluctuation becomes more pronounced (compare Figure 3.5(b) with Figure 3.5(c)). Increasing x_0 further, we observe more significant modulations from the vortex periodical movements.

For the case of α' , we find that, close to the centre of the condensate where the system is more dense, α' is constant with small fluctuations ; see Figure 3.6(a). For larger x_0 , the α' function has a trend to increase with time, until the vortex leaves the condensate, (see Figure 3.6(b) and Figure 3.6(c)).

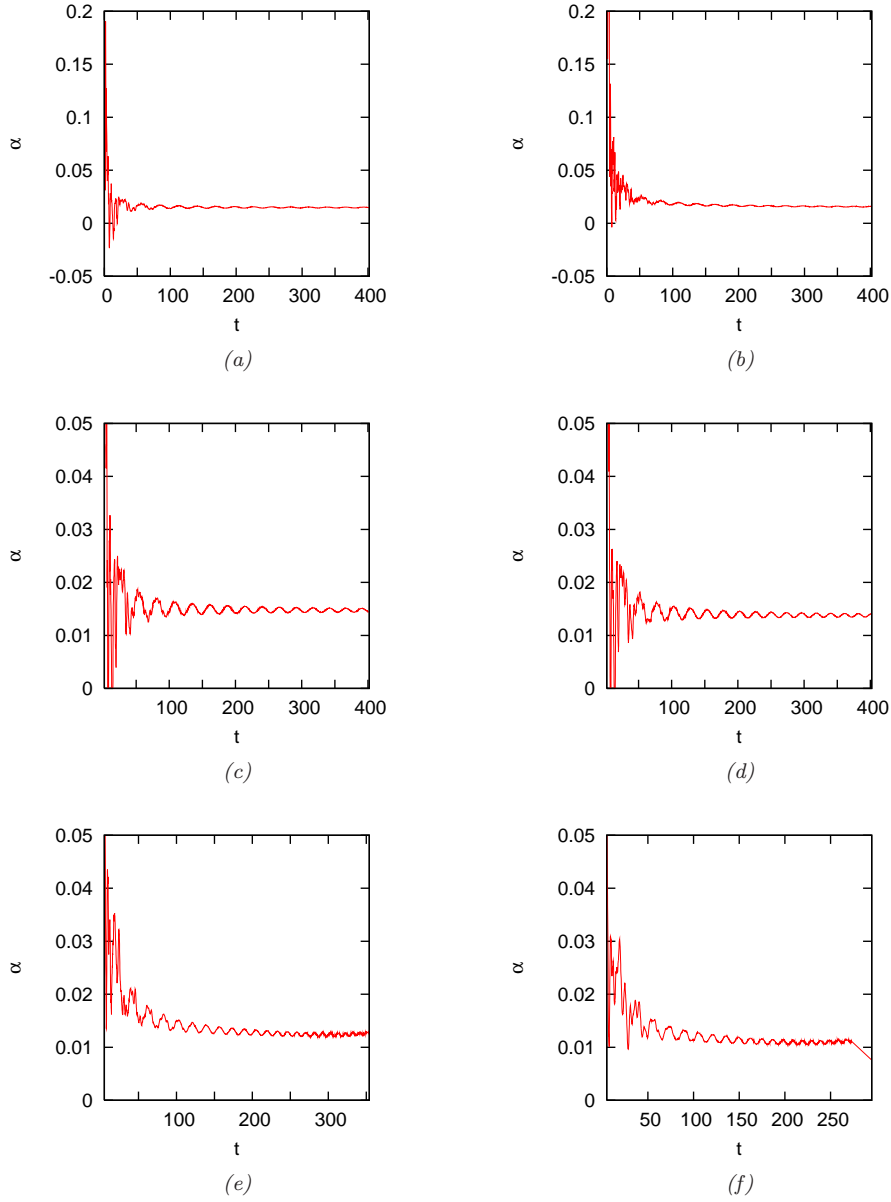


Figure 3.5: Friction coefficient α as a function of time for a single vortex for $\gamma = 0.003$ and for $x_0 = 0.9$ (a); 1.5 (b); 1.8 (c); 2.4 (d); 3.9 (e) and 4.5 (f).

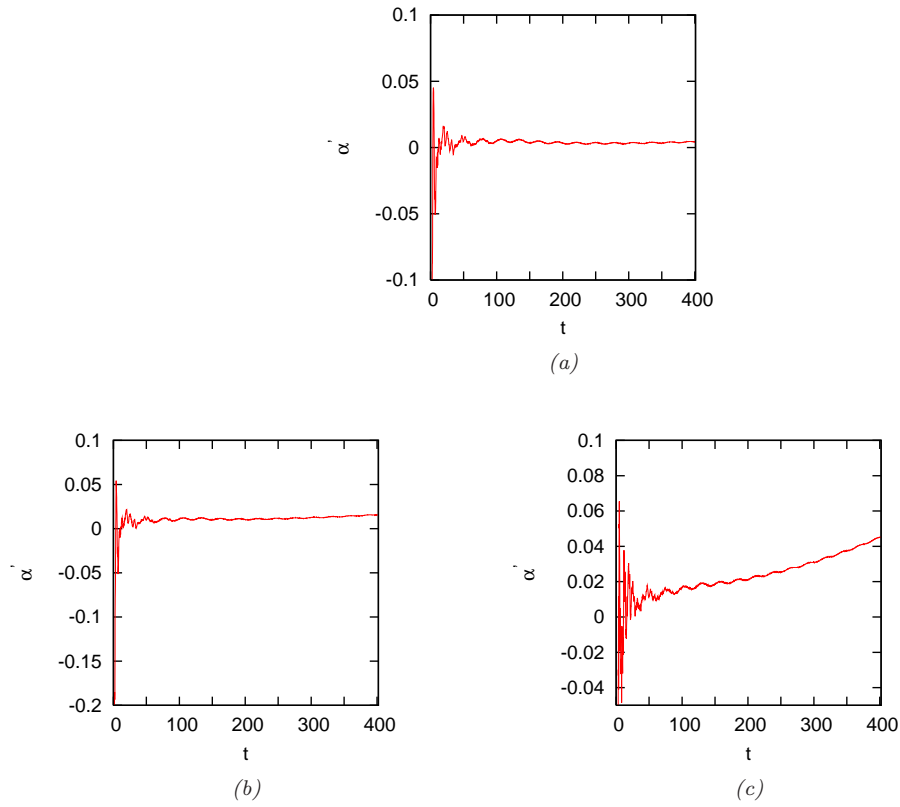


Figure 3.6: Friction coefficient α' as a function of time for a single vortex for $\gamma = 0.003$ and for $x_0 = 0.6$ (a); 0.9 (b) and 1.5 (c).

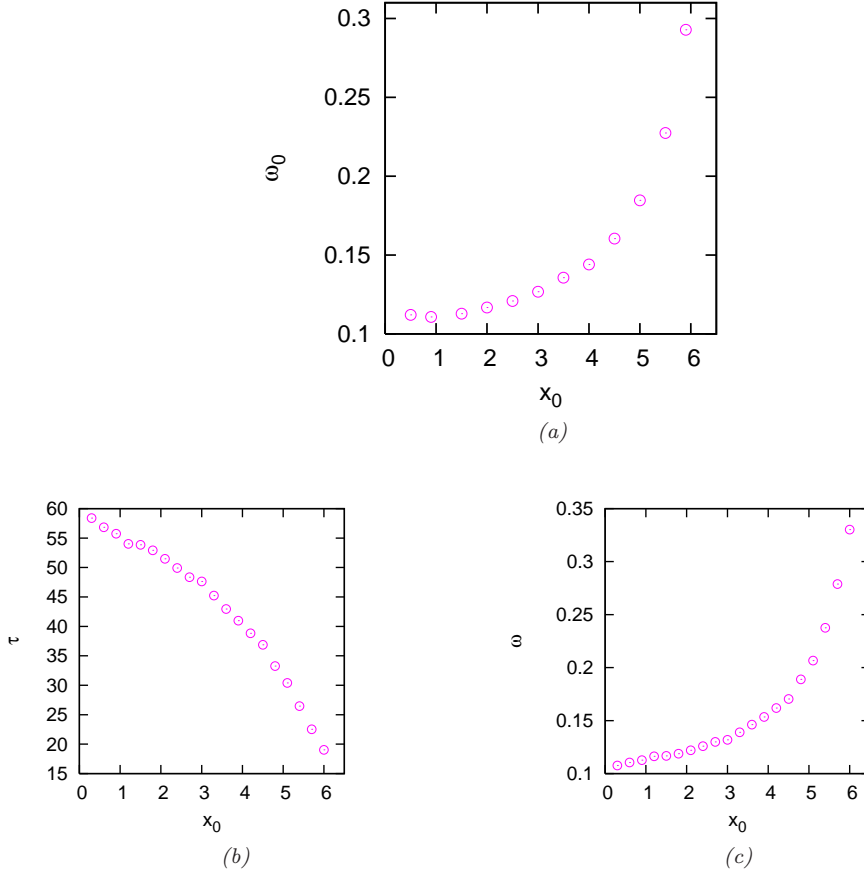


Figure 3.7: (a): Precession frequency, ω_0 as a function of initial positions, $(x_0, 0)$ for a vortex, which orbits the trap in absence of dissipation for $C = 2000$. (b,c): (left): period and (right): frequency of the first circle of motion as a function of initial positions, $(x_0, 0)$ for a single vortex for $\gamma = 0.003$.

First of all, to see the effect of dissipation on the vortex precession frequency, our strategy is to compare a plot of ω_0 vs x_0 without dissipation (see Figure 3.7(a)) with a plot of ω vs x_0 with dissipation (see Figure 3.7(c)). The frequency is calculated from $\omega = 2\pi/\tau$, which means an inverse relation between the period and frequency (see Figure 3.7(b) and Figure 3.7(c) together with Table C.6 and Table C.7).

The variation of ω_0 with γ is investigated in Figure 3.8. The precession frequency can be compared to the expression obtained by Svidzinsky and Fetter, see (Svidzinsky & Fetter, 2000b), using a time-dependent variational analysis.

$$|\omega| = \frac{3\hbar\omega_x^2}{4\mu} \ln\left(\frac{R_\perp}{\xi}\right), \quad (3.15)$$

where ω_x is the x -component of the trap frequency, μ is the chemical potential, $R_\perp^2 = 2\mu/m\omega_x^2$ and here $\xi = \hbar/(2m\mu)^{1/2}$, is the coherence length in the center of the condensate. This expression is valid for small initial position of the vortex.

In our calculations, we have used the first significant circle-like trajectory to calculate the

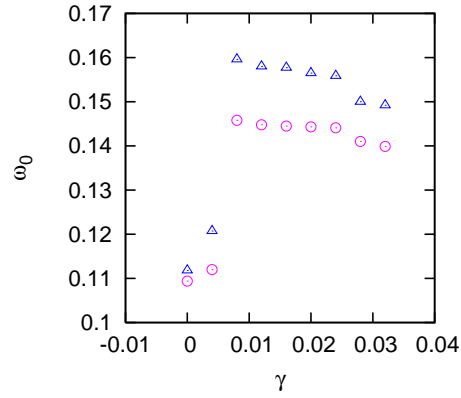


Figure 3.8: Vortex precession frequency, ω_0 for a single vortex with $(x_0, y_0) = (0.9, 0)$ (circle) and $(1.45, 0)$ (triangle) as a function of γ .

γ	α' (for $x_0 = 0.9$)	α' (for $x_0 = 1.45$)
0	0.018604	0.024306
0.004	0.018527	0.024092
0.008	0.018610	0.024320
0.012	0.018602	0.024314
0.016	0.018617	0.024364
0.02	0.018001	0.024323
0.024	0.018613	0.024313
0.028	0.018905	0.024683
0.032	0.018982	0.024624

Table 3.1: Friction coefficient α' as a function of dissipation, γ corresponding to Figure 3.8.

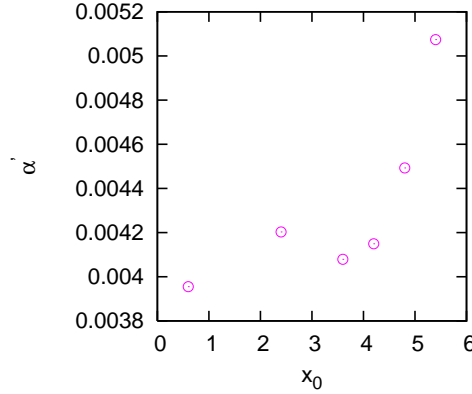


Figure 3.9: Friction coefficients α' for a single vortex vs initial positions $x_0 = 0.6$ (0.1098); 2.4 (0.132); 3.6 (0.2038); 4.2 (0.226); 4.8 (0.25); 5.4 (0.2855). (We have the frequency of motion in the bracket), ($y_0 = 0$) and for $\gamma = 0.003$. Here, we compare the values of α' for different initial positions but for almost the same times, (which vary between 313.61 and 401.63).

period and frequency. Our conclusion is that, in the beginning with small dissipation, the vortex moves similarly to the case of without dissipation.

Our observation is that, α decreases linearly with x_0 (see Figure 3.4, Table C.2 and Table C.3). Here again, we would like to point out that, the density is not constant in the whole condensate. Keeping the period of motion of the single vortex nearly constant, α' varies similarly with x_0 as ω varies with x_0 (compare Figure 3.7(c) with Figure 3.9). This variation is an exponential behaviour. So, close to the centre of the condensate, α' is small and close to the border, the values of α' increase as an exponential function (see Figure 3.9), where in parenthesis we note the corresponding frequency of vortex motion for each initial position).

3.5 Motion of Single Vortices with Different γ 's

Now, our vortices have as initial positions: $(x_0, y_0) = (0.9, 0)$ and $(1.45, 0)$. As one can see, we continue our study of α and α' vs t with larger dissipation, $\gamma = 0.016$ and $\gamma = 0.032$. Comparing Figure 3.10(c) with Figure 3.10(d), we note that for larger dissipation, the modulation from the vortex cyclical motion is more significant close to the centre. In conclusion, increasing the dissipation, for example to $\gamma = 0.032$ and for $x_0 = 1.45$, the modulation disappears.

We notice that for every γ , the α function tends to decrease with time and later to be constant, (see Figure 3.10(e)).

Let us see the effect of larger γ on the other friction coefficient, α' . After a short initial instability, until about $t = 20$ (this time is shorter than the time for smaller dissipation), α' increases until the vortex leaves the condensate (see Figure 3.11(c), Figure 3.11(d), Figure 3.11(e) and Figure 3.11(f)). Further, we note that for $\gamma = 0.016$ and $x_0 = 1.45$, the function α' begins its steeper increase earlier. If we increase the dissipation further, say $\gamma = 0.032$, we observe that the fluctuations due to the instability in the beginning are weaker and α' increases from larger

negative values to its positive final value. This last value depends on the time at which the vortex leaves the system.

Finally, let us finish our study about α and α' with the case of no dissipation, $\gamma = 0$. Both α and α' oscillate in the beginning with large fluctuations, which later transform to small fluctuations. For α , our observation is that for $(x_0, y_0) = (0.9, 0)$, the function becomes constant at an earlier time with a value of $\alpha = 0.0064$, (see Figure 3.10(a)), than in the case of $(x_0, y_0) = (1.45, 0)$, when this constant is $\alpha = 0.0035$, (see Figure 3.10(b)). In the beginning, the second friction coefficient, after some impulsive oscillations both with negative and positive values, become constant too, for $t \approx 50$. For $x_0 = 0.9$, $\alpha' = 0.01194$ and for $x_0 = 1.45$, $\alpha' = -0.02431$, with a very weak, similar modulation pattern. When $\gamma = 0$, it is always true that the system is dominated by short time fluctuations.

The friction coefficient, α increases linearly with γ , (see Figure 3.12(a) and Figure 3.13). Having more values of γ , we have noticed that for smaller γ 's, α' increases more rapidly, and from about $\gamma = 0.0125$ (see Figure 3.12(b)) α' decreases weakly. These observations are valid for both $(x_0, y_0) = (0.9, 0)$ with $\omega = 0.11; 0.115$ and $(x_0, y_0) = (1.45, 0)$ with $\omega = 0.1171; 0.1125$.

As we have indicated earlier, our simulation program is very flexible, so it permits us to study the variation of α' with γ using nearly the same frequency of motion; see Figure 3.14. Placing our vortex in the same initial position $(x_0, y_0) = (0.9, 0)$ and having almost the same frequency of motion, ω , we observe that α' varies linearly with γ . We have created an ideal situation which is useful in our study and shows us that there is a linear relation between α' and γ in that case; see Figure 3.14. This observation is really important due to the fact that α' is not so easy to study. Its value is very small and in most studies, one often neglects it, (see Tsubota *et al.* (2000); Araki *et al.* (2003)).

Let us continue our investigation about the motion of a single vortex with different dissipations γ and examine the connection between ω and γ . So, for smaller values of γ and for about $\gamma = 0.0075$ with these conditions, the variation of ω with dissipation increases strongly. We are interested to see the development of frequency with dissipation. The first step is to examine our understanding about the period of motion τ vs γ ; see Figure 3.15. With dissipation, the trajectory permanently changes, so we have used the data from the first significant circle-like trajectory. Our plot shows that τ decreases with dissipation in two steps; see Figure 3.15. Until $\gamma \approx 0.03$ it decreases slightly, but above this value, its change has a more inclined character. The same comment is valid for the frequency of motion of the trajectory vs dissipation, but in that case the function ω increases due to the fact that $\omega = 1/\tau$ (see Figure 3.15(b)).

3.5.1 Radial Position of Single Vortices as a Function of Time

Connection between dissipation and vortex initial position

In our simulations, with the help of x - and y -coordinates of the trajectory, we also have information about the radius, r of the path, $r = \sqrt{x^2 + y^2}$. From our plots we have observed that $r = r_0 e^{\Gamma_1 t}$, where Γ_1 is an exponential coefficient. In the following plots, we show a connection

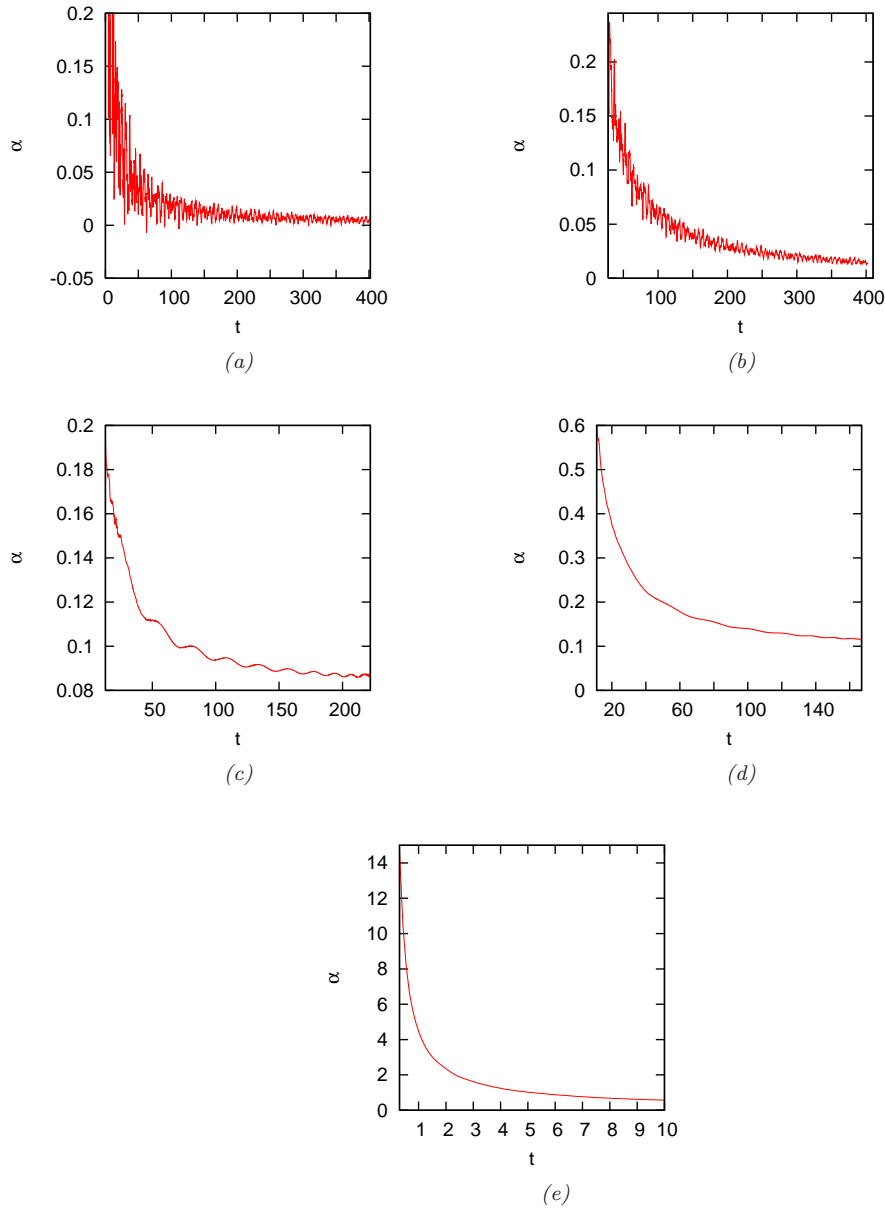


Figure 3.10: Friction coefficient α as a function of time for a single vortex for (left): $(x_0, y_0) = (0.9, 0)$ and (right): $(x_0, y_0) = (1.45, 0)$. for (a,b): $\gamma = 0$ and for (c,d): $\gamma = 0.016$ and for (e): $\gamma = 0.032$ and for $(x_0, y_0) = (1.45, 0)$.

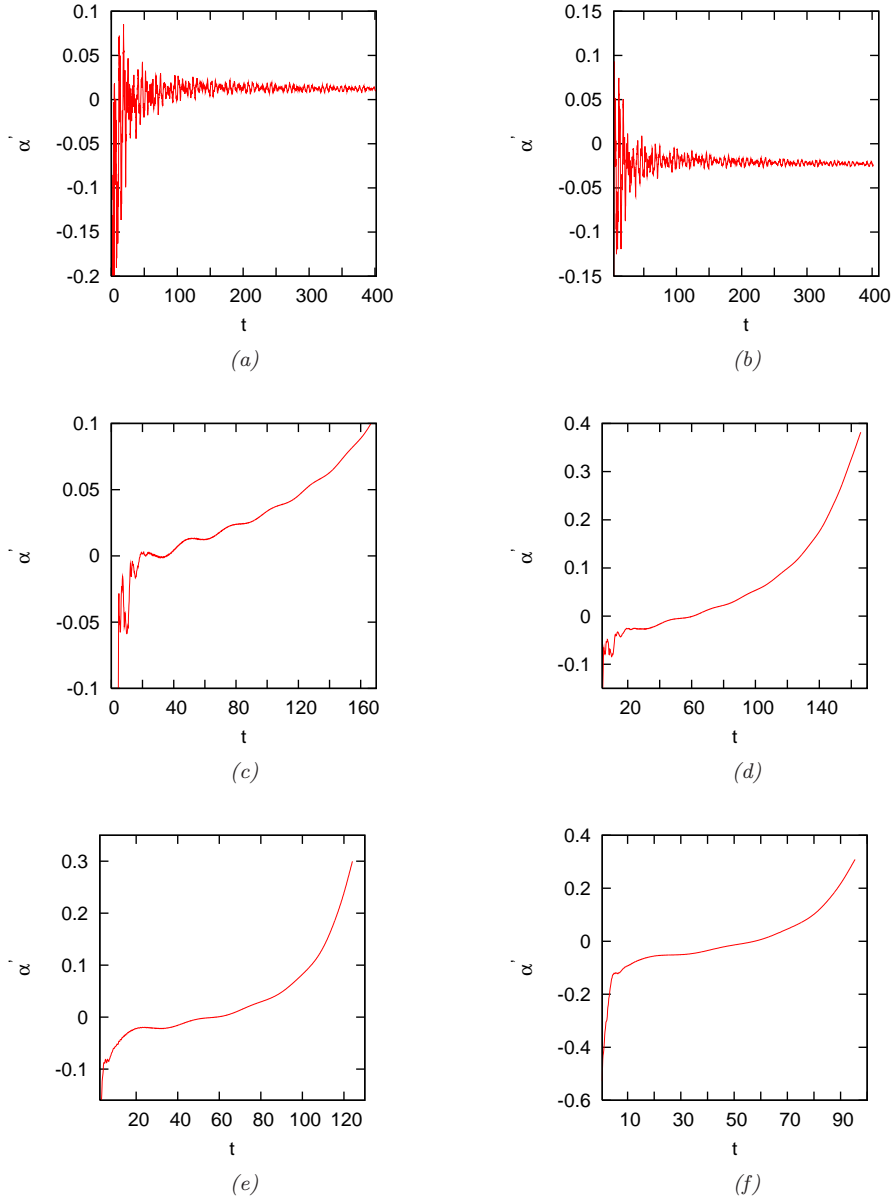


Figure 3.11: Friction coefficient α' as a function of time for (left): $(x_0, y_0) = (0.9, 0)$ and for (right): $(x_0, y_0) = (1.45, 0)$ for (a,b): $\gamma = 0$, for (c,d): $\gamma = 0.016$ and for (e,f): $\gamma = 0.032$.

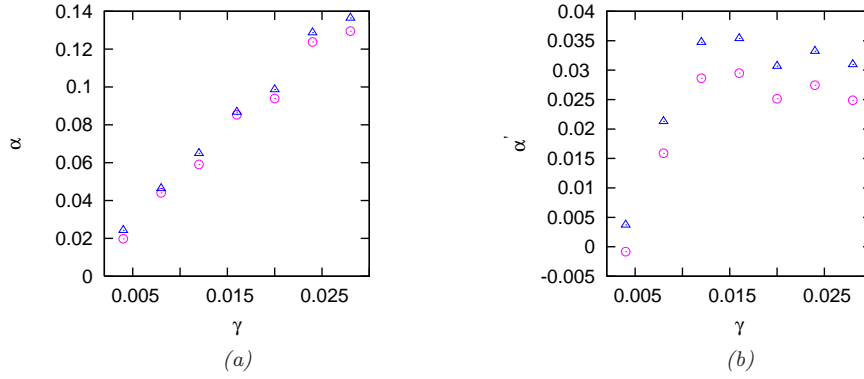


Figure 3.12: (a): Friction coefficient α for a single vortex with initial position $(x_0, y_0) = (0.9, 0)$ (triangles) and $(x_0, y_0) = (2, 0)$ (circles) as a function of γ . The linear fit for α is: $\alpha = c_1 + c_2\gamma$, where $c_1=0.007$ and $c_2=5.092$. (b): Friction coefficient α' corresponding to Figure. 3.11(a).

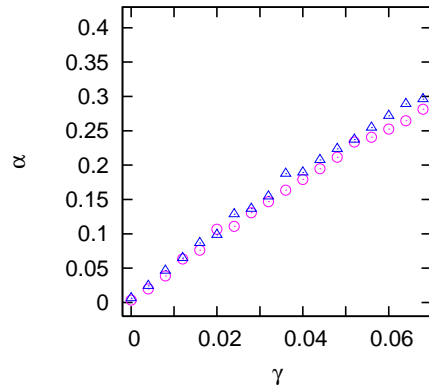


Figure 3.13: Friction coefficients α as a function of γ for a single vortex with initial positions, $(x_0, y_0) = (0.9, 0)$ and $(1.45, 0)$. Triangles represent the case when $(x_0, y_0) = (1.45, 0)$ and circles represent the case for $(x_0, y_0) = (0.9, 0)$. The linear fit for α is: $\alpha = c_1 + c_2\gamma$, where $c_1=0.007$ and $c_2=4.44$.

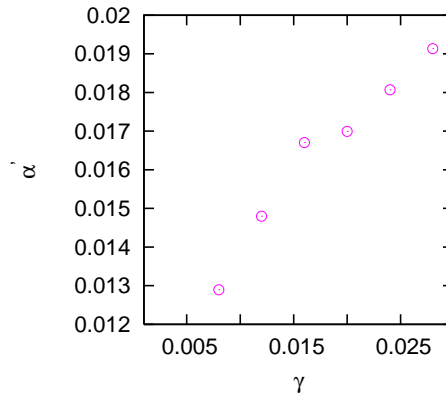


Figure 3.14: Friction coefficients α' for a single vortex with $(x_0, y_0) = (0.9, 0)$ and for dissipations, $\gamma = 0.008$ (0.1459); 0.012 (0.1459); 0.016 (0.1465); 0.02 (0.1416); 0.024 (0.1453); 0.028 (0.1413). The numbers in the paranthesis are the frequencies of motion, ω .

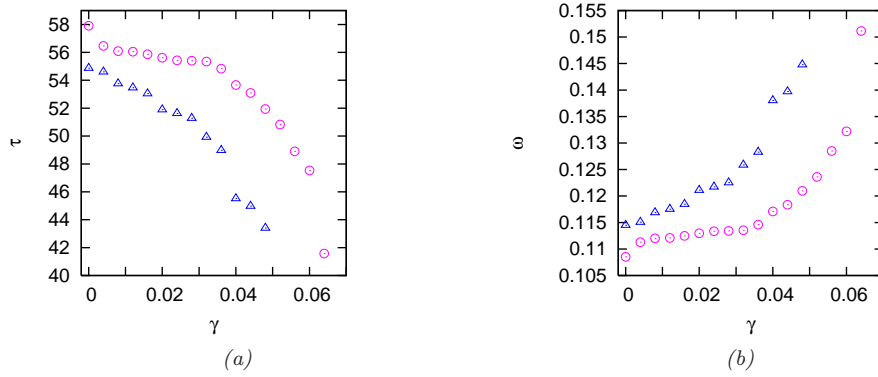


Figure 3.15: (a): Period, τ and (b): frequency, ω of the first circle like trajectory of motion for a single vortex with initial positions, $(x_0, y_0) = 0.9$ (circles) and with $(x_0, y_0) = 1.45$ (triangles).

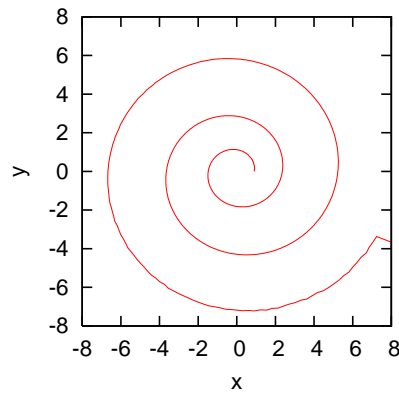


Figure 3.16: Trajectory for a single vortex with $(x_0, y_0) = (0.9, 0)$ and for $\gamma = 0.032$. We can see that in the end of its motion the vortex moves out to the border of the condensate.

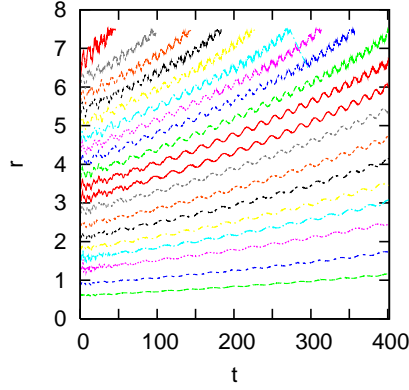


Figure 3.17: Radius of the trajectories as a function of time for a single vortex with initial positions, from bottom to top $x_0 = 0.6; 0.9; 1.2; 1.5; 1.8; 2.1; 2.4; 2.7; 3.0; 3.3; 3.6; 3.9; 4.2; 4.5; 4.8; 5.1; 5.4; 5.7; 6.0$, $y_0 = 0$ and for $\gamma = 0.003$.

between this exponential coefficient Γ_1 , the dissipations and also the vortex initial positions, x_0 (for $y_0 = 0$). From the plots of r vs t , we have calculated $\ln(r)$ vs t and the exponential constant, Γ_1 . So, from the plots we remark that r is an exponential function of time, t (see Figure 3.18(a) - Figure 3.18(d) and Figure 3.17).

For $\gamma = 0$, r does not exhibit an exponential behaviour in time. As we increase γ , the exponential function $r = r_0 e^{\Gamma_1 t}$, describes a steeper curve. Similar behaviour can be observed with the lines of $\ln(r)$, (see Figure 3.19(a) - Figure 3.20(d) and Figure 3.21(a) - Figure 3.21(d).)

From $\ln(r)$, we have calculated $\Gamma_1 = (\ln(r) - \ln(r_0))/t$. A linear increase of Γ_1 with dissipation γ is observed for both $(x_0, y_0) = (0.9, 0)$ and $(x_0, y_0) = (1.45, 0)$, (see Figure 3.22(a) and Figure 3.22(b) together with the corresponding values of the exponential constant, Γ_1 as a function of γ in Appendix C, Table C.8 and Table C.9). There are no significant differences between these two plots. Finally, we are interested to see the variation of Γ_1 in the whole condensate area, for the same dissipation $\gamma = 0.003$. For that purpose, we increase the initial position of the vortex from $(x_0, y_0) = (0.3, 0)$ to $(x_0, y_0) = (6, 0)$. The increase is very weak. On the contrary, close to the centre and the edge of the condensate, there are considerable changes, (see Figure 3.22(c) and the corresponding values of the exponential constant, Γ_1 as a function of x_0 in Appendix C, Table C.10).

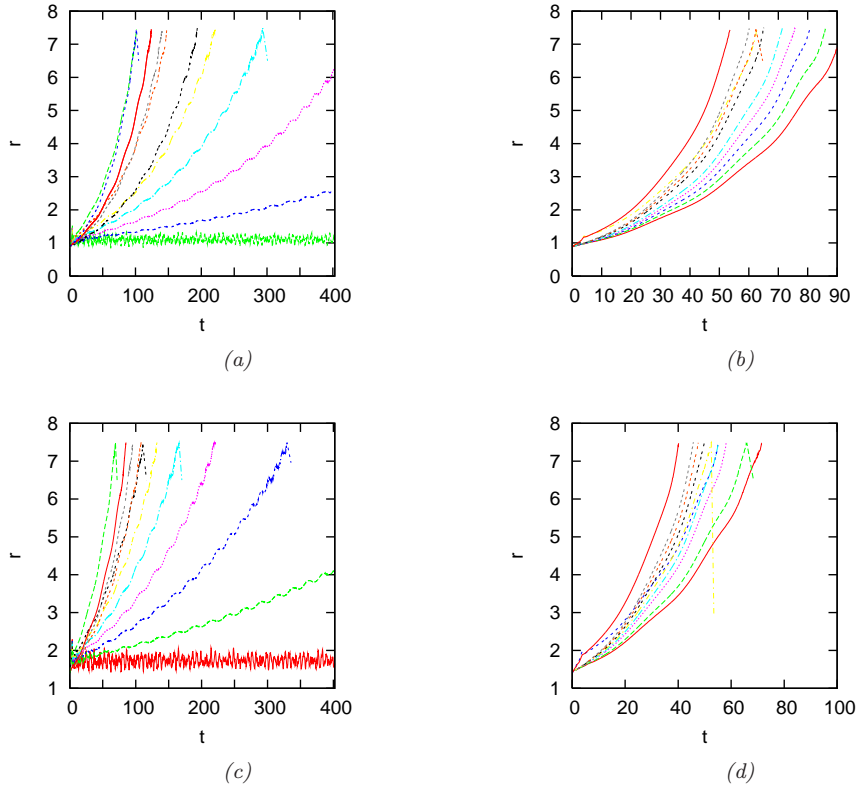


Figure 3.18: Radius of trajectories for a single vortex as a function of time with (a,b): $(x_0, y_0) = (0.9, 0)$ and with (c,d): $(x_0, y_0) = (1.45, 0)$ for dissipations (left): from the green(a)/red(c) horizontal line to the green curved line $\gamma = 0; 0.004; 0.008; 0.012; 0.016; 0.02; 0.024; 0.028; 0.032; 0.036; 0.04$ and (right): from the right red curved line to the left red curved line $\gamma = 0.044; 0.048; 0.052; 0.056; 0.06; 0.064; 0.068; 0.072; 0.076; 0.08$.

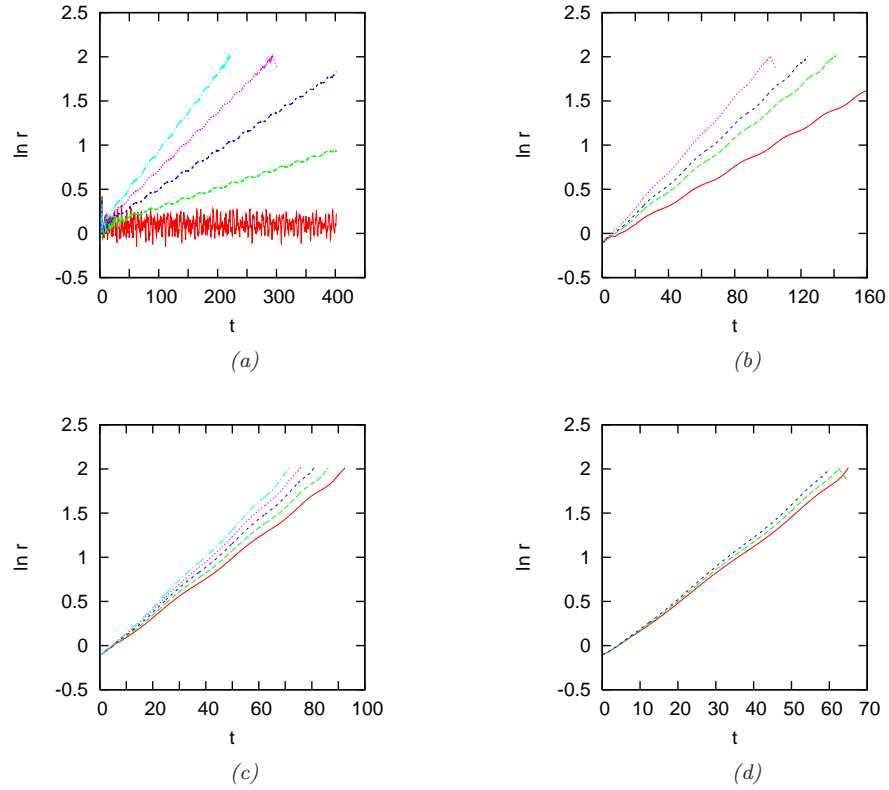


Figure 3.19: Log of radius of trajectories as a function of time for a single vortex with $(x_0, y_0) = (0.9, 0)$ and for dissipations from bottom red to top: (a): $\gamma = 0; 0.004; 0.008; 0.012$ and 0.016 and (b): $\gamma = 0.02; 0.028; 0.032$ and 0.04 and (c): $\gamma = 0.044; 0.048; 0.052; 0.056$ and 0.06 and (d): $\gamma = 0.068; 0.072$ and 0.076 .

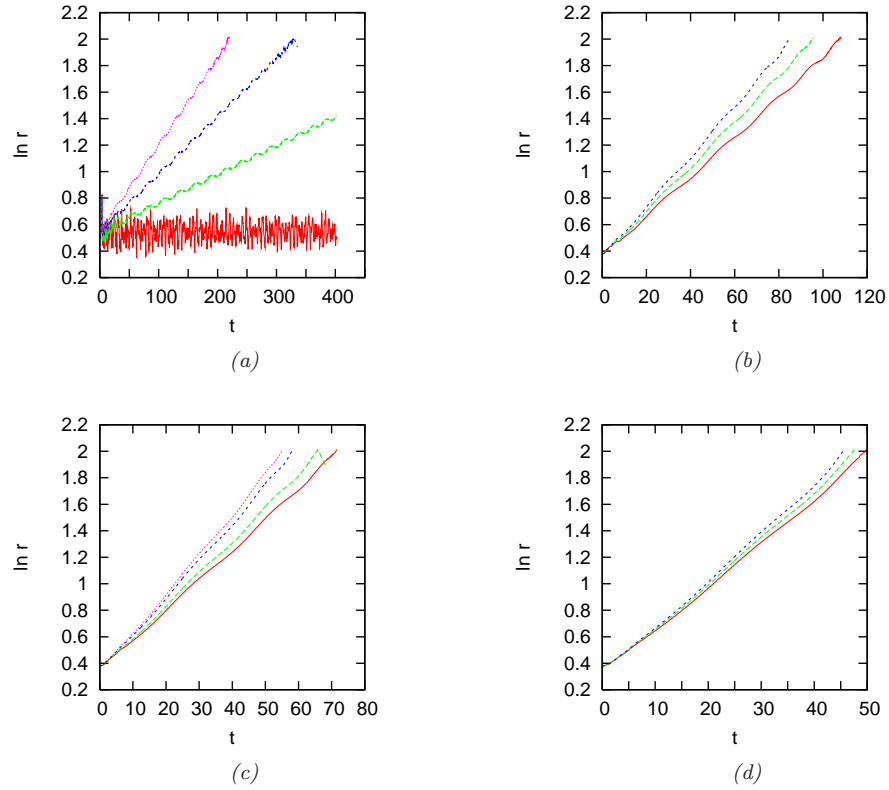


Figure 3.20: Log of radius of trajectories as a function of time for a single vortex with $(x_0, y_0) = (1.45, 0)$ and for dissipations from bottom red to top: (a): $\gamma = 0; 0.004; 0.008$ and 0.012 and (b): $\gamma = 0.028; 0.032$ and 0.036 and (c) $\gamma = 0.044; 0.048; 0.056$ and 0.06 and (d): $\gamma = 0.068; 0.072$ and 0.076 .

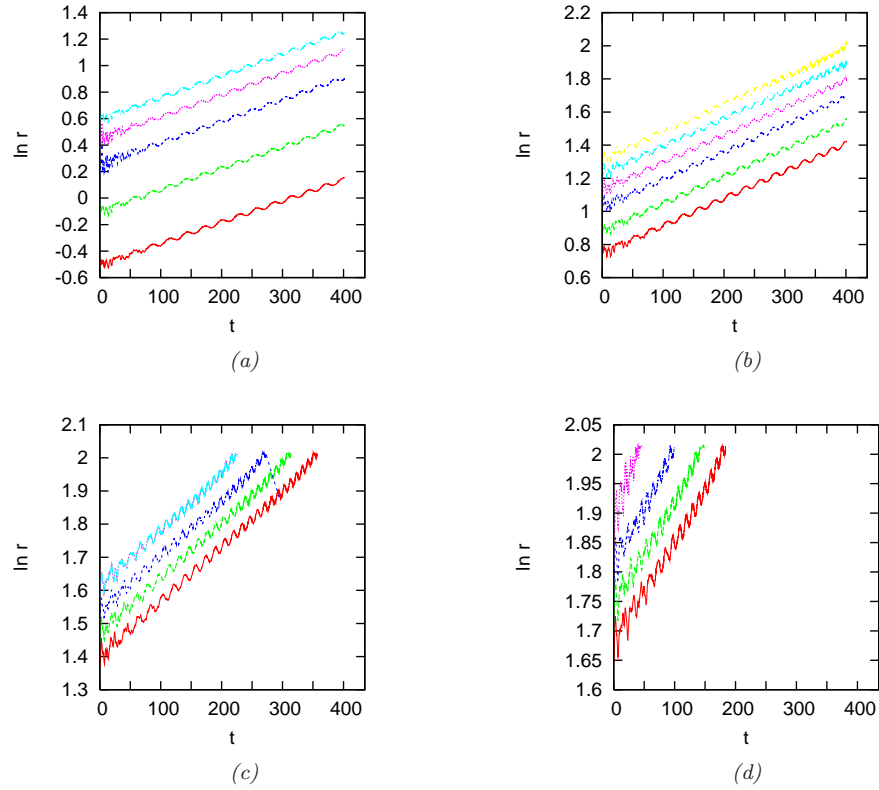


Figure 3.21: Log of radius of trajectories as a function of time for a single vortex for $\gamma = 0.003$ and with initial positions x_0 , from bottom red to top: (a): 0.6; 0.9; 1.2; 1.5; 1.8 and (b): 2.1; 2.4; 2.7; 3.0; 3.3; 3.6 and (c): 3.9; 4.2; 4.5; 4.8 and (d): 5.1; 5.4; 5.7; 6.0. ($y_0 = 0$ in every cases).

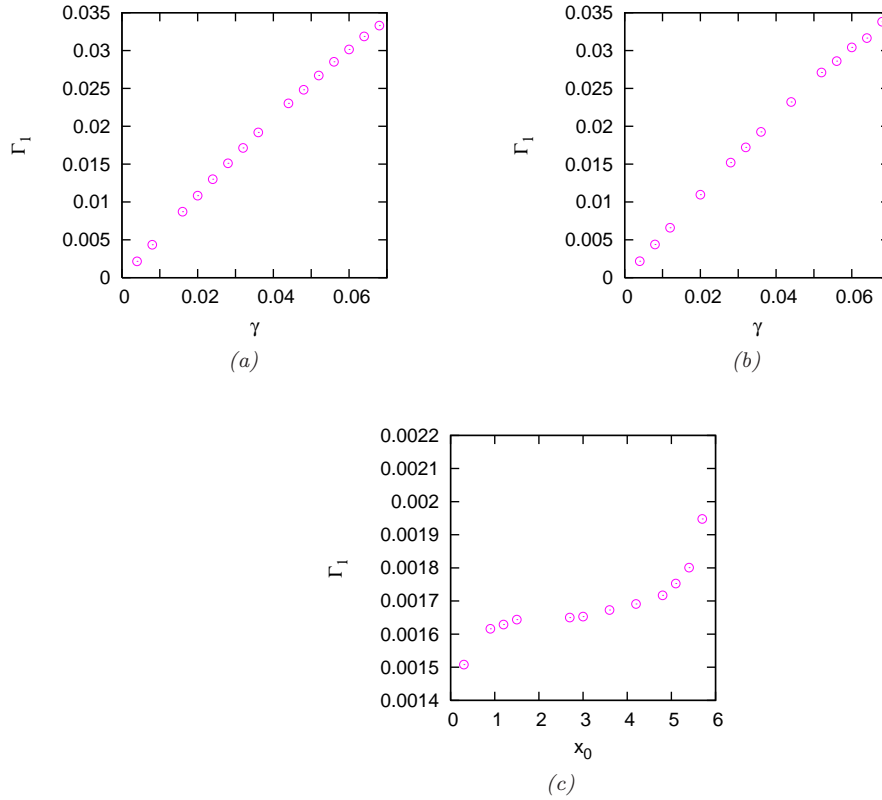


Figure 3.22: Exponential constant, Γ_1 of the radius of vortex trajectory as a function of γ for a single vortex with (a,b): (left): $(x_0, y_0) = (0.9, 0)$ and (right): $(x_0, y_0) = (1.45, 0)$ and (c) as a function of x_0 for $\gamma = 0.003$.

Chapter 4

Motion of Vortex - Anti Vortex Pair in a Trapped BEC

4.1 Introduction

Vortex -anti vortex pair is the 2D analogy of 3D vortex ring, which was observed by Anderson *et al.* (2001) and Dutton *et al.* (2001). The vortex ring motion is complicated due to the inhomogeneity of the condensate and the curvature of the vortex line, which contribute to the dynamics of the ring. A vortex structure displays both a dynamical instability of the vortices and the interactions that can happen between the vortices and fluid excitations, e.g. the sound field in the condensate, an induction from the anti-vortex et cetera.

Due to the dynamical instabilities, co-rotating vortex pairs and in homogeneous 2D superfluids, single vortices execute circular motions (Lundh & Ao, 2000; Vinen, 2001). They are considered to decay by way of sound wave emissions. With long-wavelength oscillatory modes, excitations can occur as Kelvin waves, which in superfluid dynamics, is a long scale perturbation mode of the vortex.

In this chapter among others, we study the sound energy together with other energies and show the anticorrelation between the sound and vortex energy. We calculate the vortex pair velocity with two methods. We investigate the period and frequency of motion for pair of vortices as a function of initial separation distance between vortices. We present the decay rate of the total energy as a function of time for a single vortex. Furthermore, we show that this decay rate decreases linearly with dissipation. We finish this chapter by presenting a connection between the fluid and vortex velocity.

4.2 Motion without Dissipation

Theoretically, we can estimate the precession frequency with an analytical approximation (Jackson, 1999). In our case, we use two methods to calculate the frequency of motion for a single vortex or for a vortex - anti vortex pair.

We put a pair of vortices in the condensate, (see Appendix D) at different initial separation distances on the line $y_0 = 0$. A vortex - anti vortex pair initially is located at $(\pm x_0, 0)$. The initial separation distance is $d_0 = x_0 - (-x_0) = 2x_0$, where x_0 is the vortex initial position. The first vortex in the vortex pair has a positive sign (it is a vortex) and moves from left to right, while the second one has a negative sign (it is an anti-vortex) and moves in the opposite direction, from right to left; see the snapshots of Figure 4.1(a) - Figure 4.1(f) for $d_0 = 0.8$.

It is also remarkable, that the pair follows a definite path periodically, which depends on the initial separation distance. From Figure(4.2(a) - 4.2(d)), where $d_0 = 2.86$, we note that the vortices are at the same place after $t = 35 * 36.648$ (which is a period) ≈ 1284 (in dimensionless units) seconds later, or when $d_0 = 0.8$, after $t = 28.8$ (which is one period) (in dimensionless units) seconds later; see Figure(4.3(a) - 4.3(b)).

Smaller initial separation distance causes the pair to translate faster. When the vortices meet the wall, they become forced to separate. There is some minimum distance at which the vortices can avoid annihilation. However, to be in the right domain and to have a large enough initial separation distance, we have chosen for the minimum distance to be $12h = 0.8$, and for the maximum distance, we have set $32h = 2.86$, where h is the space step, ($h = 0.0867$ h.o.u.).

Without dissipation the trajectory is almost the same as in the beginning (see Figure 2.8(a) (the red/centre path)). So, the vortices follow the same paths and have almost the same positions after a few periods have elapsed (see Figure 4.4(a) and Figure 4.4(b)), which demonstrate that the vortex - anti vortex pair (here one of them) has almost the same amplitude for the x - and y -component of the trajectory. We can see another example with $d_0 = 1.0$ and 1.43 , see Figure(4.6(a) - 4.6(d)). Observe the relation between the initial separation distance d_0 and the influence of the condensate edge, especially when $d_0 = 1.43$. When the vortices change their direction or meet each other, fluctuations appear, which are sound waves due to the density fluctuations.

It is instructive to compare the trajectory of one vortex with the trajectory of one of the vortices from the vortex pair, see Figure 4.5(a). So, we put the vortices in the vortex - anti vortex pair symmetrically to the *Origin* on the same position, where our one vortex was. Comparing their trajectories, we observe that, the pair moves together on a longer path, (compare Figure 4.5(a) with Figure 2.2(a)). The single vortex needs more times and more cyclical motions to go out to the edge of the condensate, see Figure 2.2(a) and Figure 2.3(a).

So, we observe that for a single vortex, the path has a more circular shape. Actually, from Figure(1.1(a) - 1.1(b)), we can see the influence of the antivortex as well. In that case, the trajectory becomes larger in the y -direction. Another important feature exhibited by the two vortices is that in the beginning, they move in parallel because of the opposite signs they possess. So, initially, the pair moves across the condensate. When the pair approaches the edge of the condensate, the two vortices separate, and move back toward the opposite side of the condensate, thus making a closed orbit before returning to the initial position, as showed in Figure 1.1(b).

As a result of the cyclical motion and the inhomogeneity of the condensate, the compressibility is changed, and so the moving vortex pair produce acoustic emission. Let us now study the sound

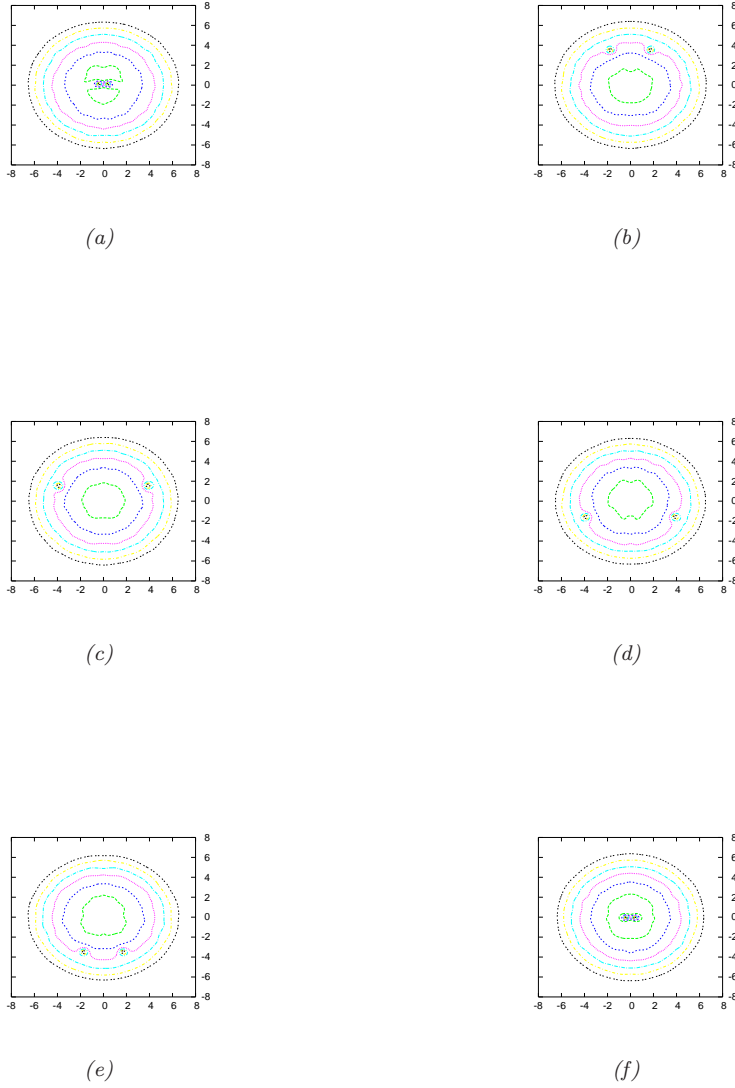


Figure 4.1: Contourplot of the density for a vortex - antivortex pair for $d_0 = 0.8$, $\rho_{max} = 0.012$, and with levels: 0.01, 0.008, 0.006, 0.004, 0.002, (the levels decrease as you move outwards) at times: (a): $t = 87.2$, (b): $t = 93$, (c): $t = 98.8$, (d): $t = 104.4$, (e): $t = 110.2$ and (f): $t = 116$.

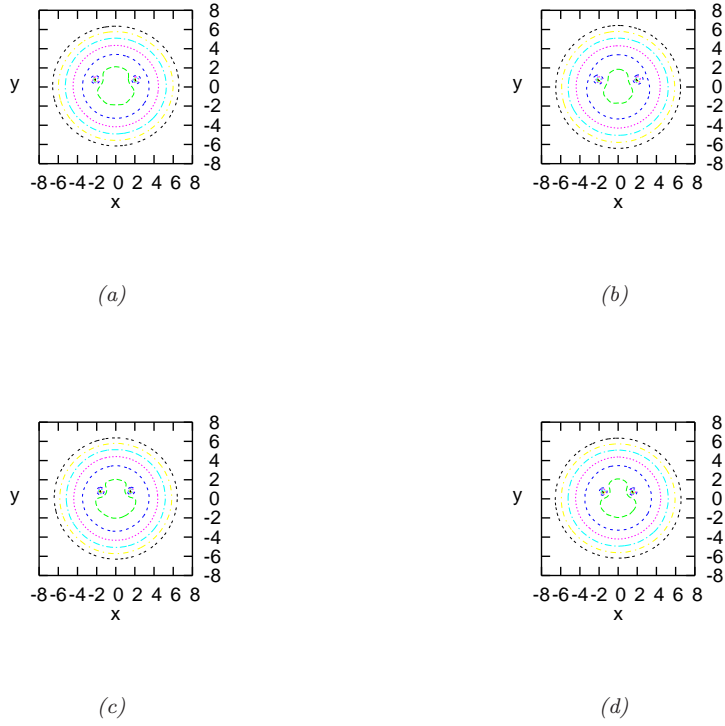


Figure 4.2: Contourplot of the density for a vortex - antivortex pair for $d_0 = 2.86$, $\rho_{max} = 0.012$, and with levels: 0.01, 0.008, 0.006, 0.004, 0.002, (the levels decrease as you move outwards) at times: (a): $t = 50$, (b): $t = 1334$, (c): $t = 750$ and (d): $t = 2034$.



Figure 4.3: Contourplot of the density for the vortex - antivortex pair corresponding to Figure 4.2 at time (a): $t = 0.2$ and at time (b): $t = 29$.

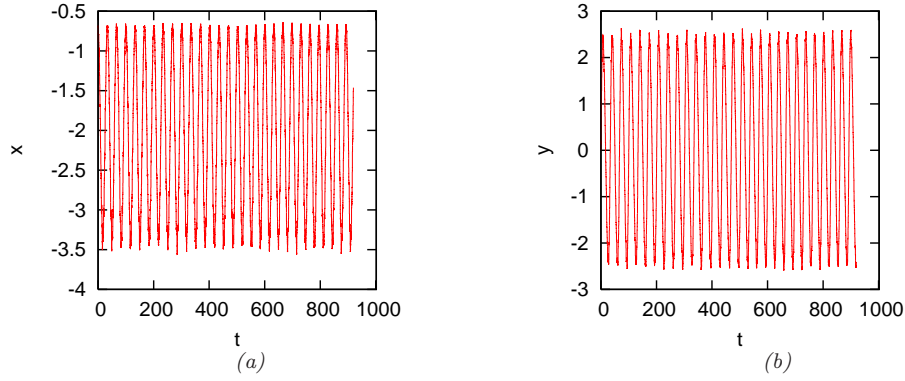


Figure 4.4: (a): x -component and (b) y -component of the trajectory as a function of time for one of the vortices in the vortex pair for $d_0 = 1.8$.

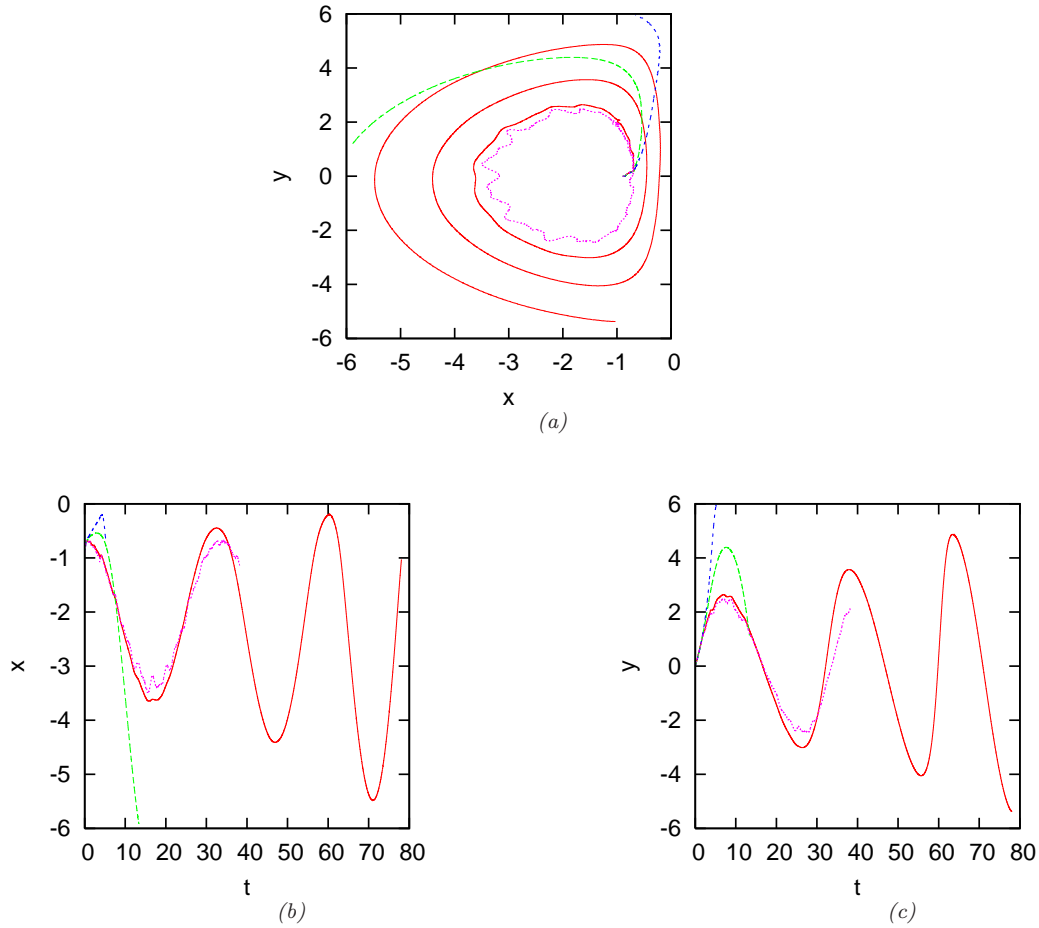


Figure 4.5: (a): Trajectories of one of the vortices from the vortex pair with $d_0 = 1.8$, (b): x -components and (c): y - components of trajectories vs. time corresponding to Figure 2.9(a) for $\gamma = 0$ (purple/dotted line); $\gamma = 0.01$ (red/solid line); $\gamma = 0.07$ (green/dashed line) and $\gamma = 0.1$ (blue/small dashed line).

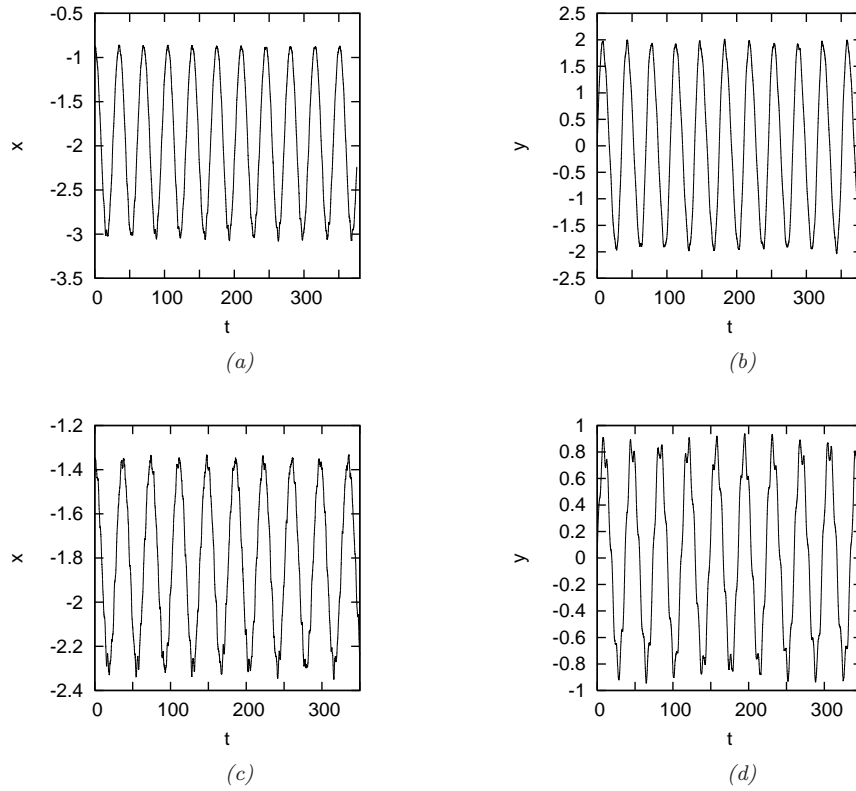


Figure 4.6: (left): x -component and (right): y -component of the trajectories as a function of time for one of the vortices in the vortex pair for d_0 (a,b): = 1 and (c,d): = 1.43.

energy together with other energies. The sound energy is the difference between the kinetic energy and the vortex energy: $E_{kin} = E_{sound} + E_{vortex}$, so $E_{sound} = E_{kin} - E_{vortex}$ (see Figure 4.8(f) and Figure 4.8(g)). These plots show a significant anticorrelation between the sound energy and the vortex energy, with correlation coefficient $cc = -0.844$.

The correlation coefficient, cc between two sets of random variables X and Y with expected values, μ_X and μ_Y and standard deviations, σ_X and σ_Y is given by: $cc = \frac{cov(X,Y)}{\sigma_X \sigma_Y}$, where $cov(X, Y)$ denotes the covariance. The covariance between two real-valued random variables X and Y , with expected values, $E(X) = \mu_X$ and $E(Y) = \mu_Y$ is defined as $cov(X, Y) = E((X - \mu_X)(Y - \mu_Y))$, where E is the expected value operator. The expected value of a random variable is the sum of the probability of each possible outcome of the experiment multiplied by the outcome value: $E(X) = \sum_{i=1}^N p_i X_i$. The standard deviation of a random variable is a measure of the spread of its values: $\sigma = \sqrt{\frac{1}{N} \sum_{i=1}^N (X_i - \bar{X})^2}$, where $\bar{X} = \frac{1}{N} \sum_{i=1}^N X_i$.

The correlation is 1 in the case of an increasing linear relationship and is -1 in the case of a decreasing linear relationship. For other correlations, cc takes some value in between and is zero when the two variables are not related to one another. The closer the coefficient is to either -1 or 1 , the stronger is the correlation between the variables. In this definition, we let X denote the sound energy and Y denote the vortex energy.

A direct visualisation can be seen in Figure 4.7. We notice that where the sound energy has a maximum, the vortex energy has a minimum. It is more clear that the sound is re-absorbed, see again Figure 4.8(f) and Figure 4.8(g). Generally, in the case of internal- and trap - energy, the oscillation amplitude of these functions is almost constant (see Figure 4.8(a) and Figure 4.8(b)). On the other hand, for quantum energy, these fluctuations have different values (see Figure 4.8(c)). From Figure 4.8(d), we can see that the average of the total energy is constant, though it displays a time modulation.

By this modulation, we mean harmonic oscillations of the vortex cyclical motions. The same modulation appears in the case of kinetic energy too, (see Figure 4.8(e)). For a vortex pair initially located at $(\pm 1.43, 0)$, we find $E_{tot} \simeq 17.47$. Because of the numerical resolution, E_{tot} is not constant, but varies of a typical amount ± 0.015 over $t = 140$, which corresponds to four orbits of the pair. That indicates a relative accuracy of $\pm 0.09\%$ in conserving the total energy.

According to the density plots, we observe that for smaller initial separation distance $d_0 = 0.793 \approx 0.8$, the sound production is more intensive with a rapidly varying density; compare Figure 4.3(b) with Figure 4.2(a). On the contrary, for larger values of d_0 ($d_0 = 2.86$), we have a nearly uniform density (See Figure 4.2(a) and Figure 4.2(b) together with Figure 4.2(c) and Figure 4.2(d)). Also, we have seen that without dissipation, the density fluctuation is more pronounced, than with dissipation, (compare Figure 4.9 with Figure 4.25).

It is well known that, in the absence of dissipation, a vortex-antivortex pair set at $(\pm x_0, 0)$ in an infinite homogeneous condensate moves with (dimensionless) translational speed $v_\infty = 1/(2x_0) = 1/d_0$, where d_0 is the initial separation distance between the vortices. We define v_{pair} ,

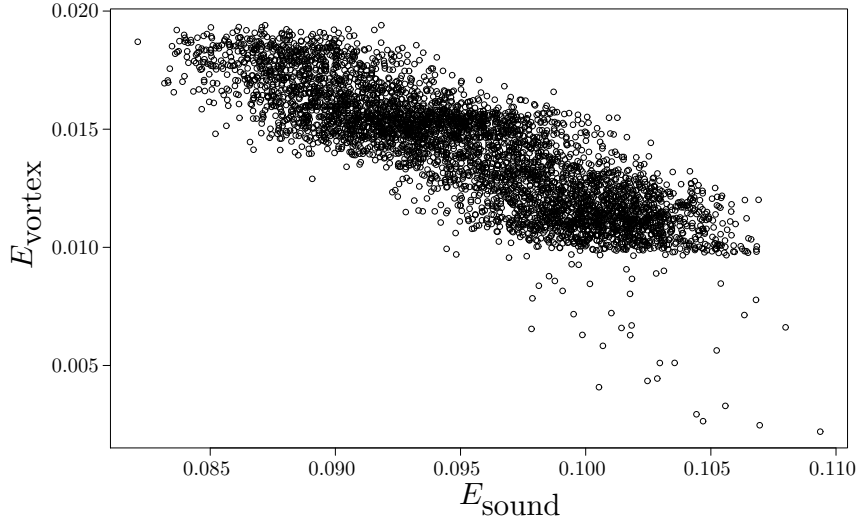


Figure 4.7: Correlation between vortex energy and sound energy for the vortex - anti vortex pair when $d_0 = 2.86$ and $\gamma = 0$. The correlation coefficient is $cc = -0.844$.

the measured velocity of the vortex pair, when it moves near the centre parallel to the y -axis and compare v_{pair} with v_∞ in Figure 4.10. We can see that our values agree well with v_∞ .

So, we calculate the translation speed with two methods and compare them in Figure 4.10. For the first method we use the y -component of the trajectory vs time, t . From the tangent to this curve, we calculate, $v'_y = v_{trans} = \Delta y / \Delta t$. We call it *the calculated values*. (see v'_y in Table. 4.1).

As we mentioned earlier the motion and the velocity of the pair of vortices depend on the initial separation distance, d_0 , between them. However, from Eq. (1.2) it follows that the velocity around a single vortex is:

$$\mathbf{v}_s = \frac{\Gamma}{2\pi r} \hat{\phi}, \quad (4.1)$$

where \mathbf{v}_s is the superfluid velocity at a point r , \mathbf{r} is the radius and $\hat{\phi}$ is the unit of angle of the vortex pair.

In our case of a vortex - anti vortex pair, the translation speed is expressed by $v_{pair} = v_y = 1/2x_0 = 1/d_0$. Actually, this formula has its origin in Eq. 4.1, which is valid for vortex points in an infinite fluid. In this expression, if $\Gamma = 1$ and $d = 2r$, represents the distance between the vortex and anti-vortex, this formula become similar with our (see the circle symbols in Figure 4.10 and v'_y in Table 4.1).

From Table 4.1, we observe that the difference between these two methods is significantly small. Table 4.2 contains more data for the second method, using $v_y \sim 1/d_0$.

It is worth stressing, that the motion of the vortex pair is periodic with a period of τ_p . The value of this period is measured from the x -coordinate and the y -coordinate vs t of the trajectory-

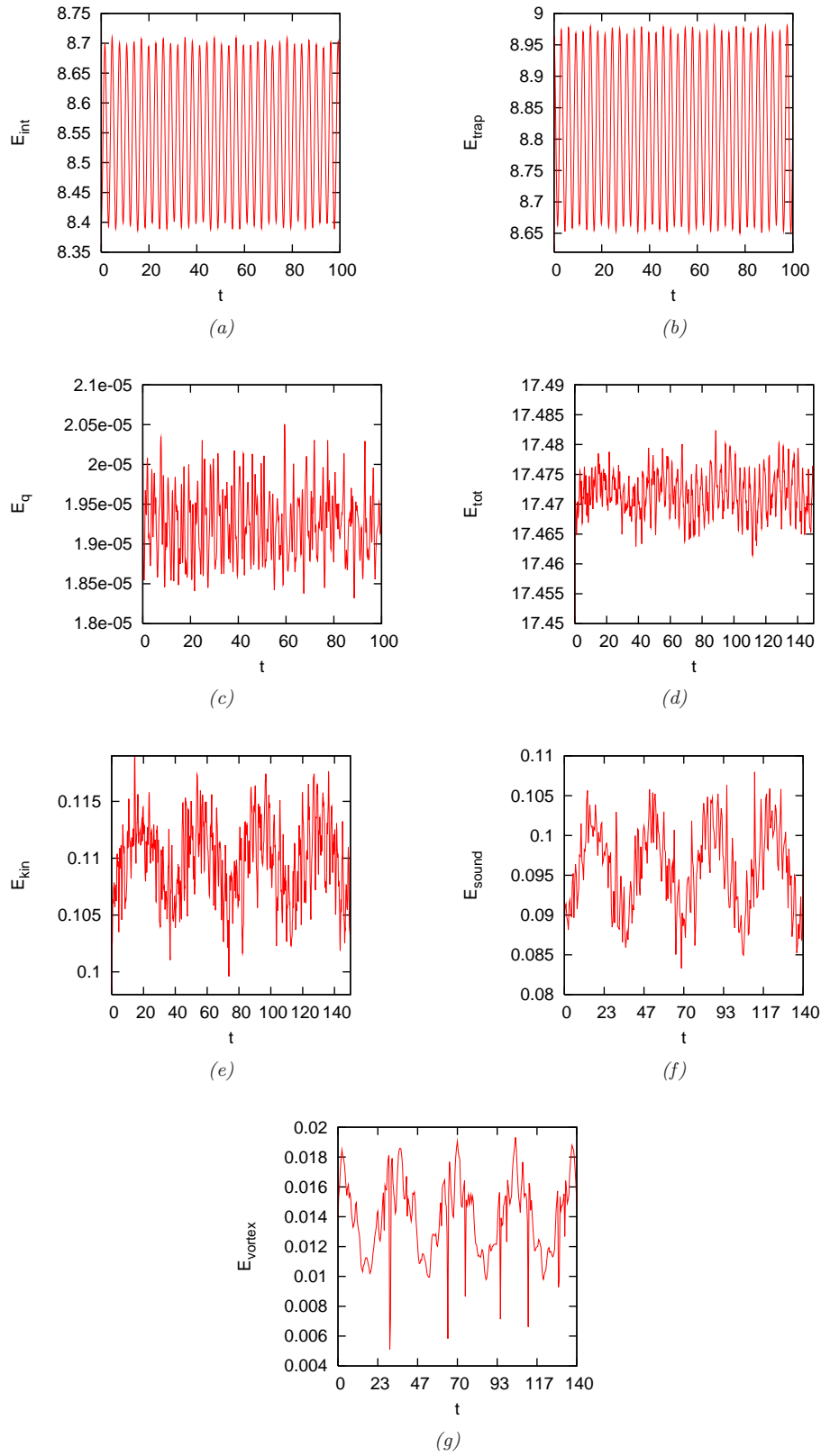


Figure 4.8: For a vortex - anti vortex pair with $d_0 = 2.86$ and $\gamma = 0$ (a): Internal energy, (b): Trap energy, (c): Quantum energy, (d): Total energy, (e): Kinetic energy, (f): Sound energy and (g): Vortex energy.

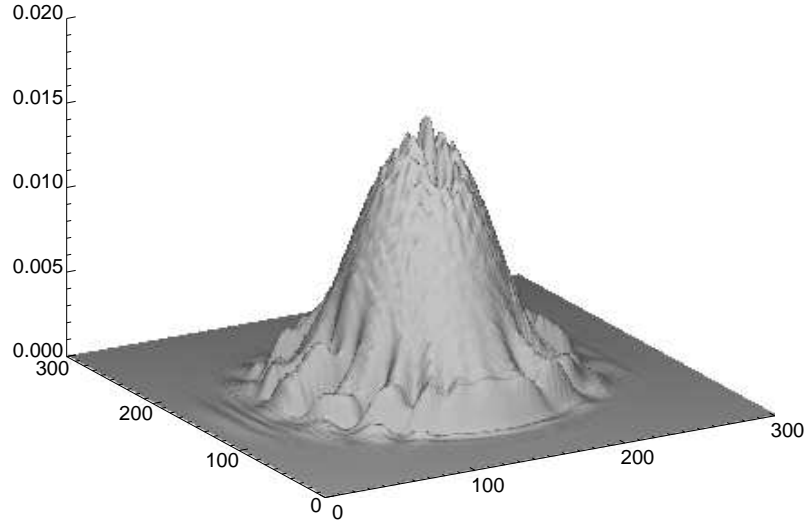


Figure 4.9: Sound waves on the density plot for the vortex - anti vortex pair for $d_0 = 2$ at $t = 2.6$ (for $\gamma = 0$).

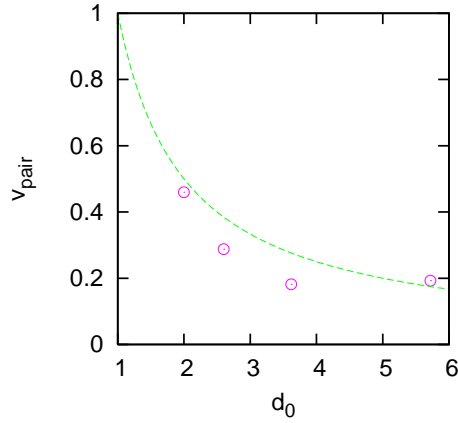
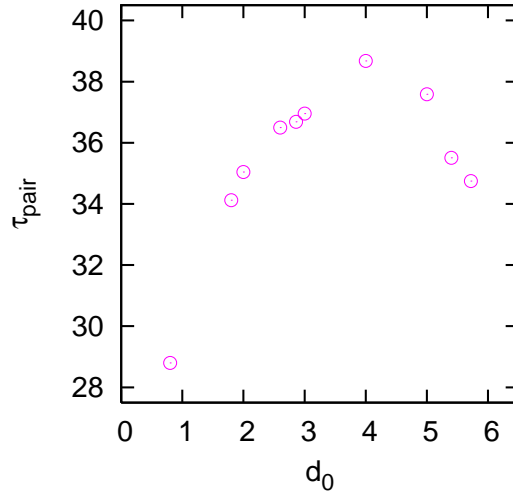


Figure 4.10: Vortex pair velocity as a function of d_0 (circle) measured at the centre of the condensate and compared to vortex pair velocity, v_∞ in homogeneous condensate (green/dashed line), for $\gamma = 0$.

x_0	d_0	$v'_y = tg\alpha = \Delta y / \Delta t$	$v_\infty \sim 1/d_0$	$diff = v'_y - v_y$
+/-1.00	2.00	0.459559	0.500000	0.040441
+/-1.30	2.60	0.287586	0.384615	0.097029
+/-1.81	3.62	0.181481	0.276243	0.094762
+/-2.86	5.72	0.192308	0.174825	0.017483

Table 4.1: The y -component of the velocity calculated with $v'_y = tg\alpha = \Delta y / \Delta t$ and with the form $v_y \sim 1/d_0$.

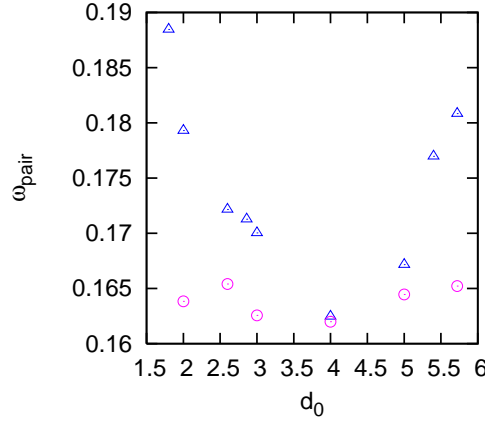
d	$v_\infty \sim \frac{1}{d}$
0.80	1.250000
1.80	0.555556
2.00	0.500000
2.60	0.384615
2.86	0.349650
3.00	0.333333
4.00	0.250000
5.72	0.174825

Table 4.2: Translation speed, v_∞ for the vortex pair.Figure 4.11: Period of motion for one of the vortices in the vortex - anti vortex pair for $\gamma = 0$.

plots; see Figure 4.11 and Table 4.3. Figure 4.11 and Figure 4.12 show that there is a symmetry about $d_0 = 4$. The explanation is that the vortices follow the same path if one were to put them close to the centre or close to the edge of the condensate. Due to the fact that they have the same path, they will have the same period and frequency as well. The peak at about $d_0 = 4$ appears due to the fact that for this initial separation distance, the pair has the largest period and the smallest frequency of motion.

In order to establish the frequency of motion, we use two methods: Firstly from $\omega_{pair} = 1/\tau_{pair}$ and secondly with the help of the period of a single vortex, which has its initial position at the centre of the path of one of the vortex pair. So, $\omega'_{pair} \sim \sqrt{2}\omega_{single}$ (see Appendix A), where $\omega_{single} = 1/\tau_{single}$ and τ_{single} are the frequency and the period of orbit for the single vortex (see Figure 4.12). Analogously, in Table 4.4, we have some values of the frequency of motion for a single vortex without dissipation. Figure 3.7(a) contains more data for the case of a single vortex, where x_0 is the distance from the centre. We can note that ω_0 , the frequency of motion for a single vortex, is almost constant near the centre of the condensate, and increases exponentially as we put the vortices close to the edge of the condensate see (Jackson *et al.*, 2000).

x_0	y_0	d_0	Period τ
0.40	0.00	0.80	28.800000
0.90	0.00	1.80	34.118880
1.00	0.00	2.00	35.042370
1.30	0.00	2.60	36.497570
1.43	0.00	2.86	36.684470
1.50	0.00	3.00	36.954320
2.00	0.00	4.00	38.673370
2.50	0.00	5.00	37.587970
2.70	0.00	5.40	35.50412
2.86	0.00	5.72	34.744530

 Table 4.3: Period, τ of motion of the vortex pair.

 Figure 4.12: Frequency of one vortex in the vortex pair calculated with two methods. Triangle symbols represent the value obtained from $\omega_{pair} = 1/\tau_{pair}$ and circle symbols represent the value which was calculated with the help of the corresponding single vortex frequency $\omega'_{pair} \sim \sqrt{2}\omega_{single}$.

x_0	y_0	d_0	x_{0s}	τ_{pair}	ω_{pair}	τ_{single}	ω_{single}	ω'_{pair}	diff
1.00	0.0	2.00	1.9200	35.04237	0.179302	54.23782	0.115845	0.163829	-0.015473
1.30	0.0	2.60	1.9384	36.49757	0.172153	53.72410	0.116953	0.165396	-0.006757
1.50	0.0	3.00	1.8373	36.95432	0.170026	54.65859	0.114953	0.162568	-0.007457
2.00	0.0	4.00	1.8050	38.67337	0.162471	54.85648	0.114538	0.161982	-0.000486
2.50	0.0	5.00	1.8444	37.58797	0.167159	54.02893	0.116293	0.164463	0.002696
2.86	0.0	5.72	1.9000	34.74453	0.180839	53.78207	0.116826	0.165218	-0.156215

 Table 4.4: This table presents the initial position (x_0, y_0) of one vortex in the vortex pair, the initial separation distance between the vortices, d_0 , the initial position for the single vortex, which was placed in the centre of the trajectory of the vortex/anti-vortex, x_{0s} , the period and frequency of motion for the pair of vortices, τ_{pair} and ω_{pair} , the period and frequency of motion for the single vortex, τ_{single} and ω_{single} , the frequency of motion of the vortex pair (calculated with the help of ω_{single}) ω'_{pair} and the difference between the two frequencies ω_{pair} and ω'_{pair} .

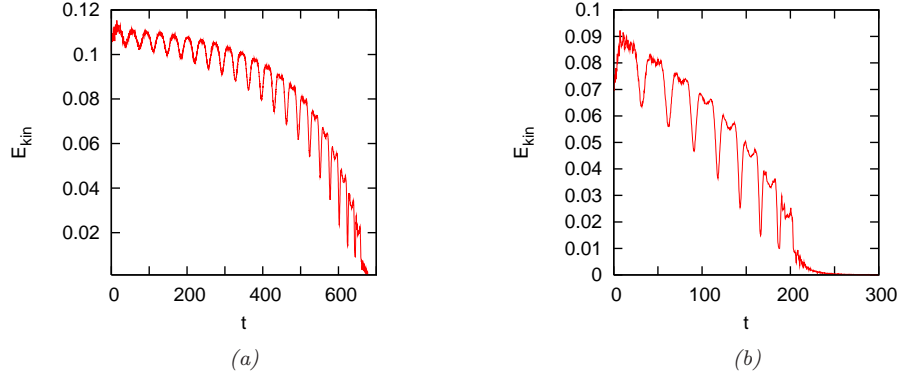


Figure 4.13: Kinetic energy for the vortex - anti vortex pair for $\gamma = 0.003$ with (a): $d_0 = 2.86$ and with (b): $d_0 = 1.5$.

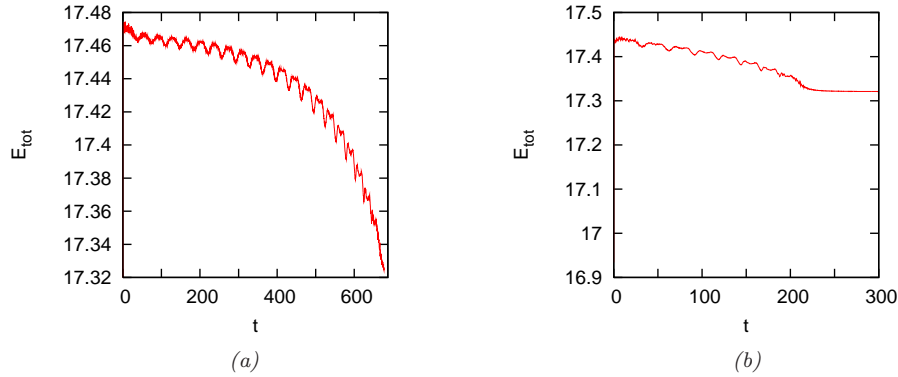


Figure 4.14: Total energy corresponding to Figure(4.13(a) - 4.13(b)). In (b) We can see that about $t = 220$, the vortex leave the condensate.

4.3 Motion with Small Dissipation

In this section, we apply dissipation with special emphasis on the case of $\gamma = 0.003$. That means that the relaxation of the condensate towards equilibrium is slow. We have introduced the dissipation term on purpose to remove short wavelength excitations in the scales smaller than the healing length.

It is useful to study the kinetic energy, the total energy, the internal energy, the quantum energy and the trap energy with the help of figures: Figure(4.13(a) - 4.13(b)), Figure(4.14(a) - 4.14(b)), Figure(4.15(a) - 4.15(b)), Figure(4.16(a) - 4.16(b)) and Figure(4.17(a) - 4.17(b)).

Let us begin with examination of different energies for the case of initial separation distances $d_0 = 1.5$ and $d_0 = 2.86$. As expected, the different energy-plots show a decrease in energy levels due to the dissipation. We compare these energies, the sound and the vortex energy with the case of no dissipation, ($\gamma = 0$). In both cases, we observe the anti-correlation phenomenon between the vortex energy and the sound energy. To have four periods of modulation with time due to the

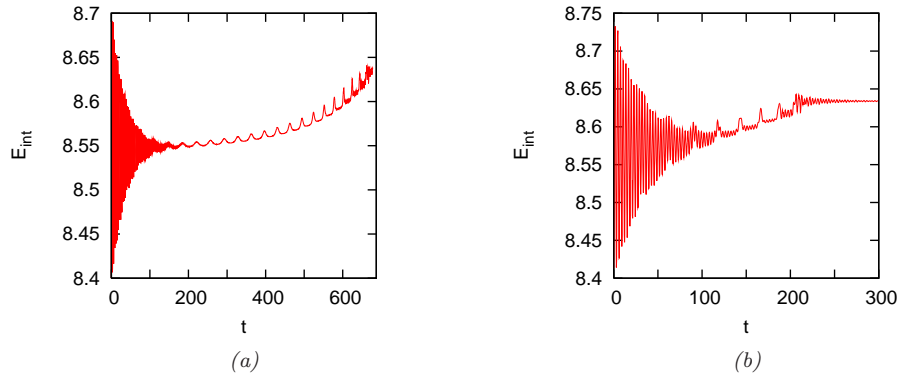


Figure 4.15: Internal energy corresponding to Figure(4.13(a) - 4.13(b)).

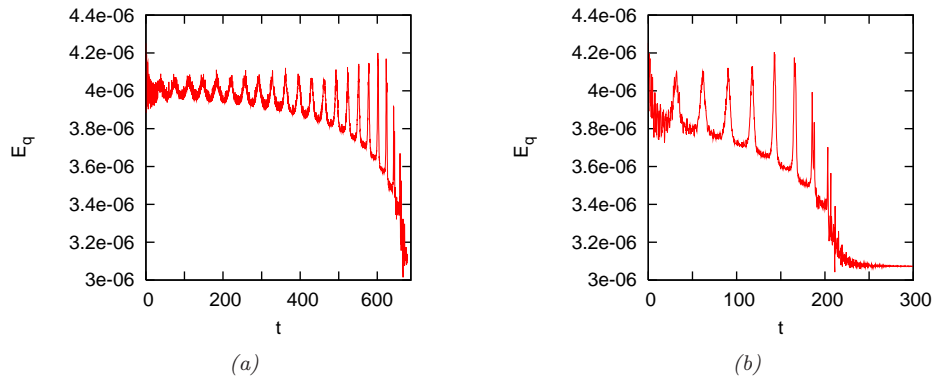


Figure 4.16: Quantum energy corresponding to Figure(4.13(a) - 4.13(b)).

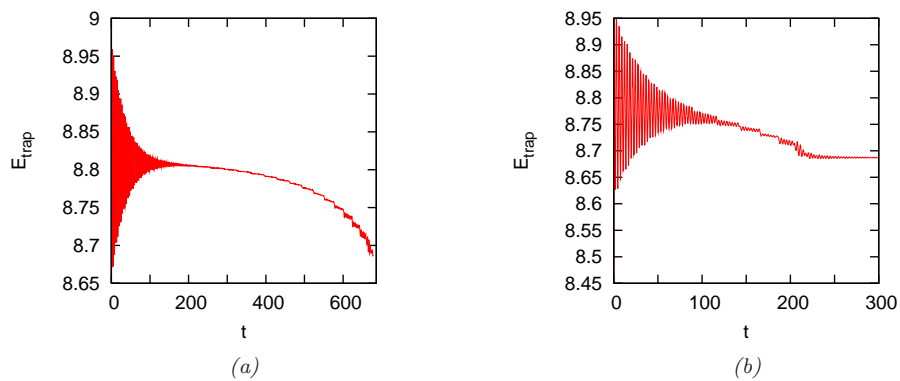


Figure 4.17: Trap energy corresponding to Figure(4.13(a) - 4.13(b)).

cyclical motion, it needs about $t = 140$ in both cases for the following energies: kinetic energy, total energy, sound energy and vortex energy.

For the case of $d_0 = 2.86$, the maximum value of the vortex energy without dissipation is about 0.019, almost twice as large as with the case of dissipation ($\gamma = 0.003$), where this value is about 0.01. For the sound energy, we note that without dissipation the oscillation varies between about 0.085 and about 0.105 and with $\gamma = 0.003$, the first oscillation varies between 0.087 and 0.103 and later it decrease with time. The modulation on these different energies, as already pointed out, is a result of the cyclical motion of the vortex.

Now, we compare the first four period-times of the total energy and of the kinetic energy (with dissipation $\gamma = 0.003$) for the case of $d_0 = 2.86$ and $d_0 = 1.5$, (see Figure 4.18(g); Figure 4.18(h) and Figure 4.18(e); Figure 4.18(f)). The maximum values of the sound and vortex energies are: $E_{kin} = E_{sound} + E_{vortex} = 0.101 + 0.0175 = 0.1185$. We compare this sum (of the maximum values) with the maximum value of the kinetic energy: $E_{kin} = 0.113$. The difference is $Diff = 0.0055$. Notice that for larger d_0 , when the vortex is closer both to the edge of the condensate and to each other, more noise is formed, especially when they move together in the centre of the condensate or they meet the edge of the condensate, see Figure(4.19(a) - 4.19(b)). In particular, from the plot of kinetic energy, total energy and sound energy, we remark that the system loses more energy (much quicker) at the end of the vortex motion, (see Figure 4.19(a), Figure 4.13(a) and Figure 4.14(a)).

With respect to Figure 4.21, we can note an out-lying point, with coordinates ($E_{sound} = 0.1027$, $E_{vortex} = 0.0024$). The explanation is that in the case of dissipation ($\gamma = 0.003$), the correlation is different from the case of no dissipation, when $cc = -0.844$ is a *constant*. With dissipation, the correlation coefficient (cc) varies with time. Until $t = 150$, $cc = -0.841$, when $t = 300$, $cc = -0.601$ and at $t = 400$ the correlation coefficient has reduced its magnitude to $cc = -0.215$. The above discussion is the ground for our opinion that this *out-lying point* is due to these changes. Furthermore, the condensate needs time for relaxation, in order to be stable. This can be checked from, for example internal energy and trap energy, see Figure(4.15(a) - 4.15(b)) and Figure(4.17(a) - 4.17(b)). As expected, in the beginning they are unstable but after some short time oscillations, whose amplitude decreases with time, these energy functions take up the cyclical-motion modulations at about $t = 150$ for $d_0 = 2.86$.

However, the trap energy, see Figure(4.23(a) - 4.23(b)) shows a similar tendency as the internal energy, see Figure(4.22(a) - 4.22(b)). The only difference between them is that the internal energy increases from about 8.54 to about 8.64 and the trap energy decreases from about 8.8 to about 8.7 in their values with time. The average values of these energies are the same for both $\gamma = 0$ and for $\gamma = 0.003$, when $d_0 = 2.86$. So, there is a similarity between the case of no dissipation with the case of small dissipation.

In fact, we can compare the average values of the quantum energy without dissipation, $E_q = 1.94 \times 10^{-5}$, with the case of $\gamma = 0.003$ (for $d_0 = 2.86$), when $E_q = 4 \times 10^{-6}$ in the beginning and decreases later; see Figure 4.8(c) and Figure 4.16(a). The periodic modulation of the vortex motion is present here as well.

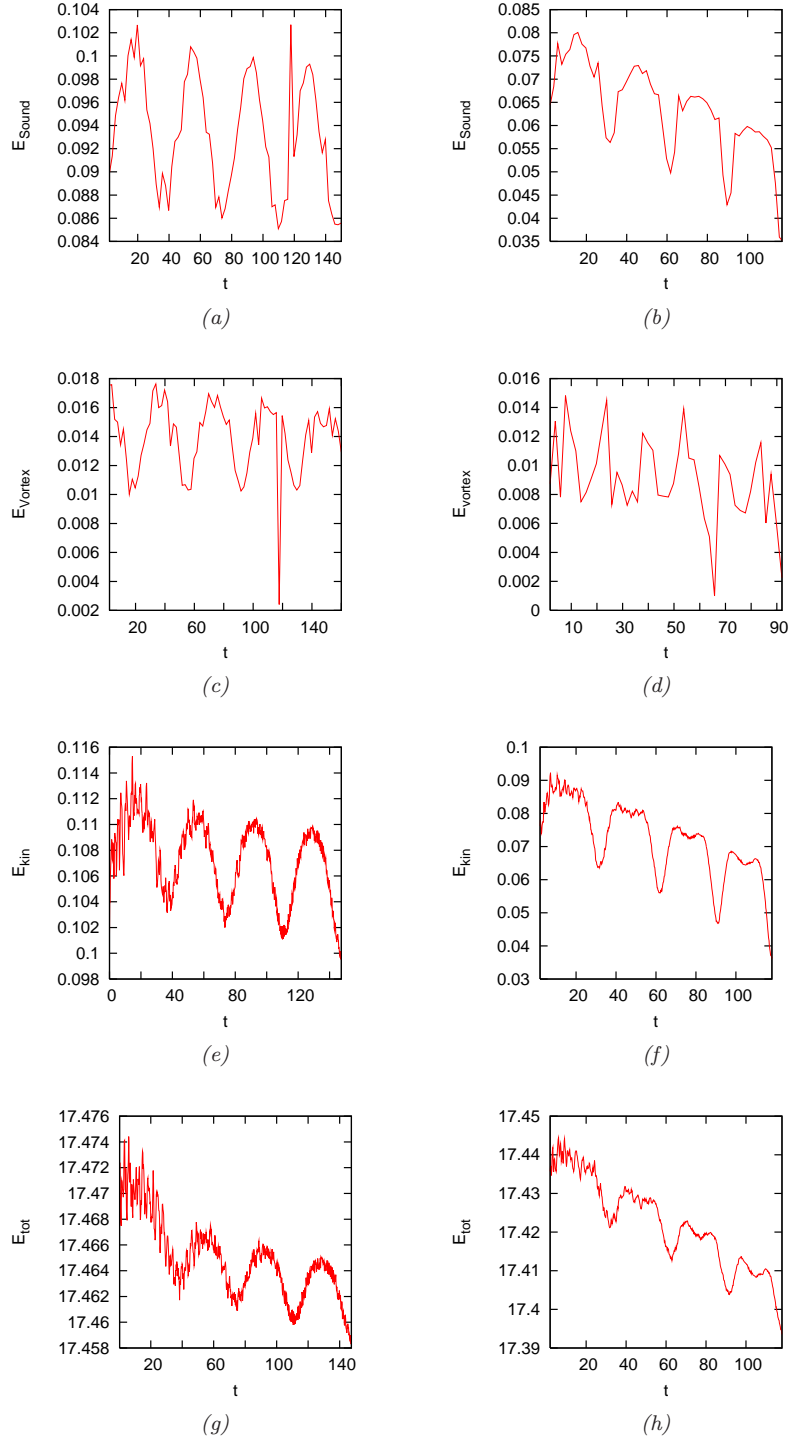


Figure 4.18: Energies corresponding to Figure(4.13(a) - 4.13(b)): (a,b): Sound energy for shorter time (compare with Figure 4.19(a) and Figure 4.19(b)), (c,d): Vortex energy for shorter time (compare with Figure 4.20(a) and Figure 4.20(b)), (e,f): Kinetic energy for shorter time (compare with Figure 4.13(a) and Figure 4.13(b)) and (g,h): Total energy for shorter time (compare with Figure 4.14(a) and Figure 4.14(b)).

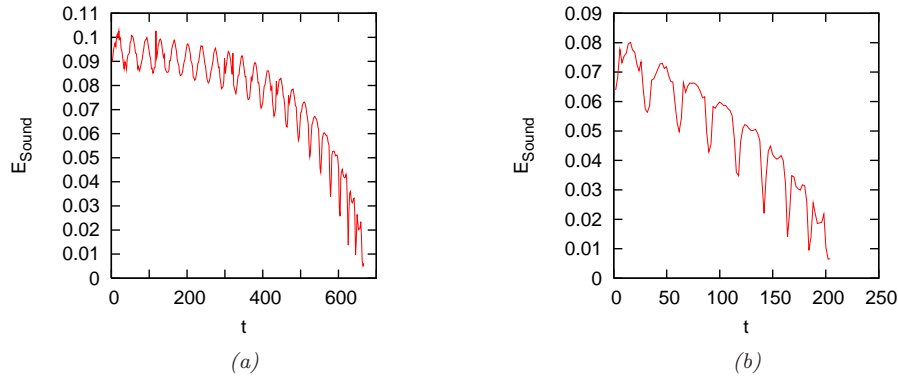


Figure 4.19: Sound energy corresponding to Figure(4.13(a) - 4.13(b)).

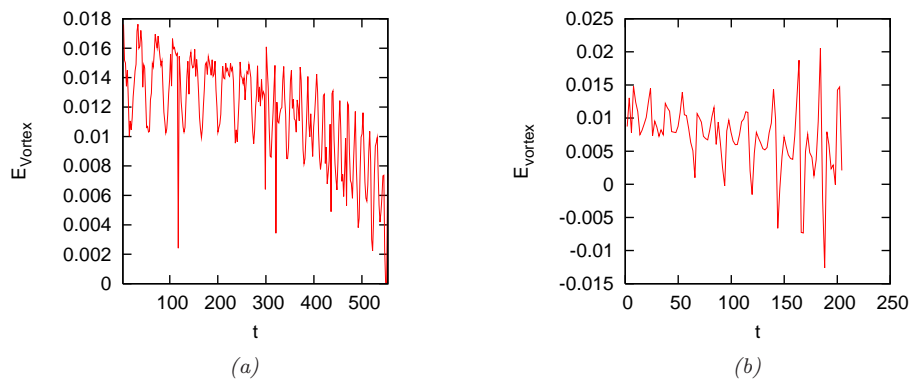


Figure 4.20: Vortex energy corresponding to Figure(4.13(a) - 4.13(b)).

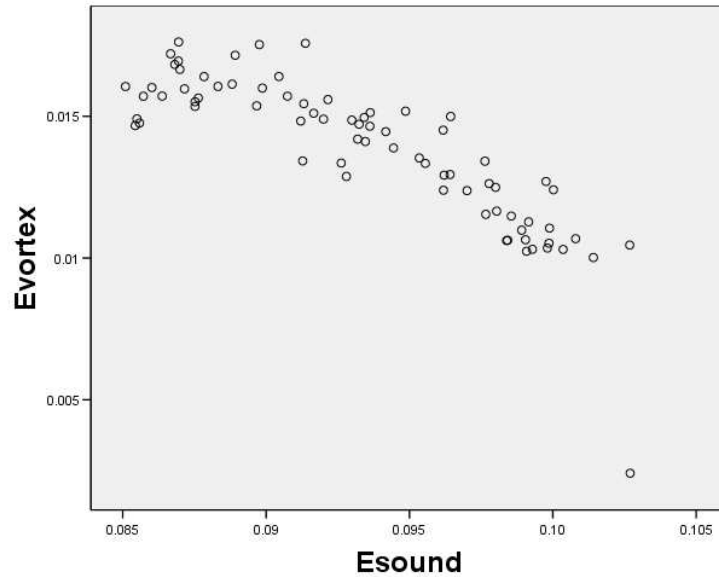


Figure 4.21: Correlation between vortex energy and sound energy for the vortex - anti vortex pair with $d_0 = 2.86$ and $\gamma = 0.003$. The correlation coefficient is $cc = -0.841$.

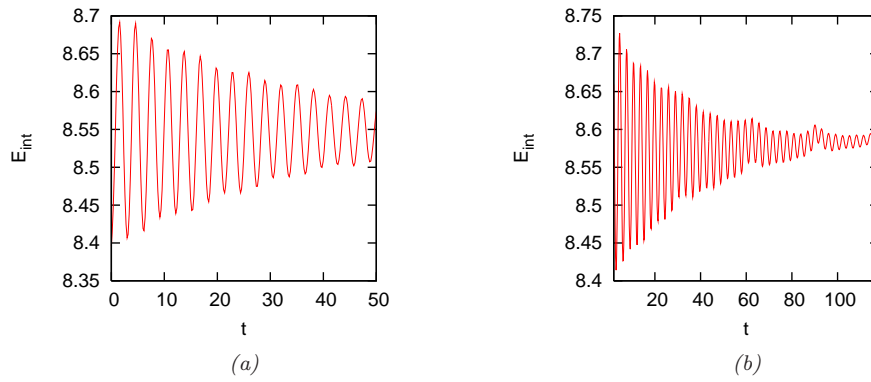


Figure 4.22: Internal energy corresponding to Figure(4.13(a) - 4.13(b)) for shorter time (compare with Figure 4.15(a) and Figure 4.15(b)).

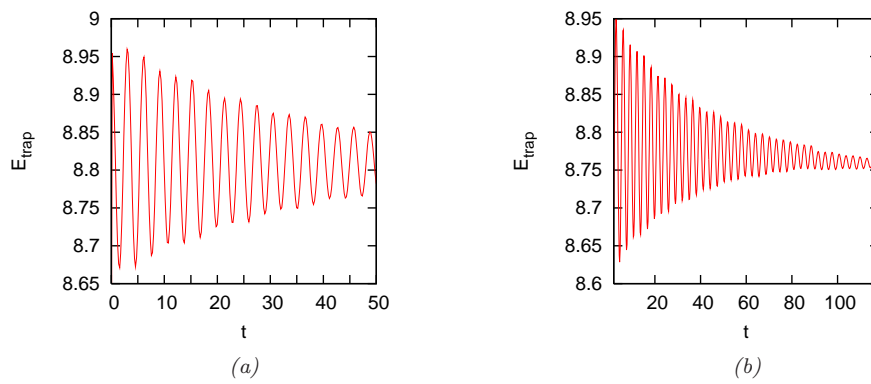


Figure 4.23: Trap energy corresponding to Figure(4.13(a) - 4.13(b)) for shorter time (compare with Figure 4.17(a) and Figure 4.17(b)).

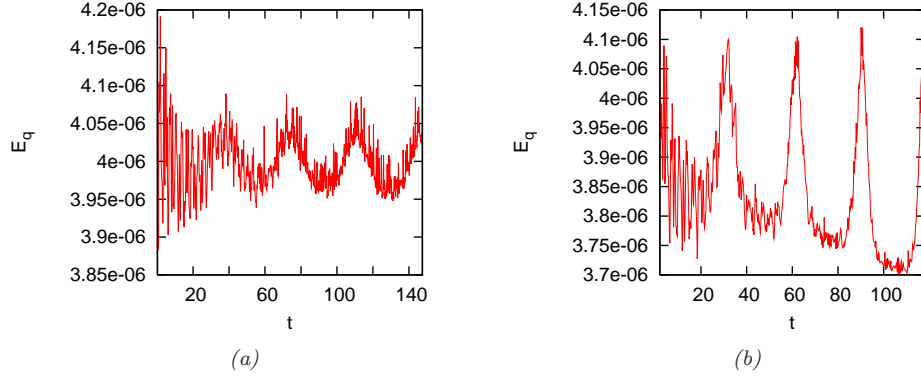


Figure 4.24: Quantum energy corresponding to Figure(4.13(a) - 4.13(b)) for shorter time (compare with Figure 4.16(a) and Figure 4.16(b)).

Let us conclude this section by discussing the behaviour of the strange shape of the quantum energy, in the case of dissipation. We believe that, this figure, see Figure(4.16(a) - 4.16(b)), can be explained by the fact that in the centre of the system the density is higher and the vortex has a smaller diameter than at the edge, where the density is more dilute. So, on the border of the system, the vortex becomes larger because of the dilute nature of the fluid. Notice that the vortex always comes back to the centre of the condensate, where the density is higher.

4.4 Motion with $d_0 = 1.8$ and Different γ 's

In this section we continue our investigation with dissipation, applying more values for γ . One can see that, when the dissipation, γ is different from 0, for example $\gamma = 0.01$, the density fluctuation is much smoother than without dissipation (see Figure 4.25). It is worth noticing that with dissipation, the total energy decreases from the same initial value as without dissipation (≈ 17.525) to its final value of approximately 17.32 (see Figure 4.26(a)).

Note, that in the case of no dissipation, for $d_0 = 2.86$, the average value of the total energy is 17.47. It is worth pointing out that, with larger dissipation, the vortices travel towards the edge of the condensate earlier and the different energies reach their final values earlier as well. The same observation is valid for the kinetic energy, quantum energy, internal energy and trap energy, (see Figure 4.26(b), Figure 4.27(a), Figure 4.27(b), Figure 4.28(a), Figure 4.28(b), Figure 4.29(a) and Figure 4.29(b)).

In particular, by increasing the dissipation, we note that the initial short time fluctuations become fewer in the case of internal energy and trap energy. In general, for smaller γ , (which value is close to the case of no dissipation) the short time fluctuations are the same as with $\gamma = 0$. The only difference is that with small dissipations, the amplitude of these oscillations decreases exponentially in time (see Figure 4.29(a)). Our conclusions, from the case of dissipation with $\gamma = 0.003$ and separation distances $d_0 = 2.86$ and 1.5 are partially valid here as well, in the case of small dissipation, like $\gamma = 0.01$. With time the internal energy increases and whilst the trap energy

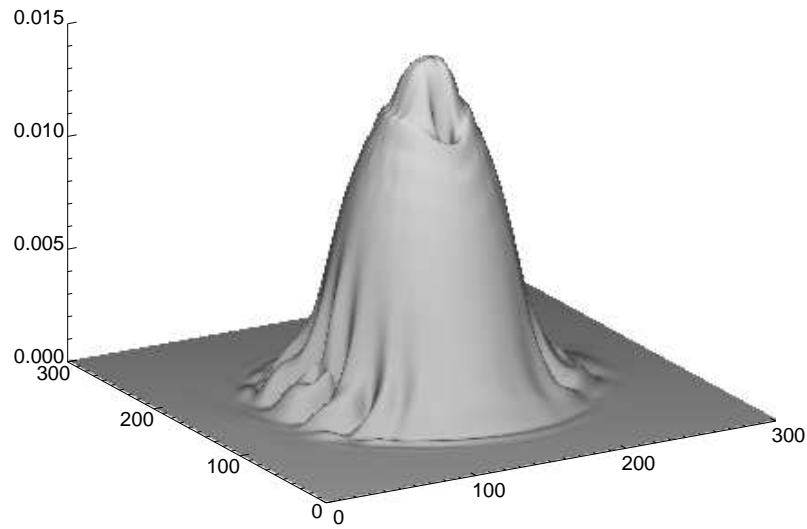


Figure 4.25: Sound waves on the density plot for the vortex - anti vortex pair with $d_0 = 1$ and $\gamma = 0.01$ at time, $t = 2.4$.

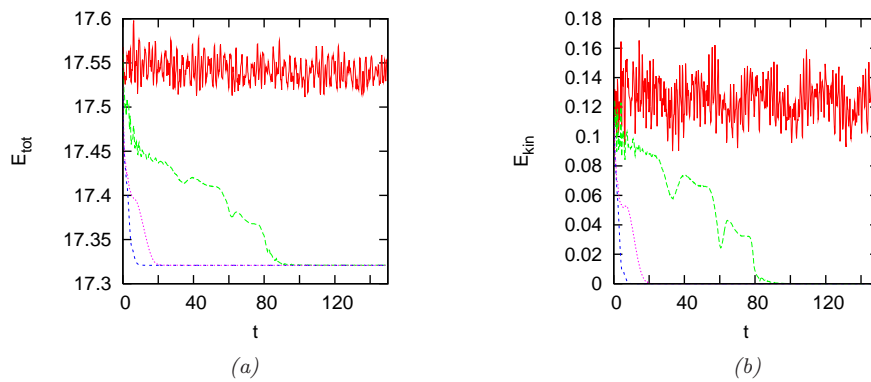


Figure 4.26: (a): Total energies and (b): Kinetic energies for the vortex - anti vortex pair with $d_0 = 1.8$ and $\gamma = 0$ (red line/solid line); $\gamma = 0.01$ (green line/dashed line); $\gamma = 0.07$ (purple line/dotted line); $\gamma = 0.1$ (blue line/small dashed line)

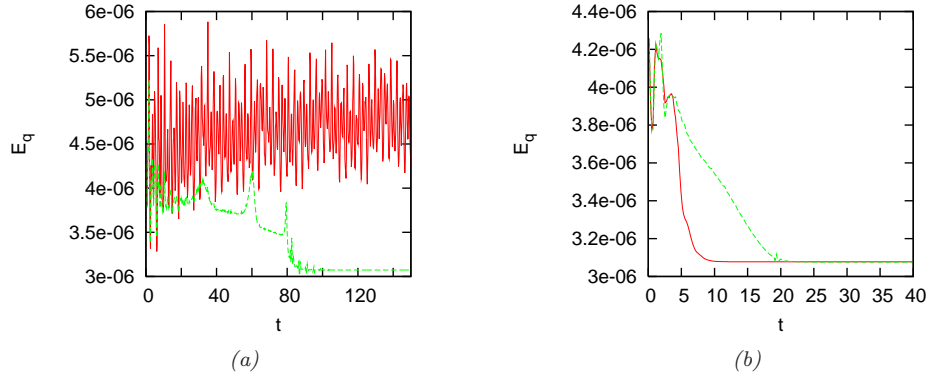


Figure 4.27: (a): Quantum energies for the vortex - anti vortex pair with $d_0 = 1.8$ for (a): $\gamma = 0$ (red line/solid line) and $\gamma = 0.01$ (green line/dashed line) and for (b): $\gamma = 0.07$ (green line/dashed line) and $\gamma = 0.1$ (red line/solid line).

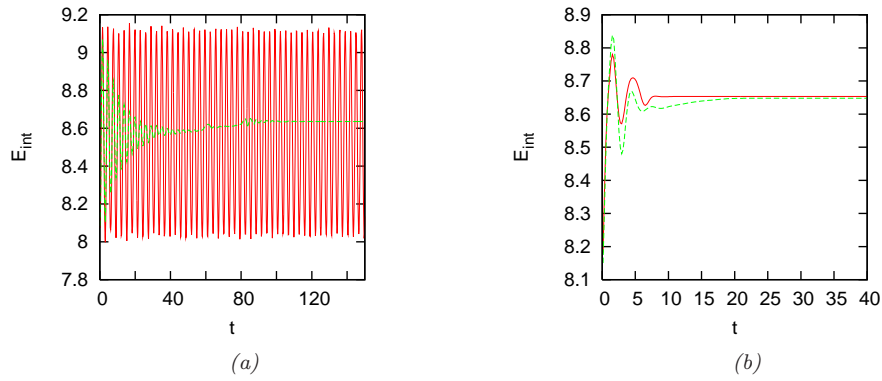


Figure 4.28: Internal energies for the vortex - anti vortex pair with $d_0 = 1.8$ for (a): $\gamma = 0$ (red line/solid line) and $\gamma = 0.01$ (green line/dashed line) and for (b): $\gamma = 0.07$ (green line/dashed line) and $\gamma = 0.1$ (red line/solid line).

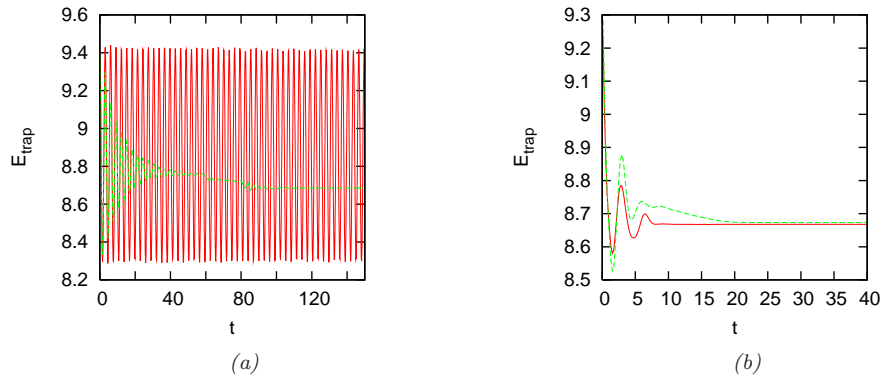


Figure 4.29: Trap energies for the vortex - anti vortex pair with $d_0 = 1.8$ for (a): $\gamma = 0$ (red line/solid line) and $\gamma = 0.01$ (green line/dashed line) and for (b): $\gamma = 0.07$ (green line/dashed line) and $\gamma = 0.1$ (red line/solid line).

decreases; but as we can see from Figure 4.28(a) and Figure 4.29(a), the trap energy decreases a bit more than the internal energy increase, thus there is a net loss of energy.

4.4.1 Energy Balance

From the energy plots we see that the internal energy behaves inversely than the other energies. To understand this phenomenon, we do the energy balance for a vortex - anti vortex pair with dissipations γ : 0.003; 0.03 and 0.01 and for the case of a single vortex for $\gamma = 0.01$.

Let us begin our study with the case of small dissipation, $\gamma = 0.003$ and $d_0 = 2.86$. The quantum energy in every case is neglected because it is too small. Its initial value is about $4 * 10^{-6}$. Due to the dissipation, the energies decrease; $\Delta E_{tot} = -0.14$, $\Delta E_{kin} = -0.106$, $\Delta E_{trap} = -0.113$ and $\Delta E_{int} = +0.08$. So for the change in the total energy, we have $\Delta E_{tot} = \Delta E_{kin} + \Delta E_{trap} + \Delta E_{int}$, which gives $-0.140 = -0.106 - 0.113 + 0.08$, which means $-0.14 = -0.139$. So, we have a good balance. That explains why the internal energy increases.

We do a similar thing for the case of the same dissipation $\gamma = 0.003$ but with smaller initial separation distance, $d_0 = 1.5$. For $\Delta E_{tot} = \Delta E_{kin} + \Delta E_{trap} + \Delta E_{int}$, we have $-0.105 = -0.0725 - 0.08 + 0.05$, which gives $-0.105 = -0.1025$. This is not bad but is not as accurate as in the first example and similarly our vortex energy function is not as good as for $d_0 = 2.86$. One of the explanation is that the vortices in the second example are more close to each other, so they have more influence upon each other and the system uses a smaller energy resource. Our purpose now is to compare the energy balance for the case of a vortex - anti vortex pair with the case of a single vortex.

Let us continue our investigation by putting our single vortex at initial position $(x_0, y_0) = (0.9, 0)$ and compare it with the case of vortex - anti vortex pair for $d_0 = 1.8$. For the vortex pair, $\Delta E_{tot} = \Delta E_{kin} + \Delta E_{trap} + \Delta E_{int}$, which gives $-0.2 = -0.13 - 0.09 + 0.04$, i.e. $-0.2 = -0.18$. A different scenario takes place for a single vortex: We have $\Delta E_{tot} = \Delta E_{kin} + \Delta E_{trap} + \Delta E_{int}$, so $-0.1 = -0.075 - 0.075 + 0.055$, which means $-0.1 = -0.095$.

Also, in this section among other things, we have discussed the problem of the energy balance and we summarise it with our conclusions in Table 4.5 with two remarks. The first one is that for $\gamma = 0.01$ our energy balance is better for a single vortex than for the case of a vortex - anti vortex pair, where the condensate uses less energy. The second remark is that we have the best energy balance for the case of small dissipation, $\gamma = 0.003$ and large initial separation distance, $d_0 = 2.86$, which is valid for the case of vortex - anti vortex pair.

4.5 Motion of a Single Vortex and Vortex - Anti Vortex Pair with Different Dissipations

It is well known that in a dissipative environment the total energy is not conserved. So, in this short chapter, we discuss the question about *whether or not* the decrease of the total energy with

γ	d_0	ΔE_{tot}	ΔE_{kin}	ΔE_{trap}	ΔE_{int}	$\Delta E_{kin} + \Delta E_{trap} + \Delta E_{int}$	Diff
0.003	2.86	-0.140	-0.1060	-0.113	+0.08	-0.1390	0.0010
0.003	1.50	-0.105	-0.0725	-0.080	+0.05	-0.1025	0.0025
0.010	1.80	-0.200	-0.1300	-0.090	+0.04	-0.1800	0.0200
γ	x_0	ΔE_{tot}	ΔE_{kin}	ΔE_{trap}	ΔE_{int}	$\Delta E_{kin} + \Delta E_{trap} + \Delta E_{int}$	Diff
0.01	0.9	-0.1	-0.075	-0.075	+0.055	-0.095	0.005

Table 4.5: Energy balance for the case of vortex - anti vortex pairs with initial separation distance, $d_0 = 2.86, 1.5$ and 1.8 and for the case of a single vortex with initial position, $x_0 = 0.9$.

γ	β_1	β_2	β_3
0.003	-0.00000177	-0.00000964	-0.00002123
0.010	-0.00001456	-0.00003135	-0.00012980
0.030	-0.00003955	-0.00008946	-0.00048760
0.070	-0.00008791	-0.00018650	-0.00125300
0.100	-0.00012570	-0.00025730	-0.00179100

Table 4.6: Decay rate of the total energy for a single vortex with initial positions, $x_0 = 0.9$ (β_1); 2.86 (β_2), $y_0 = 0$ and for vortex - anti vortex pair with initial separation distance, $d_0 = 1.8$ (β_3) as a function of γ .

time depends on the vortex initial position (for different dissipations). We give for the dissipations the following values, γ : 0.003; 0.01; 0.03; 0.07 and 0.1 and the vortices have as initial positions, $x_0 = 0.9$; 2.86 and $y_0 = 0$. In order to calculate the decay rate of the total energy, β for different dissipations, we put first a single vortex at initial position $(x_0, y_0) = (0.9, 0)$ (see the result in Figure 4.30(a)).

We repeat the same procedure for $x_0 = 2.86$ (see the result in Figure 4.30(c)). In this respect, our first conclusion is that the decay rate, β of the total energy depends on the vortex initial position x_0 . We continue systematically our investigation with a vortex - anti vortex pair too. Now, we put one of the vortices from the vortex pair at the same position where the single vortex was but symmetrically about the *Origo* ($(x_0, y_0) = (0, 0)$), $x_0 = \pm 0.9$ (see the result in Figure 4.30(b)). Notice that, we have again different values for β . As expected, we have an exponential decrease of the total energy with time in these three cases, with different decay rates, β (see Table 4.6). So, our second conclusion is that the variation of the decay rate β with dissipation γ is linear, that is to say, if we increase γ , β decreases linearly.

Also, after some oscillations in the beginning the internal energy decreases and at the same time the trap energy decreases (see the result in Figure 4.31(c) and Figure 4.31(d)).

Now, we turn our attention to the connection between the fluid and the vortex velocity. We wish to describe the velocity field at those positions, where the vortex pair was located originally. The initial positions of the vortices are: $x_0 = \pm 2.99$ and ± 0.65 for $y_0 = 0$. The considered dissipations are: $\gamma = 0$ and 0.03 .

We place two vortices symmetrically about the *Origo* at $(x_0, y_0) = (\pm 2.99, 0)$. In the following, we will consider only the short time decrease of the fluid velocity. Consequently, we omit the periodic motions of the vortices.

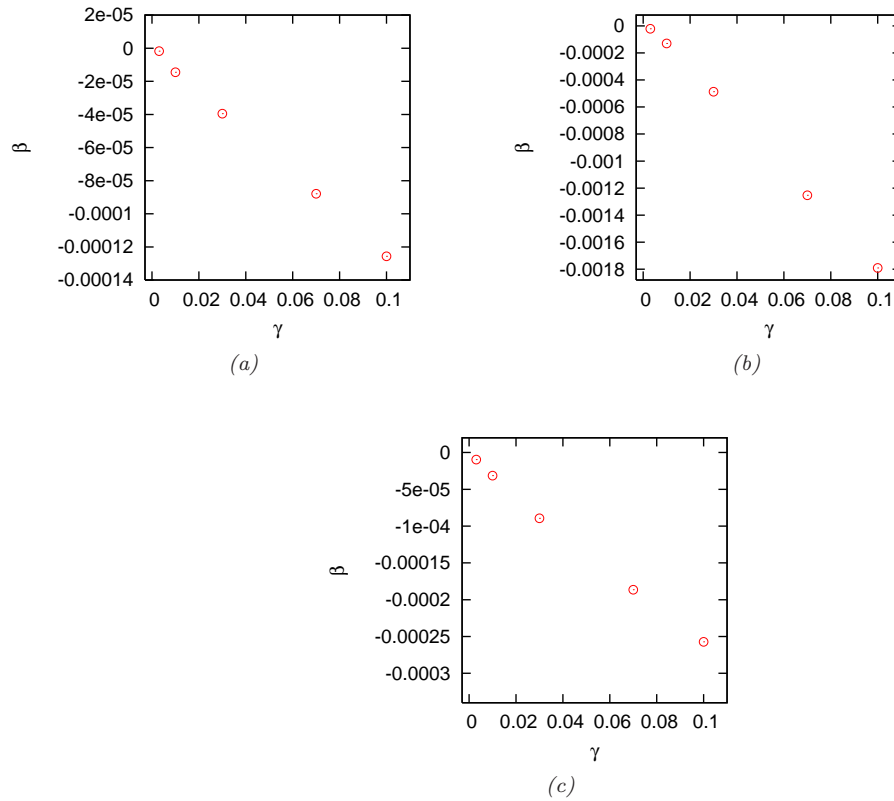


Figure 4.30: Decay rate of the total energy, $\beta = dE/dt$ as a function of γ (a,b): (left): for a single vortex with $(x_0, y_0) = (0.9, 0)$ and (right): for a vortex - anti vortex pair with $d_0 = 1.8$ and (c): for a single vortex with $(x_0, y_0) = (2.86, 0)$.

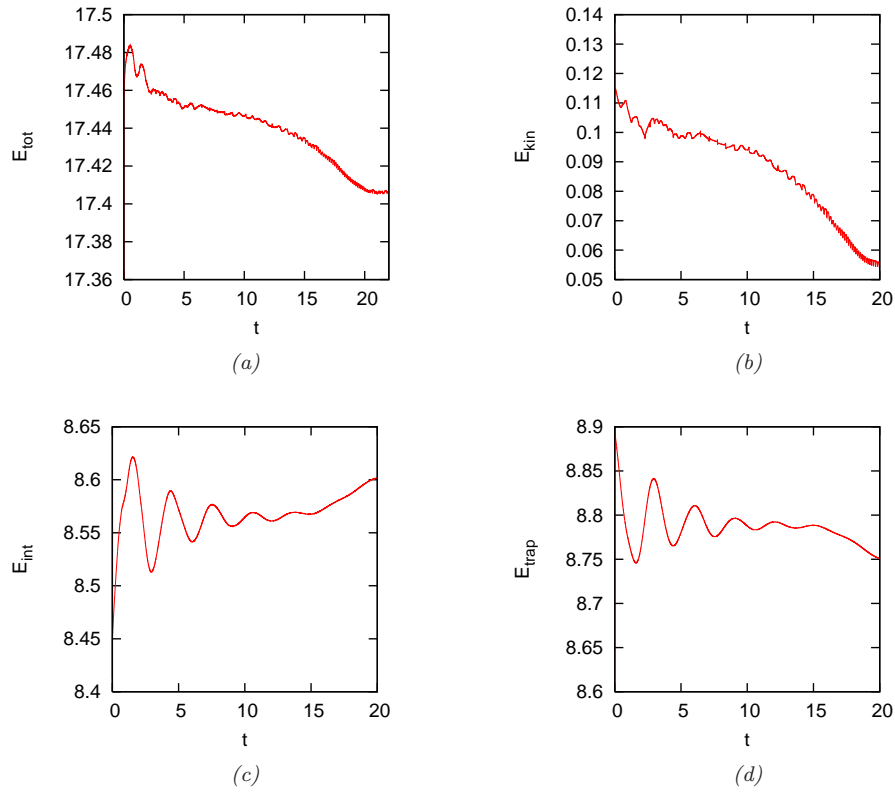


Figure 4.31: For a vortex - anti vortex pair with $d_0 = 5.98$ and $\gamma = 0.03$ the decrease of (a,b): (left): the total energy and (right): of the kinetic energy and the (c,d): (left): the increase of the internal energy and (right): the decrease of the trap energy.

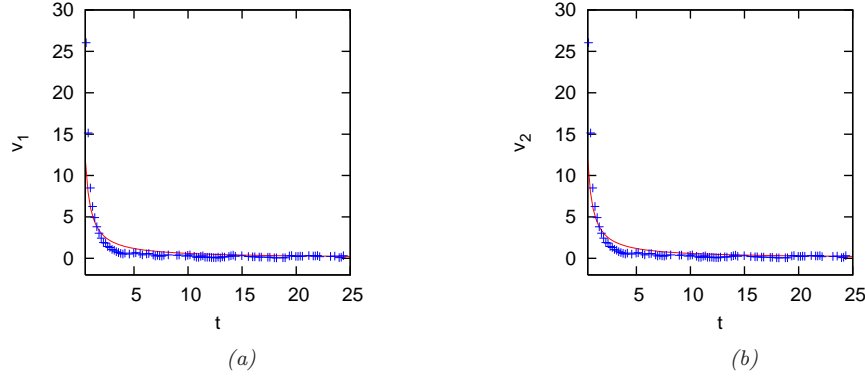


Figure 4.32: For $\gamma = 0$, the red/solid line stands for the function, $f(t) = a/t$ and (a): (+) represents the fluid velocity, $v_1 = \sqrt{v_x^2 + v_y^2}$, at the position, where the first vortex from the vortex - anti vortex pair was placed originally, $(x_0, y_0) = (2.99, 0)$ and (b) (+) represents the fluid velocity, $v_2 = \sqrt{v_x^2 + v_y^2}$, at the position, where the second vortex from the vortex - anti vortex pair was placed originally, $(x_0, y_0) = (-2.99, 0)$.

In the first case $\gamma = 0$, and the vortices move without dissipation. In that case the fluid velocity $v_f \propto 1/r$, where r is the radius of the circle having its centre at that point where the vortex was originally located. Since $r = v_{vort} * t$, $v_f \propto 1/v_{vort} * t$. So, the fluid velocity, v_f , varies as an inverse function with t , $v_f = a/t$, where a is a constant, $a \simeq 1/v_{vort}$. By fitting v_f with an inverse function we obtain a and with the help of a , we have v_{vort} .

In Figure 4.32(a) and Figure 4.32(b), the red/solid line represents the function, $f(t) = a/t$, where $a = 5.89$ and (+) represents, in Figure 4.32(a), the fluid velocity at the position, where the vortex was placed originally ($x_0 = 2.99$) and in Figure 4.32(b), the fluid velocity at the position, where the anti-vortex was placed originally ($x_0 = -2.99$), calculated using the following equations:

$$v_x = -\frac{i}{2}|\psi|^2 \left(\psi^* \frac{\partial \psi}{\partial x} - \psi \frac{\partial \psi^*}{\partial x} \right), \quad (4.2)$$

and

$$v_y = -\frac{i}{2}|\psi|^2 \left(\psi^* \frac{\partial \psi}{\partial y} - \psi \frac{\partial \psi^*}{\partial y} \right). \quad (4.3)$$

These are evaluated at the points: $x_0 = \pm 2.99$ and $y_0 = 0$ and we use them in calculation of the fluid velocity, v_1 and v_2 .

So, if $a \simeq 1/v_{vort}$, the vortex velocity is approximated by $1/a = 1/5.89 = 0.169779$. We compare this value with the vortex velocity using our earlier method (see Table. 4.1). Then, the translation speed of the vortices is, $v_y \sim 1/d_0$, that is to say, $v_y \sim 1/2 * 2.99 = 0.169779$. Putting the two vortices on the line $y_0 = 0$, they will move first in the y direction. So $v_y (= 0.16977)$ and $v_{vort} (= 0.1698)$ coincide! That is a proof that our two methods to calculate the vortex velocity are quite accurate. In both cases our two different methods agree very well.

Let us continue our investigation by putting the vortex - antivortex pair at the same initial positions as before, $x_0 = \pm 2.99$, but now with $\gamma = 0.03$ (see Figure 4.34(a) and Figure 4.34(b)).

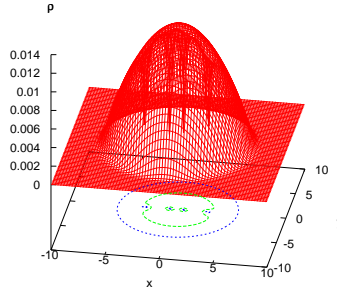


Figure 4.33: 3D plot of the density for two vortex - antivortex pairs with $d_0 = 1.3$ and 5.98 ($x_0 = \pm 2.99$ and ± 0.65) for no dissipation at $t = 0$.

We can see, that when the program is switched from imaginary time to real time, the decrease of the fluid velocity begins from a larger value. In the presence of dissipation ($\gamma \neq 0$), the decrease of the fluid velocity is less than with no dissipation ($\gamma = 0$). So, in a dissipative fluid the decrease of the fluid velocity is slower than without dissipation.

4.5.1 Additional Vortices

Finally, we are interested to see the influence of additional vortices, which we placed in the condensate. So, we put two additional vortex - anti vortex pairs at $x_0 = \pm 0.65$; $y_0 = 0$, as it is shown in Figure 4.33.

The velocities were taken at the points, $x_0 = \pm 2.99$. From the way the fluid velocity decreases, we can infer how the four vortices move. The fluid velocity at these particular points is always the result of the sum of four vector velocities. Notice also that, the difference in that last case is that we have a peak in the decrease of the velocity (see Figure 4.34(c) and Figure 4.34(d)). This is due to the fact that the fluid has received an impulse from the neighbouring vortex. Our explanation is that the two vortices, which are closer to the centre of the condensate move faster and upwards than the others having their initial positions at the measured points and moving downwards.

Accordingly, the other two vortex pairs begin their motion parallel with the first ones, but in opposite directions. However, in the chosen points the velocity first decreases as the vortices move, but after a short time, they are influenced by the other vortices moving in opposite directions with higher velocities. This influence becomes weaker and the velocity continues to decrease as in the two other cases presented earlier.

It is worthwhile also, to compare the initial values of the fluid velocity for these three cases. We choose, for the first and second cases, $t = 0.371$ and for the third case, two times close to that time (see Table. 4.7).

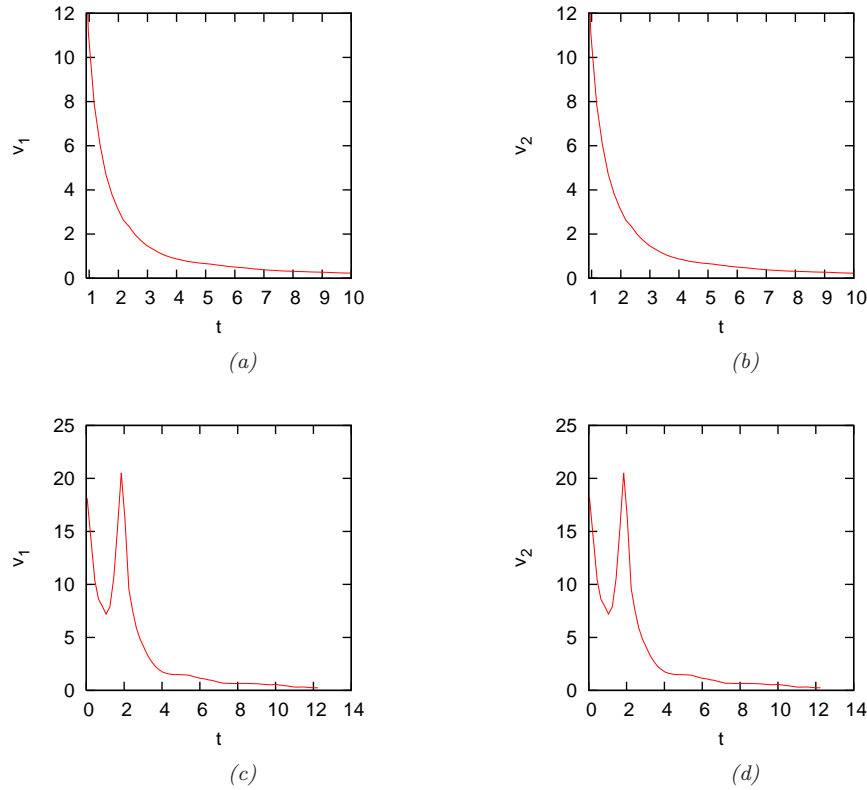


Figure 4.34: For a vortex - anti vortex pair with initial positions, $x_0 = \pm 2.99$; $y_0 = 0$ and for $\gamma = 0.03$, the fluid velocity at position where (a): the vortex of the vortex -anti vortex pair was placed originally, $x_0 = 2.99$; $y_0 = 0$ and where (b): the anti vortex of the vortex -anti vortex pair was placed originally, $x_0 = -2.99$; ($y_0 = 0$). For two vortex - anti vortex pairs with initial positions, $x_0 = \pm 0.65$; ± 2.99 ($y_0 = 0$) and for $\gamma = 0$, the fluid velocity at position where (a): the vortex of the vortex -anti vortex pair was placed originally, $x_0 = 2.99$; $y_0 = 0$ and where (b): the anti vortex of the vortex -anti vortex pair was placed originally, $x_0 = -2.99$; ($y_0 = 0$).

γ	No of vort	t	v_1	v_2
0	2	0.371	37.2422	37.2444
0.03	2	0.371	40.3349	40.3259
0	4	0.247	14.2484	14.2482
0	4	0.447	10.3824	10.3796

Table 4.7: Fluid initial velocity at the same position, where the firsts vortex - antivortex pair were placed originally as a function of γ for two and four vortices.

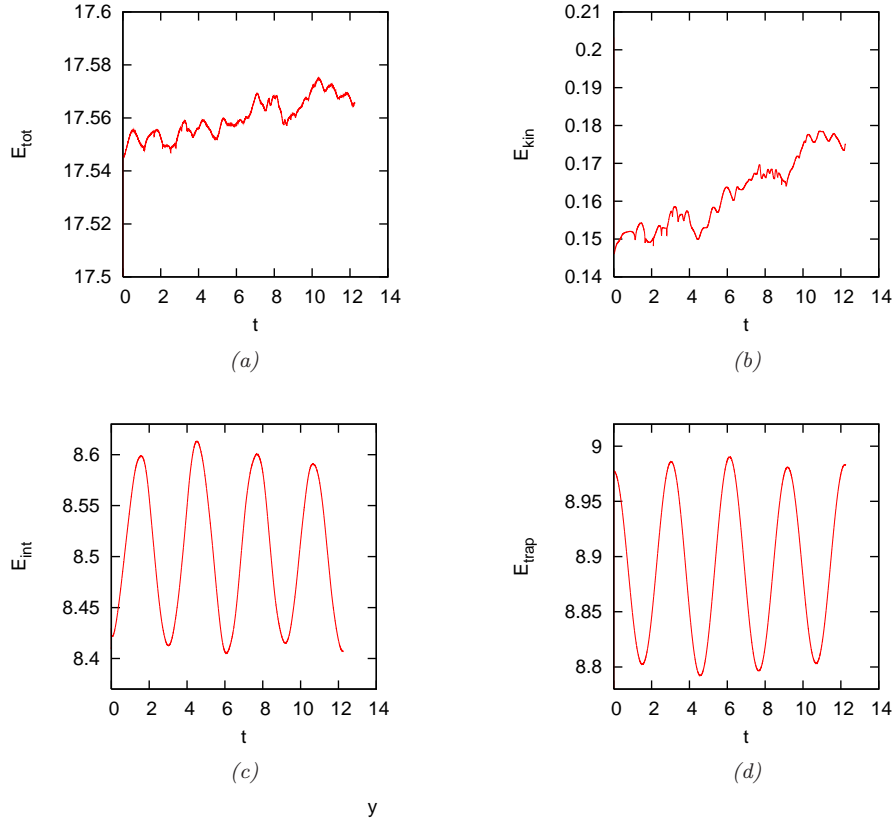


Figure 4.35: For two vortex - antivortex pairs with $d_0 = 1.3$ and 5.98 ($x_0 = \pm 2.99$ and ± 0.65), and for $\gamma = 0$ (a,b): (left): the total energy and (right): the kinetic energy and (c,d): (left): the internal energy and (right): the trap energy.

In this part of the thesis, we have examined for the vortex and anti-vortex pair, the decrease with time of the fluid/condensate velocity, with its x - and y -components, v_1 and v_2 in three different environments, at those points, where the vortex pair began to move. In the case of two vortex - antivortex pairs for that short time, when the data was taken, we investigate the total energy, (E_{tot}), kinetic energy (E_{kin}), internal energy (E_{int}) and trap energy (E_{trap}) with the help of figures: Figure(4.35(a) - 4.35(d)).

Chapter 5

Motion of Random Vortex - Anti Vortex Pairs and Vortex Lattice Formation

5.1 Introduction

In this chapter, we present for an array of vortices the increase/decrease rate of different energies and L_z with time as a function of dissipation (for the time corresponding to the entering of the vortices in the condensate).

In different dissipative environments, for the case of randomly placed vortex - anti vortex pairs, we study the decrease/increase rate of different energies and L_z together with the number of vortices with time and find exponential behaviours.

5.2 Motion of an Array of Vortices

Before beginning with the random case, let us study the variation of different energies and the z - component of the angular momentum with time and different dissipations for an *array of vortices* (see Figure 5.1).

Now, $\Omega \neq 0$. So, for $\Omega = 0.75$ the vortices come in automatically in the condensate. To have the right shape and initial conditions (the Thomas-Fermi approximation), the *GPE* first runs in imaginary time. Then the program is switched to real time with suitable values for Ω and γ . For small values of dissipation, like $\gamma = 0.003$, the *decrease* of different energies and L_z with time is *not* so significant (see the saturated values in Figure 5.2(a) and Figure 5.2(b)). These plots show the development of E_{tot} and L_z . When the vortices enter the condensate, L_z increases and E_{tot} oscillates (Observe, that the y -axis of L_z begins from 0, but for the case of E_{tot} , its value begins from larger value!), which is in accordance with both experiments (see Madison *et al.* (2001)) and with other simulations (see Tsubota *et al.* (2002)).

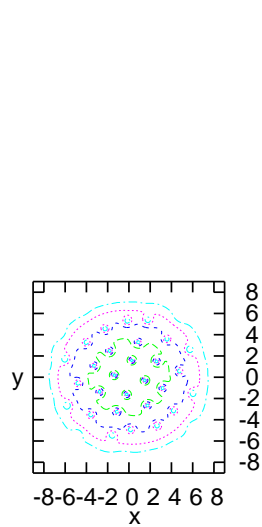


Figure 5.1: Contour plot of density with an array of vortices in case of $\gamma = 0.03$ and for $\Omega = 0.75$.

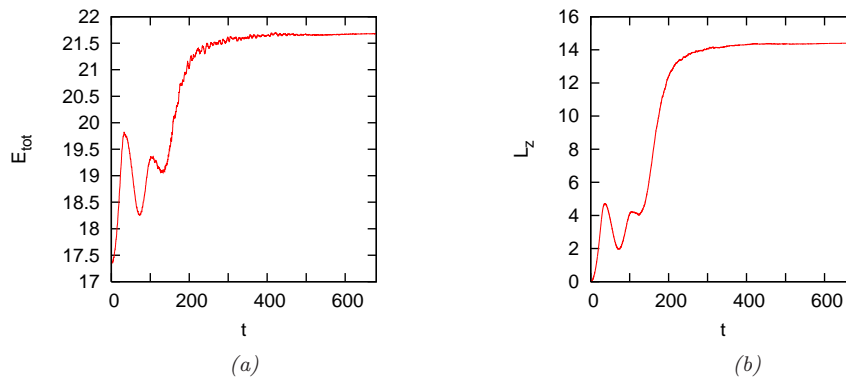


Figure 5.2: For an array of vortices with $\gamma = 0.003$ and for $\Omega = 0.75$ (a): the total energy as a function of time and b): the z -component of the angular momentum as a function of time. (With small dissipation the decay of the saturated values due to γ is not so significant.)

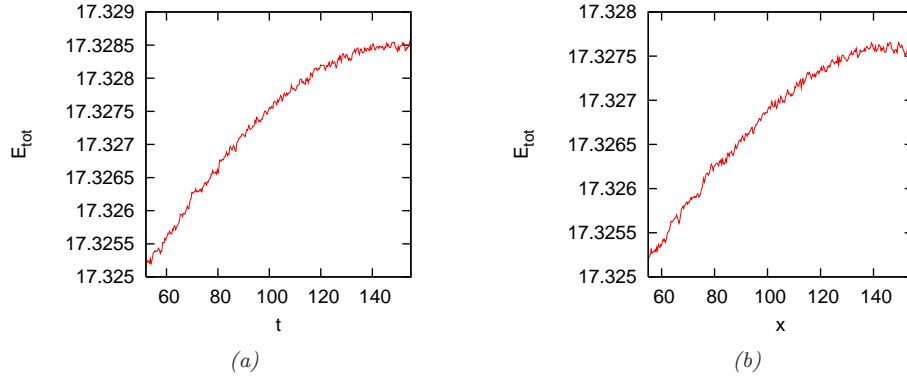


Figure 5.3: For an array of vortices with $\gamma = 0.003$ the increase of the total energy until its saturated value for (a): $\Omega = 0.7$ and (b): $\Omega = 0.85$.

For small γ , we have a considerable change only in that time when the vortices come in (see Figure 5.3(a) and Figure 5.3(b) for $C = 1400$). That was the reason to study for larger value of dissipation, like $\gamma = 0.03$ the increase of different energies and L_z , in the above-mentioned case.

We are only interested to see the maximum values, the saturated values and the difference between them.(see Table C.11 for the case of $\gamma = 0.03$ and $\Omega = 0.75$ and Table C.12 for the case of $\gamma = 0.07$ and $\Omega = 0.75$).

A more detailed study of increase/decrease of energies/ L_z with time was done with the help of their corresponding values in Appendix C (see Table C.13) together with Figure(5.5(a) - 5.5(l)) and Figure(5.6(a) - 5.6(c)).

In contrast to the case of $\gamma = 0.03$, increasing the dissipation, for example to $\gamma = 0.07$, we observe that the decrease of the saturated values become exponential again (see Figure 5.4(a)). We obtain for the decay rate, $\beta = -0.002084$ as one can see in Figure 5.4(c).

So, for larger values of γ , the fluctuations of these functions disappear (compare Figure 5.2(a) or Figure 5.2(b) with Figure 5.4(a) and Figure 5.4(b)). Notice that, in the case of $\gamma = 0.07$, the decrease became smoother as well with an exponential decrease (see Figure 5.4(c)).

5.3 Randomly Placed Vortex - Anti Vortex Pairs

We place randomly vortex pairs in the condensate and in that way we create turbulence. Eight pairs of vortex - anti vortex with initial separation distance, $d_0 = 1.8$ between them were established (for details ,see Table. C.14).

Our program chooses randomly a pair of numbers, nrx and nry , together with nrr between 0 and 1. Then with the help of $\alpha = nrr * 2\pi$, we obtain random angles. In the beginning our vortex, will move in that direction. From the random points, nrx and nry , we have obtained the coordinates x and y by: $(nrx - 0.5) * 16$ and $(nry - 0.5) * 16$. Having for all (now) 16 vortex pairs

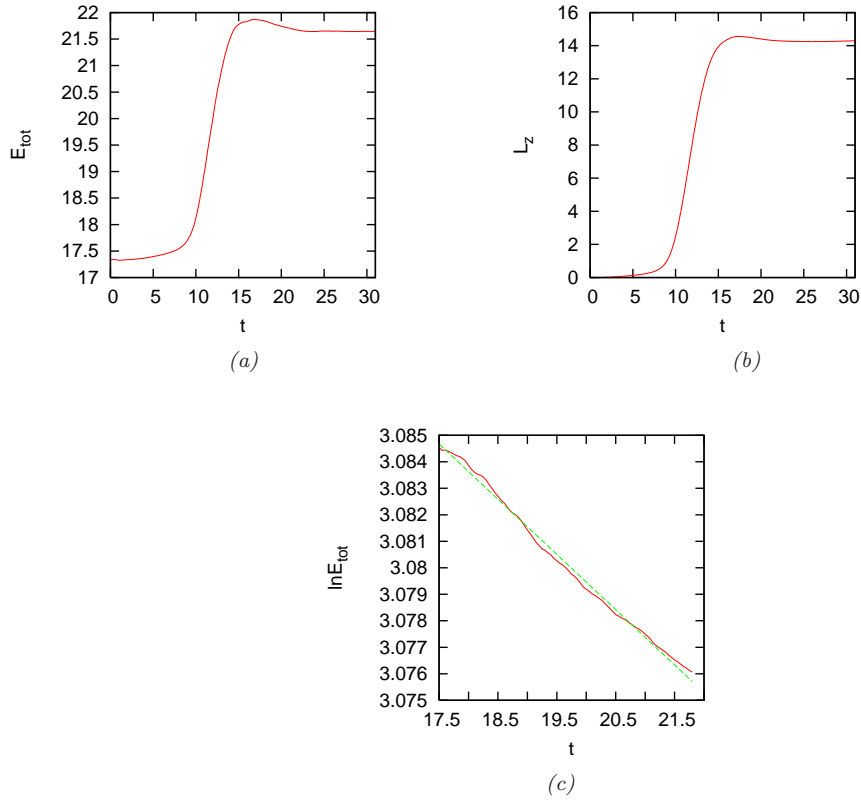


Figure 5.4: For an array of vortices with $\gamma = 0.07$ and $\Omega = 0.75$ (a,b): (left): the total energy as a function of time and (right): the z -component of the angular momentum as a function of time and the (c): log (base e) of the total energy as a function of time compared with $f(x) = a + bx$, where $a = 3.1211$ and $b = -0.002084$. We can see that with dissipation the total energy decreases. For larger values of γ , this decrease is more significant.

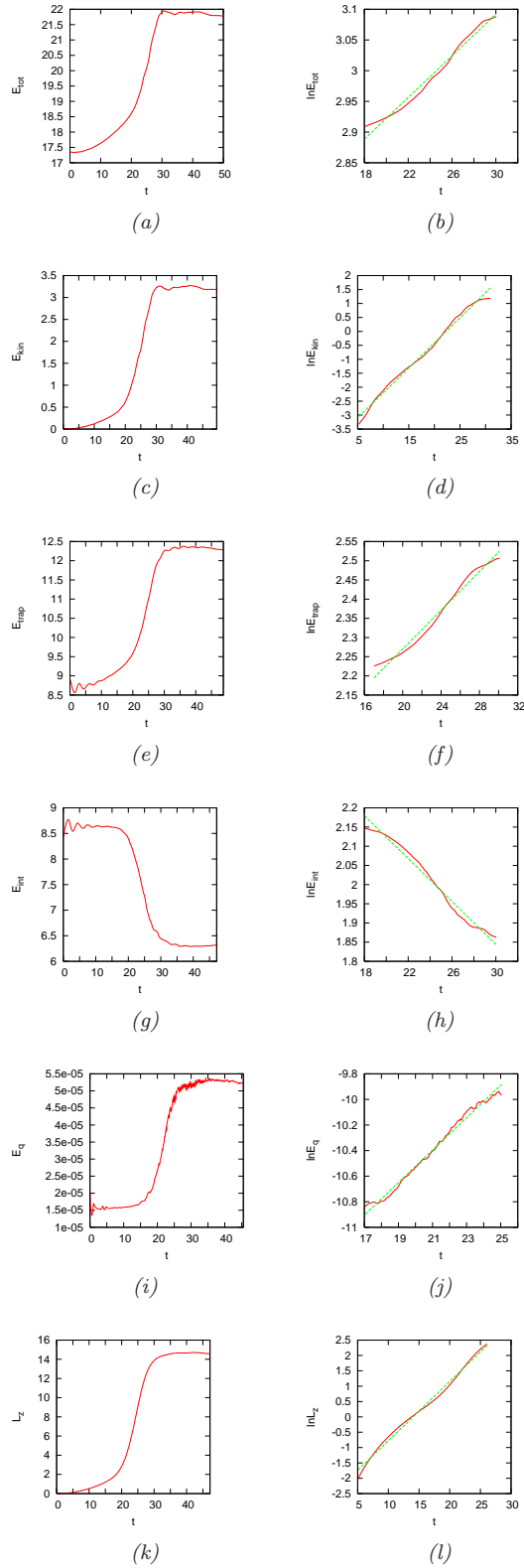


Figure 5.5: For an array of vortices with $\gamma = 0.03$ and $\Omega = 0.75$, (left): the different energies/ L_z of the (a): total energy, (c): kinetic energy, (e): trap energy, (g): internal energy, (i): quantum energy, (k): L_z and (right): the corresponding log (base e) values as a function of time (compared with $f(x) = a + bx$), where (b): $a = 2.5832$ and $b = 0.016962$, (d): $a = -3.9922$ and $b = 0.179224$, (f): $a = 1.7665$ and $b = 0.025185$, (h): $a = 2.6821$ and $b = -0.027926$, (j): $a = -13.0613$ and $b = 0.126919$ and (l): $a = -2.7013$ and $b = 0.192771$.

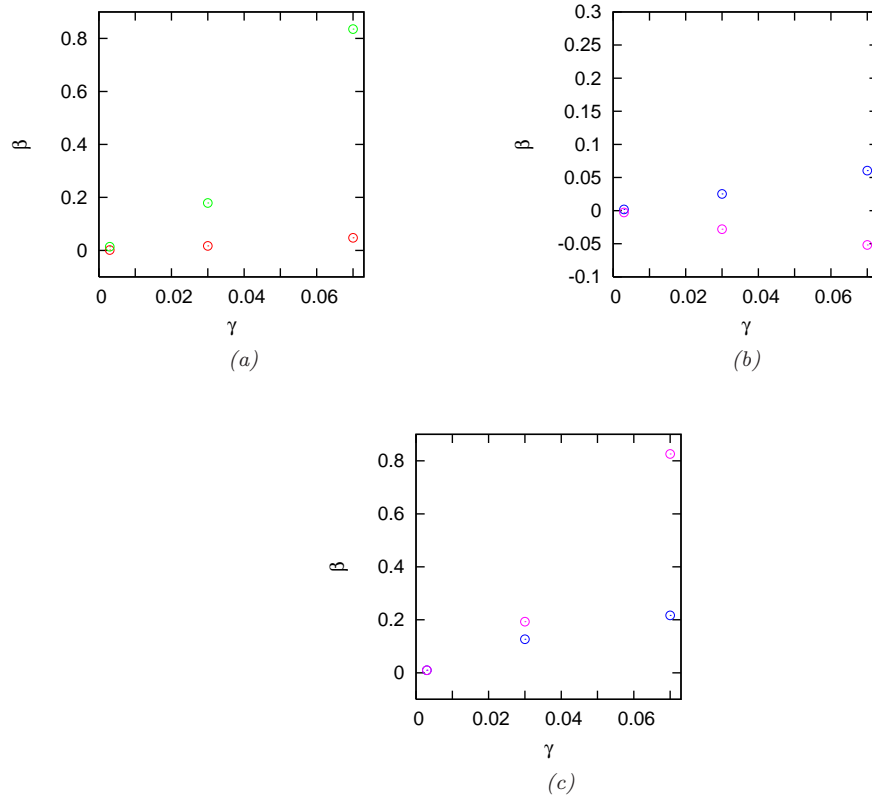


Figure 5.6: For an array of vortices for $\Omega = 0.75$ (a,b): (left): the increase rate of the total energy (red circles/lower circles) and kinetic energy (green circles/upper circles) and (right): the increase rate of the trap energy (blue circles/upper circles) and the decay rate of the internal energy (purple circles/lower circles) and (c): the increase rate of the quantum energy (blue circles/lower circles) and the z -component of the angular momentum (purple circles/upper circles) as a function of γ .

the right starting-points, x and y , we put our vortex and anti-vortex pairs on the $\pm\pi/2$ directions, on $\pm r_0 = 0.9$ locations, so the initial distance between every vortex - anti vortex pair becomes, $d_0 = 1.8$.

Also, in the case of random vortex - anti vortex pairs, the different energies (except of the internal energy, E_{int} and L_z , which increase) decrease exponentially, see Figure(5.7(a) - 5.7(f)). Notice that, we have calculated with the help of $f(x) = \alpha + \beta x$, the decay rate β , see Figure(5.8(a) - 5.8(c)). The proper values of β , can be seen in Appendix C (see Table. C.15 and Table. C.16).

So, as we mentioned earlier, we place eight pairs of random vortex - anti vortex pairs in the condensate. Finally, we obtain eight vortices due to the loss in the case, when the program is running in imaginary time and due to the fact that some of the vortices have their initial position outside of the system. The decrease of the number of these eight vortices divided by the initial vortex - number vs. time for dissipations $\gamma = 0.003; 0.048; 0.07$ and 0.1 can be seen in Figure(5.9(a) - 5.9(e)). These functions are exponential functions and by that, we illustrate the behaviour of the number of randomly placed vortices with time.

Our first conclusion is that the decay rate of number of the vortices vs. time varies linearly with dissipation, γ (see Figure 5.9(f) and Table. C.17). Our second conclusion is that with smaller γ the exponential function of number of vortices vs. time needs more time to decrease and for larger γ 's, these exponential functions becomes steeper.

5.4 Motion of Vortex - Anti Vortex Pairs and Formation of a Mini Turbulent System

For $\Omega = 0$ and $\gamma = 0.003$, we show with the help of some density plots, the parallel motion of a vortex-anti vortex pair with time, see Figure(5.10(a) - 5.10(d)) and also the development of annihilation scenario, see Figure(5.10(e) - 5.11(d)), with sound wave production (see Figure 5.11(a), Figure 5.11(b) and Figure 5.11(e)), that transform the condensate into a turbulent system, see Figure 5.11(f).

5.5 Vortex Lattice Formation in a Rotating Bose-Einstein Condensate

According to our original equation (see Eq. 1.52), we solve numerically the Gross-Pitaevskii equation. This form is prepared for our *Fortran* codes, (see Eq. 1.55). In this case, first we have an equilibrium condensate (with stationary potential, $\Omega = 0$) with a circular shape, (see Figure 5.12(a) and Figure 5.12(b)).

The dynamics of the condensate density $|\Psi|^2$ is investigated with the help of some contour-plots of the density (see plots (a)), and of the phase (see plots (b)). This method is a direct proof of a test of our computer code. We stress that this result is not new; (Tsubota *et al.*, 2002) has obtained similar results.

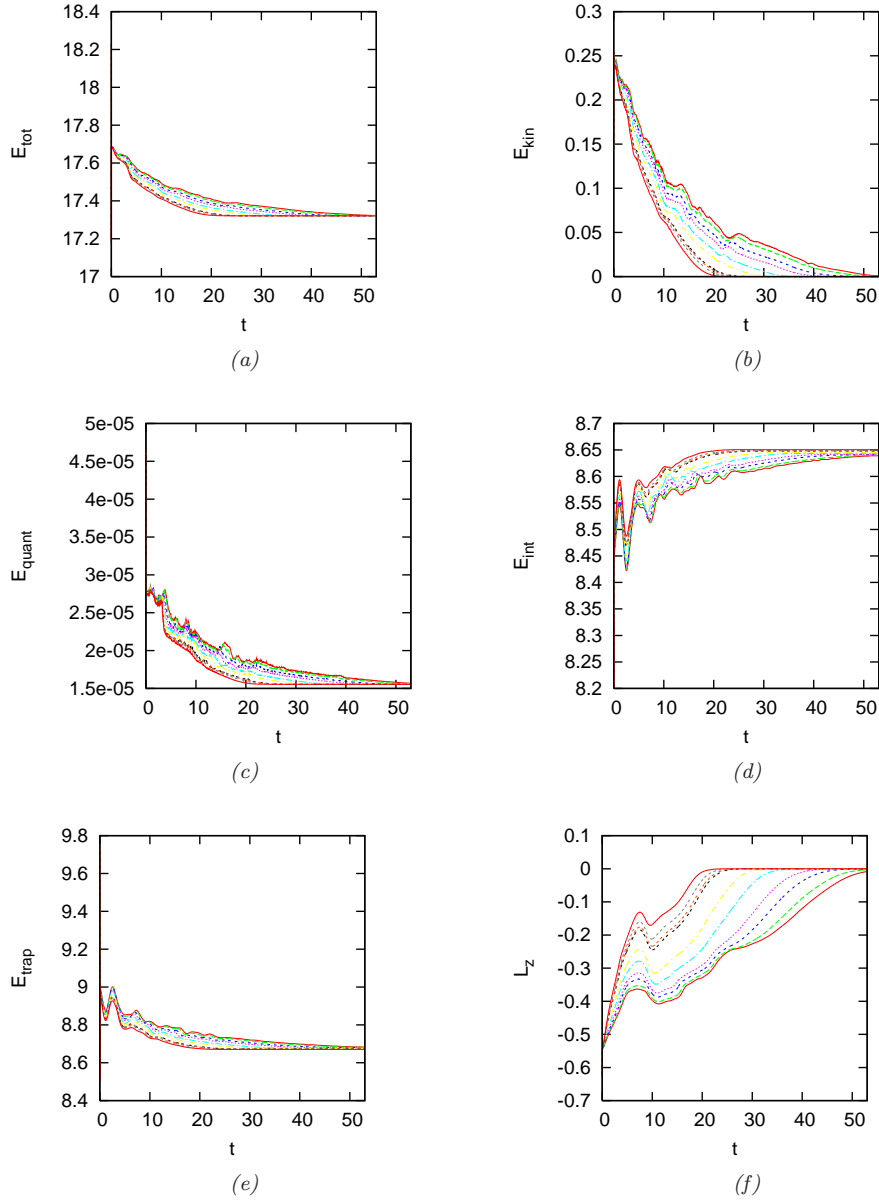


Figure 5.7: For randomly placed vortex - anti vortex pairs and for dissipations: $\gamma = 0.03; 0.032; 0.036; 0.04; 0.048; 0.056; 0.07; 0.072; 0.076$ and 0.084 (from the red upper line to the red lower line) (a,b): (left): the total energy and (right): the kinetic energy and (c,d): (left): the quantum energy and (right): the internal energy and (e,f): (left): the trap energy and (right): the z-component of the angular momentum as a function of time.

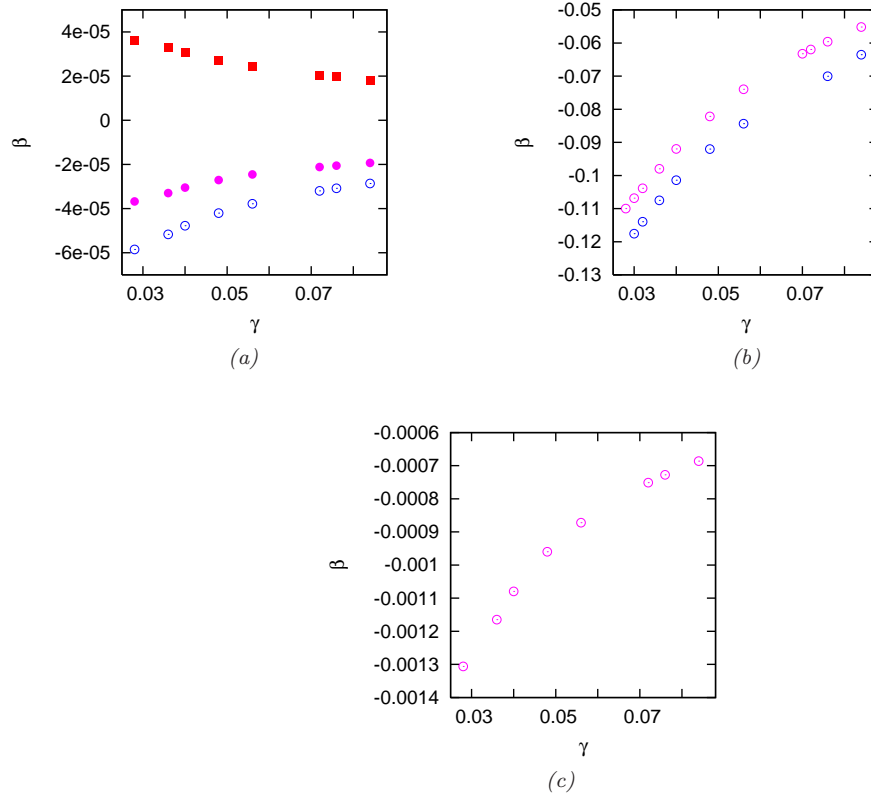


Figure 5.8: For random vortex - anti vortex pairs with $d_0 = 1.8$ (a,b): (left): the decay/increase rate, β of the total energy (purple filled circles/middle filled circles), of the trap energy (blue circles/lower circles) and of the internal energy (red filled squares/ upper filled squares) and (right): the increase rate, β of the kinetic energy (purple circles/upper circles) and of the z -component of the angular momentum (blue circles/lower circles) and (c): the increase rate, β of the quantum energy (purple circles) as a function of γ .

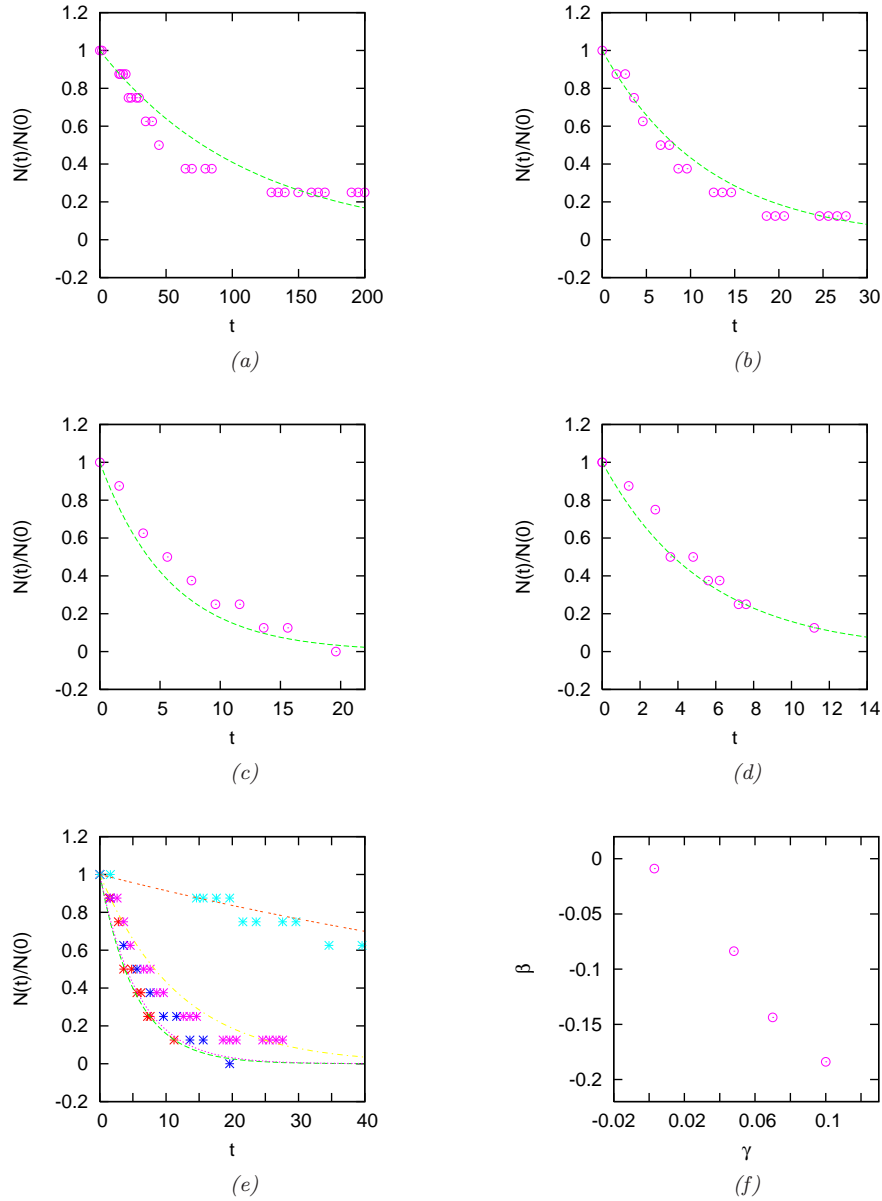


Figure 5.9: Number of vortices divided by the number of vortices at $t = 0$ as a function of time, for random vortex - anti vortex pairs with $d_0 = 1.8$ compared with $f(x) = \exp(\beta t)$ for (a): $\gamma = 0.003$ and $\beta = -0.0089$, (b): $\gamma = 0.048$ and $\beta = -0.0837$, (c): $\gamma = 0.07$ and $\beta = -0.1437$, (d): $\gamma = 0.1$ and $\beta = -0.184$, (e): $\gamma = 0.003; 0.048; 0.07; 0.1$ (from top to bottom) and the corresponding β 's: $-0.0089; -0.0837; -0.1437; -0.184$, (f): Decay rate, β of the number of vortices as a function of γ , corresponding to Figure(5.9(a) - 5.9(d))

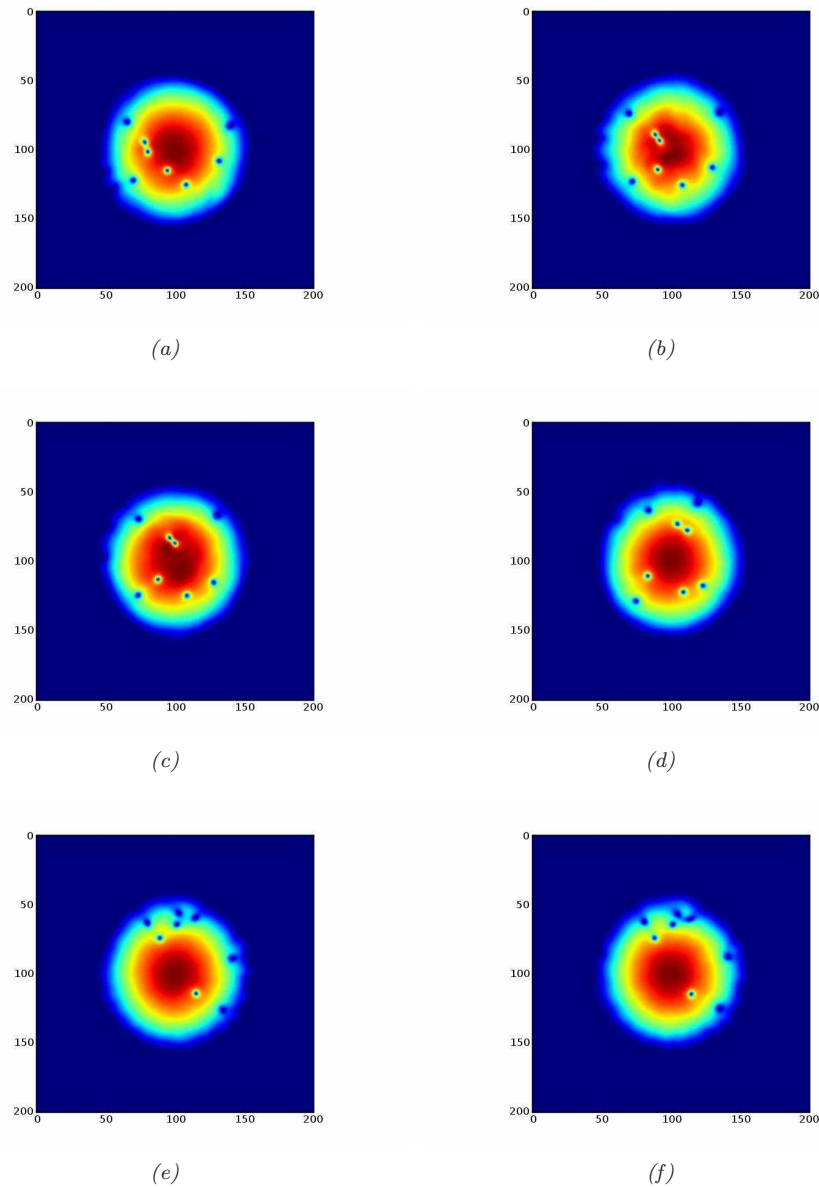


Figure 5.10: Density profile of the condensate for a vortex-anti vortex pair at (a): $t_1 = 15$ and (b) $t_2 = 21$. (A vortex-anti vortex pair begins to move together.) and at (c): $t_1 = 25$ and (d) $t_2 = 33$. (The pair stops to move together.) and at (e): $t_1 = 175$ and (f) $t_2 = 176$. (A vortex-anti vortex pair begins to destroy each other).

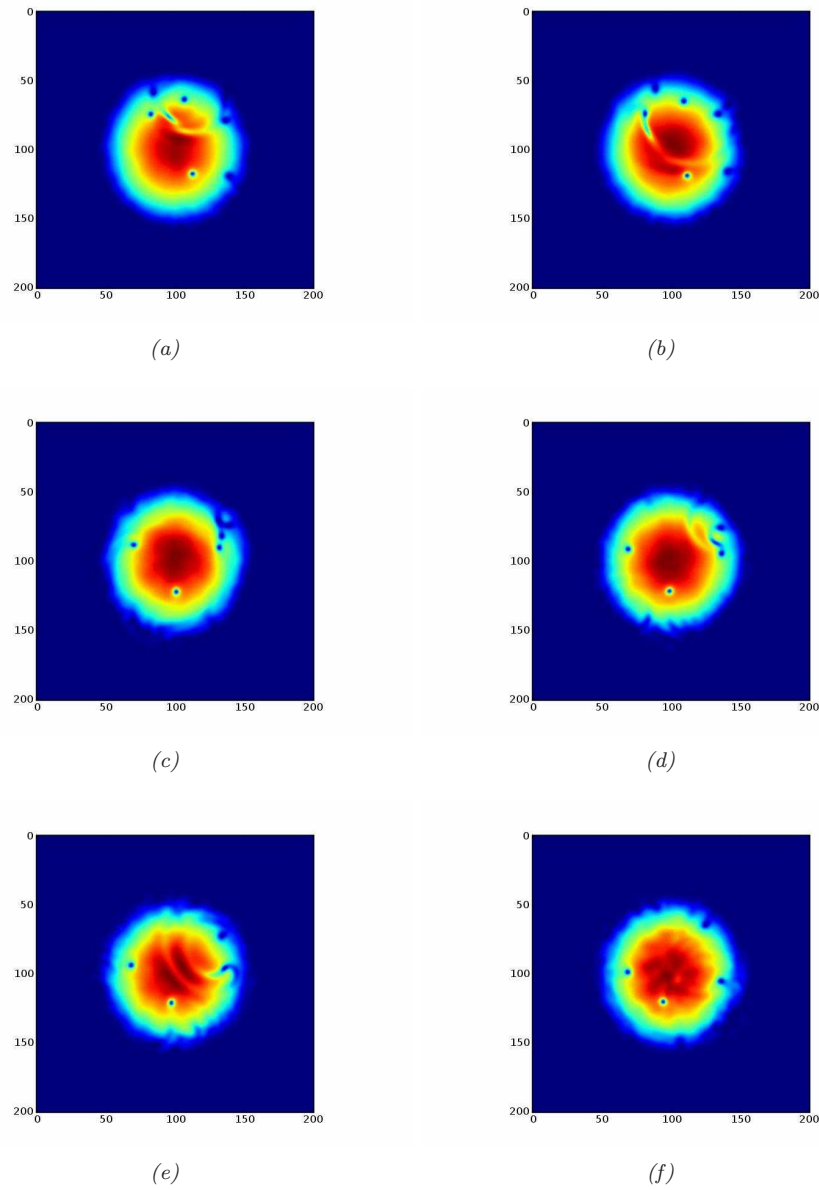


Figure 5.11: Density profile of the condensate for a vortex-anti vortex pair at (a): $t_1 = 182$ and (b) $t_2 = 185$. (We can see the annihilation and the sound wave production,) and at (c): $t_1 = 208$ and (d) $t_2 = 212$. (Two vortices annihilate each other.) and at (e): $t_1 = 215$ and (f) $t_2 = 222$. (Two big sound waves cross the condensate (e) and the system becomes turbulent (f)).

As a consequence of setting for $\Omega = 0.85$, the trapping potential begins to rotate. Because of the small anisotropy of the trapping potential, V_{tr} , the condensate is elongated, (see Figure 5.12(c) together with Figure 5.12(d)).

Later, since the boundary surface is unstable, the surface with low curvature becomes host to surface waves, (see Figure 5.12(e) and Figure 5.12(f)). These ripples make themselves visible at vortex cores, (see Figure 5.12(g) and Figure 5.12(h)).

More and more vortices enter the condensate, (see Figure 5.13(a); Figure 5.13(b); Figure 5.13(c) and Figure 5.13(d)), and form a vortex lattice, (see Figure 5.13(e) and Figure 5.13(f)). At that point, the angular momentum is transferred into quantised vortices and the condensate recovers its circular like form.

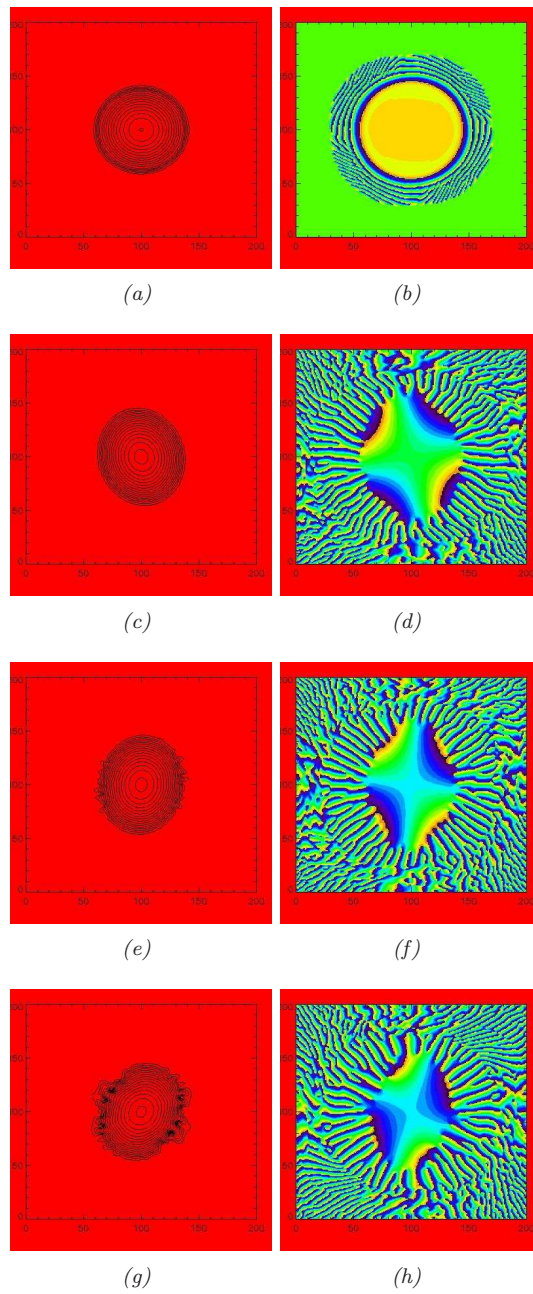


Figure 5.12: Density profile (left) and phase profile (right) of the condensate for $\Omega = 0.85$ at (a,b) $t = 0.2$, (c,d) $t = 11$, (e,f) $t = 16.4$, (g,h) $t = 20$.

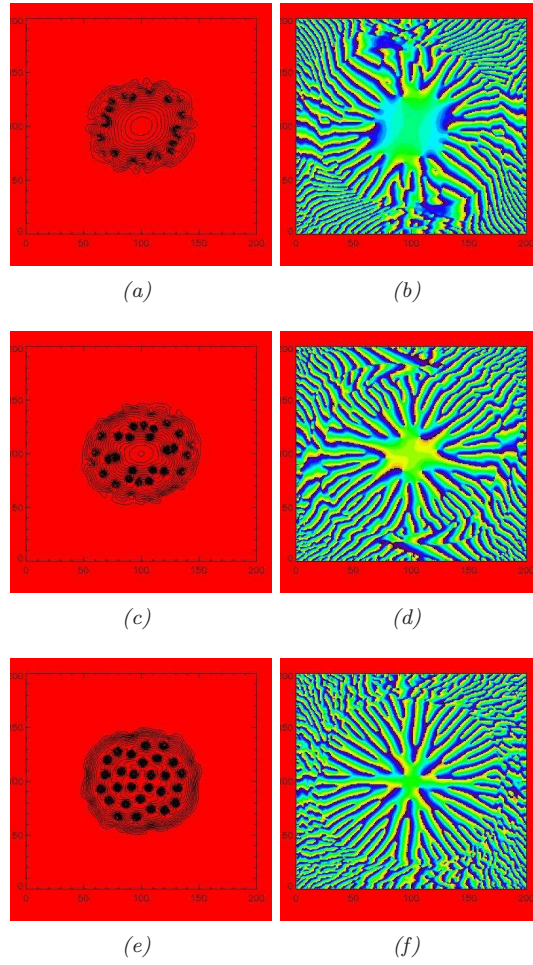


Figure 5.13: Density profile (left) and phase profile (right) of the condensate for $\Omega = 0.85$ at (a,b) $t = 22.4$, (c,d) $t = 26.8$, (e,f) $t = 54.8$.

Chapter 6

Summary - Future Work

6.1 Conclusions

We performed numerical simulations of vortex motion in a trapped Bose-Einstein condensate by solving the two-dimensional Gross-Pitaevskii Equation in the presence of a simple phenomenological model of interaction between the condensate and the finite temperature thermal cloud.

At zero temperature, the trajectories of a single, off - centred vortex precessing in the condensate, and of a vortex - antivortex pair orbiting within the trap, excite acoustic emission. At finite temperatures the vortices move to the edge of the condensate and vanish. Our calculation showed that, some features of the motion of vortices in a Bose-Einstein condensate can be modelled relatively well using Schwarz's vortex dynamics. In particular, we had been able to relate our phenomenological damping parameter, γ , to friction coefficients α and α' .

So, by fitting the calculated vortex position (at given value of γ) to the solution of Schwarz's equation, we deduced the friction coefficients α and α' . The results slightly depends on the initial position of the vortex because the condensate is not homogeneous near the edge. For initial condition sufficiently close to the centre of the condensate, we found that, α is proportional to the dissipation parameter γ . The transverse friction coefficient, α' , is much smaller than α , thus more difficult to determine it. We found that, α' is approximately proportional to γ only for small values of γ .

It is well known that, in the absence of dissipation, a vortex - antivortex pair set at $(\pm x_0, 0)$ in an infinite homogeneous condensate moves with (dimensionless) translational speed $v_\infty = 1/(2x_0) = 1/d_0$, where d_0 is the initial separation distance between the vortices. We defined v_{pair} , which is the measured velocity of the vortex pair when it moves near the centre parallel to the y -axis. Then, we compared v_{pair} with v_∞ .

Our result was compared to the classical velocity of a pair of point vortices, which was studied by (Jones & Roberts, 1982). For larger initial separation distance, our result, v_o was similar to the authors' result, v_a . For example, for $d_0 = 3.5$, $v_o = 0.29$ and $v_a = 0.3$. For smaller distance, our result was different from their. For example, for $d_0 = 1.78$, $v_o = 0.56$ and $v_a = 0.4$.

The natural question which arised was then, the relation between γ and the temperature ratio T/T_c , where T_c is the critical temperature. To answer this question we used results of unpublished preliminary investigations (Jackson *et al.*, 2008) using the Zaremba-Nikuni-Griffin (ZNG) finite-temperature theory Zaremba *et al.* (1999), which showed that, for $C = 500$ and for a single vortex initially located at $(x_0, y_0) = (1.3, 0)$, the effective friction coefficient is $\alpha \approx 0.0018$ at $T/T_c = 0.15$ and $\alpha = 0.0025$ at $T/T_c = 0.267$. Similar results were found for $(x_0, y_0) = (0.65, 0)$. Setting $C = 500$, we reran our calculations of single - vortex trajectories with the same initial condition $(x_0, y_0) = (1.3, 0)$ and found, that we needed to set $\gamma = 0.044$ to obtain the same value $\alpha = 0.0020$ of ref Jackson *et al.* (2008), and $\gamma = 0.08$ to obtain $\alpha = 0.0025$. We concluded (Madarassy & Barenghi, 2008a) that $\gamma = 0.044$ and 0.08 correspond respectively to $T/T_c = 0.15$ and 0.27 . The effective friction coefficient, α from unpublished investigations of Jackson *et al.* (2008) quantitatively agreed with that found in (Berloff & Youd, 2007b,a): $\alpha = 0.1(T/T_c)^2$, which gave $\alpha = 0.0022$ for $T/T_c = 0.15$ and $\alpha = 0.007$ for $T/T_c = 0.267$ (compared with 0.0018 and 0.0025 respectively). Finally, our small values of α' were consistent with the result of the ZNG theory (Jackson *et al.*, 2008) and with Berloff's model (Berloff & Youd, 2007b,a).

In the presence of dissipation, the total energy, E_{tot} , of the vortex - antivortex pair decreases with time, and so do the contributions E_{kin} , E_{int} , E_q and E_{trap} to E_{tot} . We observed, that the energy decay was faster if the vortices of the pair had smaller initial separation distances. Our study, in regard to the system's energy balance showed, that we had the best values for the case of small dissipation and large initial separation distance between the vortices.

We studied the sound production with the help of sound energy and found an anti-correlation between the sound energy and vortex energy. We observed that for different dissipations, the radial position of the vortex vs time behaved as an exponential function. The same was valid for random vortex - anti vortex pairs, when we investigated the number of vortices as a function of time for different γ 's.

We suggested a method to create turbulence in a Bose-Einstein condensate. Our aim was to show that the phase imprinting method could be used to study the formation of rotating turbulence accompanied by acoustic emissions in a simple 2-dimensional condensate. This method consisted firstly, in creation of an ordered vortex array, and, secondly, in imprinting a phase difference in different regions of the condensate. By solving the two-dimensional Gross-Pitaevskii equation, we showed that the motion of the resulting positive and negative vortices was disordered (Madarassy & Barenghi, 2008b).

6.2 Decay of Soliton - like Perturbations into Vortices. Creation of a Mini Turbulent Vortex System

Finally, we suggest a method to create turbulence in a Bose-Einstein condensate. The method consists in, firstly, creation of an ordered vortex array, and, secondly, imprinting a phase difference in different regions of the condensate in the case of no vortices and a vortex array.

The study of the turbulence in superfluids - atomic Bose-Einstein condensates and liquid helium II. (Barenghi *et al.*, 2001) - help us to understand better issues of classical Euler fluid dynamics. The large scale turbulence of quantised vortices, was well studied in superfluid helium II and $He - 4$ (Tsubota *et al.* (2004); Araki *et al.* (2003)). Many remarkable similarities between classical turbulence and superfluid turbulence have been noticed. For example the classical $k^{-5/3}$ Kolmogorov energy spectrum (where k is the wavenumber) was observed in helium II, when agitated by rotating propellers (Maurer & Tabeling, 1998). The same spectrum was apparent in the numerical simulations of Nore et al (Nore *et al.*, 1997) and of Tsubota and collaborators (Araki *et al.*, 2002; Kobayashi & Tsubota, 2005). Another example is the classical $t^{-3/2}$ temporal decay of turbulence (where t is time) which was measured in helium II behind a towed grid (Smith *et al.*, 1993).

The disadvantage of studying turbulence in BEC is that the system is small with few vortices. On the other hand, such a system can aid the study of turbulence, for example there is a relatively good visualisation of individual vortices with more details. Particularly, we can study details of transformations of the kinetic energy into acoustic energy due to the vortex reconnection and vortex acceleration.

With the *Phase Imprinting Method* $\psi \rightarrow \psi e^{i\pi}$, we produce dark soliton-like perturbations in two ways. In the Case I (initially no vortices in the condensate), in the upper two quadrants: $\psi' = \psi$ for $y < 0$ and $\psi' = \psi e^{i\pi}$ for $y > 0$ (see Figure 6.1(b)). In the Case II, we use this method in the upper left quadrant, $x < 0$ and $y > 0$ and bottom right quadrant, $x > 0$ and $y < 0$ (see Figure 6.4(b), Figure 6.5(a) and Figure 6.5(b)).

Dark solitons, in matter waves are characterised by a particular *local density minimum* and a *sharp phase gradient* of the wave function at the position of the minimum. Dark solitons are 1D objects and in 2D and 3D systems are characterised to be unstable. They decay into more stable vortex structures. This phenomenon is known as the *snake-instability* and it was observed first in nonlinear optics (Mamaev *et al.*, 1996).

In the Case I, a plot of the density profile, for $\Omega = 0$ and $\gamma = 0$, shows that the perturbation starts to move and bends due to the difference in the density (see Figure 6.2(a)). Its velocity is larger in the centre and three pairs of vortices go into the boundary, therefore finally we have only two vortex - anti vortex pairs (see Figure 6.2(b)).

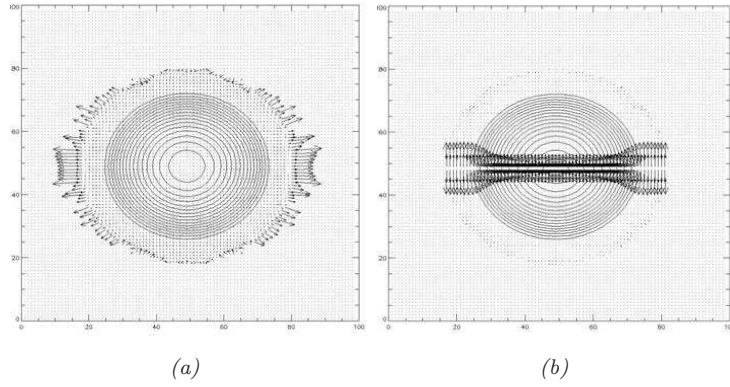


Figure 6.1: (a): Density of the condensate at the beginning without perturbations/vortices. (b): Perturbation created from the phase change. An original sound wave forms and propagates.

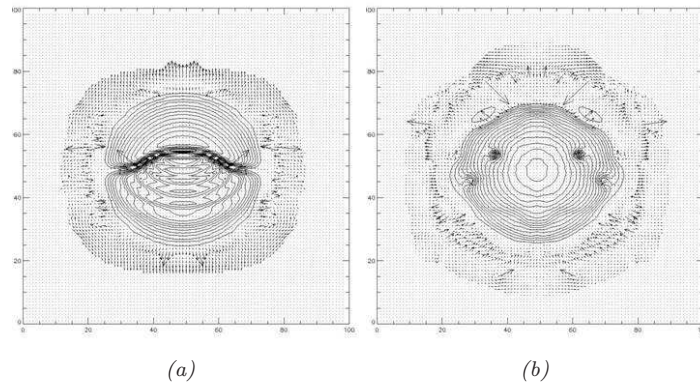


Figure 6.2: (a): Perturbation decays into vortex pairs and simultaneously sound waves appear. (b): From originally five pairs of vortices, only two pairs have survived.

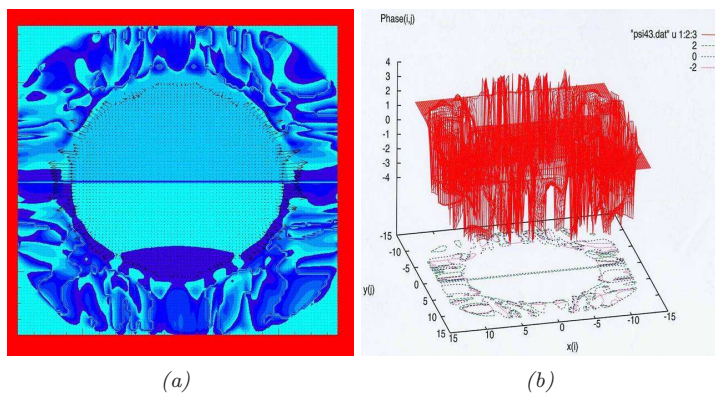


Figure 6.3: (a): Phase of the condensate for Case I. At the edge of the condensate both $Imag(\psi)$ and $Real(\psi) \rightarrow 0$. Clearly, the phase, which is: $Phase = \tan^{-1}(Imag\psi/Real\psi) \rightarrow 0$. We note the large fluctuations of the phase on the outer part of the condensate. (b): We can see the different phase in the two regions: $y > 0$ and $y < 0$.

We define the phase as: $Phase = \tan^{-1}(Im\psi/Re\psi)$ (see Figure 6.3(a), where the different colours describe the phase change, $\Delta\Phi$ which is π and vary from 0 to π). In Figure 6.3(b), we present a 3D description of the phase function.

In the Case II, following Leadbeater *et al.* (2001), at $t = 0$ we start with a non-rotating condensate to have our initial Thomas -Fermi condition. Later, we put $\Omega = 0.85$ and we create a stable lattice of 20 vortices. Density and phase profiles of the condensate are shown in Figure 6.4(a) and Figure 6.4(b). At $t = 200$ (see Figure 6.4(b)), we suddenly perform the following phase imprinting as we explained before:

$$\psi \rightarrow \psi \quad \text{for} \quad x < 0, y < 0 \quad \text{and} \quad x > 0, y > 0, \quad (6.1)$$

$$\psi \rightarrow e^{i\pi}\psi \quad \text{for} \quad x < 0, y > 0 \quad \text{and} \quad x > 0, y < 0. \quad (6.2)$$

Figure 6.5(a) and Figure 6.5(b) show the condensate after the phase imprinting. Positive and negative vortices interact and move due the velocity field which they induce on each other. Figure 6.6(a) and Figure 6.6(b) show density and phase profiles at $t = 201.95$ and reveal that large density oscillations (sound waves) are present in the condensate.

Also, in the Case II, by applying twice the *Phase Imprinting* method we create *mini turbulence* in the BEC, (see Figure 6.6(a) and Figure 6.6(b)).

So, the development of the turbulence is visualised by the snapshots of the density and phase profile, (see Figure 6.4(a), Figure 6.4(b), Figure 6.5(a), Figure 6.5(b), Figure 6.6(a) and Figure 6.6(b)).

On account of the confined and finite size of the condensate, the sound waves are reflected from the edge of the condensate and reinteract with the vortex pairs. When E_{sound} is approaching its maximum, E_{vortex} is approaching its minimum. As we know, $E_{kin} = E_{sound} + E_{vortex}$, (see Figure 6.7). The interaction of positive and negative vortices leads to a disordered motion of the vortices, see (Madarassy & Barenghi, 2008b).

In our future work, we plan to examine the formation of patterns of the same type of vortices in the case of vortex - anti vortex pairs placed randomly in the condensate. In order to observe this phenomenon, we need a larger condensate with more vortex - anti vortex pairs.

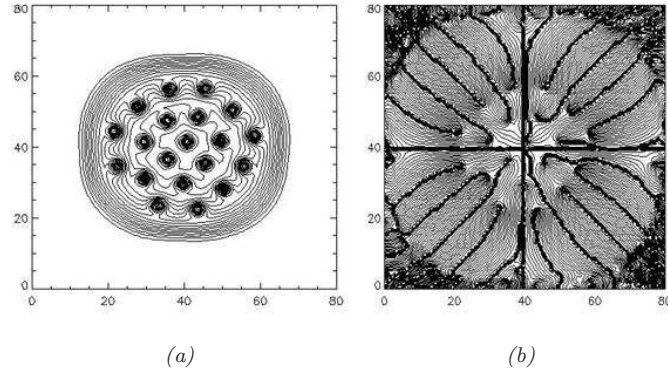


Figure 6.4: Stable condensate with $N = 20$ vortices for $\Omega = 0.85$ (a): at $t = 199.8$ before the phase imprinting. The vortices are visible as holes in the density profile or (b): as discontinuities from 0 to 2π of the phase profile at $t = 200$.

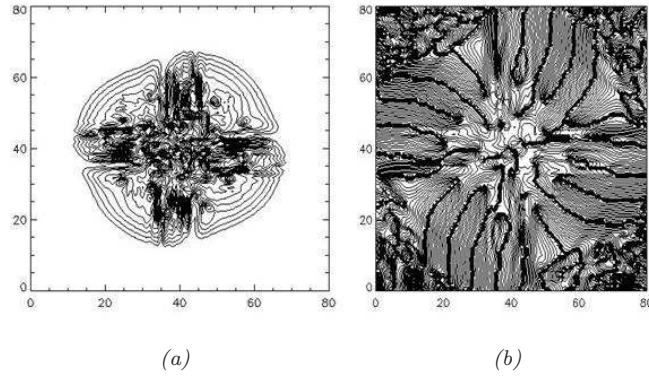


Figure 6.5: (a): Density and (b): phase profiles at $t = 200.4$ corresponding to Figure 6.4.

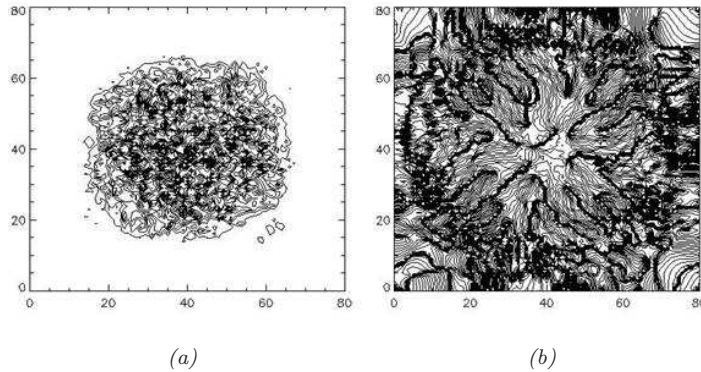


Figure 6.6: (a): Density and (b): phase profiles at $t = 201.95$ corresponding to Figure 6.4. (*mini turbulence*).

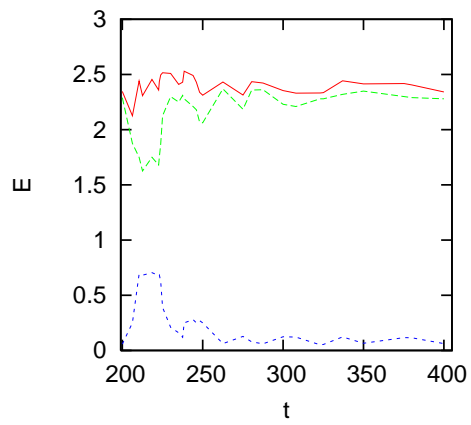


Figure 6.7: Kinetic energy (solid curve, top), vortex energy (dashed curve, middle) and sound energy (dotted curve, bottom).

l

k

Appendix A

Connection Between the Precession Frequency of a Single Vortex and Vortex Pair

We would like to find a connection between the vortex precession frequency in the case of a single vortex and in the case of vortex - anti vortex pairs. Let us use \mathbf{v}_t , for the tangential velocity and \mathbf{v}_i , for the velocity induced by the other vortex from the vortex pair.

In the beginning, the vortex-anti vortex pair move parallelly in the y -direction, having as initial positions x_1, x_2 and $y_1 = y_2 = 0$; the separation distance between them is $2x$. These two velocities act on both vortices, but for simplicity let us study only one of them. So, we have,

$$\mathbf{v}_t = \frac{\hbar}{2mx} \hat{y} = \frac{\hbar}{2m} (0, x) \quad (\text{A.1})$$

and

$$\mathbf{v}_i = -\omega r \hat{\Phi} = \omega(y, -x). \quad (\text{A.2})$$

The velocity v_i is arising from the inhomogeneous density in the condensate, and is the velocity a single vortex would have at that point. At some point, on a line parallel with the y -axis, the following is true:

$$\frac{dx}{dt} = \omega y \quad (\text{A.3})$$

and

$$\frac{dy}{dt} = \frac{\hbar}{2mx} - \omega x. \quad (\text{A.4})$$

Form:

$$\frac{d^2x}{dt^2} = \omega \frac{dy}{dt}. \quad (\text{A.5})$$

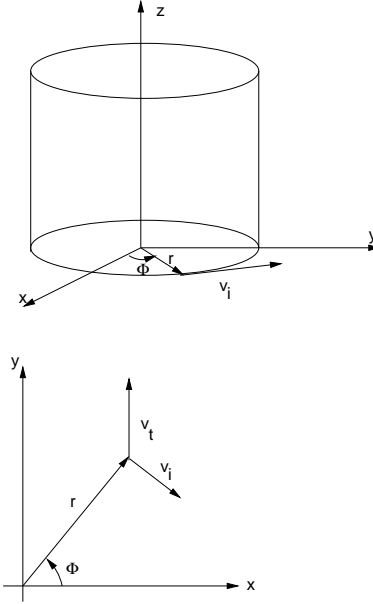


Figure A.1: .The velocities acting on both vortex and anti-vortex. Here, we choose one of them. Upper plot: The velocity induced by the neighbour vortex being on a distance of \mathbf{r} . Lower plot: The vortex-anti vortex move parallelly on the y -direction (because of their initial positions) with a tangential velocity, \mathbf{v}_t . We can see the relation between \mathbf{v}_t and \mathbf{v}_i .

Substituting Eq.(A.4) in Eq.(A.5) and putting $\hbar = 1$ and $m = 1$,

$$\frac{d^2x}{dt^2} = \frac{\omega}{2x} - \omega^2x. \quad (\text{A.6})$$

To find the equilibrium state, x_0 for a single vortex we write:

$$\frac{d^2x}{dt^2} = 0, \quad \Rightarrow \frac{\omega}{2x_0} = \omega^2x_0. \quad (\text{A.7})$$

This condition gives:

$$x_0 = \frac{1}{\sqrt{2\omega}}, \quad \text{or} \quad \omega = \frac{1}{2x_0^2}. \quad (\text{A.8})$$

Here, x_0 is the equilibrium position and ω is the frequency of motion for a single vortex. Introduce a small deviation, δ

$$\delta = \frac{x - x_0}{x_0} \leq 1, \quad (\text{A.9})$$

or

$$\delta = \frac{x}{x_0} - 1 \leq 1, \quad (\text{A.10})$$

from which,

$$x = x_0(\delta + 1), \quad \frac{x}{x_0} = \delta + 1. \quad (\text{A.11})$$

Substitute ω from Eq.(A.8) into Eq.(A.6) to find

$$\frac{d^2x}{dt^2} = \frac{1}{4xx_0^2} - \frac{x}{4x_0^2} = \frac{1}{4x^3} \left(\frac{x^2}{x_0^2} - \frac{x^4}{x_0^4} \right), \quad (\text{A.12})$$

from which we can remark that:

$$\frac{d^2x}{dt^2} = x_0 \frac{d^2\delta}{dt^2}. \quad (\text{A.13})$$

Substitute Eq.(A.11) into Eq.(A.12). The strategy then consists of writing $x/x_0 = \delta + 1$ and (A.13) and then substituting these in (A.12). By using $(1 + \delta)^2 \simeq (1 + 2\delta)$ and $(1 + \delta)^4 \simeq (1 + 4\delta)$, after some arrangements we obtain:

$$x_0 \frac{d^2\delta}{dt^2} = \frac{1 [(1 + \delta)^2 - (1 + \delta)^4]}{4x_0^3(1 + \delta)^3} \quad (\text{A.14})$$

or

$$\frac{d^2\delta}{dt^2} = \frac{(1 - 3\delta)}{4x_0^4} [(1 + 2\delta) - (1 + 4\delta)], \quad (\text{A.15})$$

which becomes

$$\frac{d^2\delta}{dt^2} = \frac{1 - 3\delta}{4x_0^4} (-2\delta). \quad (\text{A.16})$$

So, finally we get

$$\frac{d^2\delta}{dt^2} \approx \frac{-2\delta}{4x_0^4} \approx \frac{-1}{2x_0^4} \delta. \quad (\text{A.17})$$

Now, define the *Harmonic Oscillator Equation*:

$$\frac{d^2\delta}{dt^2} = -\omega_v^2 \delta, \quad (\text{A.18})$$

with solution:

$$\delta = A \sin(\omega_v t). \quad (\text{A.19})$$

Here A is the amplitude of the oscillator and ω_v the frequency of motion for a vortex-anti vortex pair. Under these conditions, from (A.18) and (A.17) we conclude:

$$\omega_v^2 = \frac{1}{2x_0^4}, \quad \Rightarrow \omega_v = \sqrt{\frac{1}{2x_0^4}}. \quad (\text{A.20})$$

We know from Eq.(A.8), that

$$x_0^2 = \frac{1}{2}\omega, \quad (\text{A.21})$$

so finally, the frequency of the vortex pair become:

$$\omega_v = \sqrt{\frac{1}{2x_0^4}} = \sqrt{\frac{1}{2\frac{1}{4\omega^2}}} = \sqrt{2\omega^2}. \quad (\text{A.22})$$

From here, the desired expression for the frequency of motion of the vortex-anti vortex pair with the help of the frequency of motion for a single vortex is:

$$\omega_v \simeq \sqrt{2}\omega. \tag{A.23}$$

Here, ω_v is the frequency of motion for the vortex-anti vortex pair and ω is the frequency of motion for a single vortex.

Appendix B

Detailed Calculations of the Hydrodynamic Equations

Firstly, we calculate:

$$\nabla\psi = \nabla R e^{iS} + i\nabla S R e^{iS} = e^{iS}(\nabla R + iR\nabla S), \quad (\text{B.1})$$

and then

$$\nabla \cdot \nabla\psi = e^{iS}[\nabla^2 R + 2i\nabla S \nabla R + i\nabla^2 S R - R(\nabla S)^2]. \quad (\text{B.2})$$

Secondly, we calculate the time derivative of ψ :

$$\frac{\partial\psi}{\partial t} = \left(\frac{\partial R}{\partial t} + i \frac{\partial S}{\partial t} R \right) e^{iS}. \quad (\text{B.3})$$

We substitute equations B.2 and B.3 into the NLSE, (see Eq.(1.30)), and hence

$$(i - \gamma)\hbar \left(\frac{\partial R}{\partial t} + i \frac{\partial S}{\partial t} R \right) e^{iS} = -\frac{\hbar^2}{2m} e^{iS} [\nabla^2 R + 2i\nabla S \cdot \nabla R + iR\nabla^2 S - R(\nabla S)^2] + gR^3 e^{iS} - \mu R e^{iS}. \quad (\text{B.4})$$

Consider now, the real and imaginary parts of the NLSE. The real part is expressed as:

$$-\hbar \left(R \frac{\partial S}{\partial t} + \gamma \frac{\partial R}{\partial t} \right) = -\frac{\hbar^2}{2m} (\nabla^2 R - R(\nabla S)^2) + gR^3 - \mu R, \quad (\text{B.5})$$

and the imaginary part is given by:

$$\hbar \left(\frac{\partial R}{\partial t} - \gamma R \frac{\partial S}{\partial t} \right) = -\frac{\hbar^2}{2m} (2\nabla S \cdot \nabla R + R\nabla^2 S). \quad (\text{B.6})$$

Using $\rho = mR^2$, $\mathbf{v} = (\hbar/m)\nabla S$, and $(\partial R/\partial t) = (1/2mR)(\partial\rho/\partial t)$, divide Eq.(B.5) by mR and rearrange for $\partial S/\partial t$, to obtain:

$$\frac{\partial S}{\partial t} = -\frac{\gamma}{R} \frac{\partial R}{\partial t} + \frac{\hbar}{2mR} (\nabla^2 R - R(\nabla S)^2) - \frac{gR^2}{\hbar} + \frac{\mu}{\hbar}. \quad (\text{B.7})$$

Substitute $\partial S/\partial t$ into the imaginary part of the NLSE, Eq.(B.6). So that,

$$\hbar \left\{ \frac{\partial R}{\partial t} - \gamma R \left[-\frac{\gamma}{R} \frac{\partial R}{\partial t} + \frac{\hbar}{2mR} (\nabla^2 R - R(\nabla S)^2) - \frac{gR^2}{\hbar} + \frac{\mu}{\hbar} \right] \right\} = -\frac{\hbar^2}{2m} (2\nabla S \cdot \nabla R + R\nabla^2 S). \quad (\text{B.8})$$

and

$$\hbar \frac{\partial R}{\partial t} + \frac{\gamma^2 R \hbar}{R} \frac{\partial R}{\partial t} - \frac{\hbar^2 \gamma R}{2mR} (\nabla^2 R - R(\nabla S)^2) + \frac{\hbar \gamma R^3 g}{\hbar} - \frac{\hbar \gamma R \mu}{\hbar} = -\frac{\hbar^2}{2m} (2\nabla S \cdot \nabla R + R\nabla^2 S). \quad (\text{B.9})$$

Multiply both sides of Eq.(B.9) by $2mR/\hbar$.

We form:

$$\nabla \cdot (\rho \mathbf{v}) = \nabla \cdot \left(mR^2 \frac{\hbar}{m} \nabla S \right) = \hbar \nabla \cdot (R^2 \nabla S) = \hbar (2\nabla R \nabla S) + R \nabla^2 S. \quad (\text{B.10})$$

Note, the first and last two terms. Use them together with substitution of $R = \sqrt{\rho/m}$, $R^2 = \rho/m$, $\nabla S = v m/\hbar$ and $\partial R/\partial t = (1/2mR)(\partial \rho/\partial t)$ into the Eq.(B.9).

$$\frac{\partial \rho}{\partial t} (1 + \gamma^2) - \hbar \gamma \sqrt{\frac{\rho}{m}} \left(\nabla^2 \sqrt{\frac{\rho}{m}} - \sqrt{\frac{\rho}{m}} \left(\frac{v^2 m^2}{\hbar^2} \right) \right) + \frac{2m\gamma}{\hbar} g \frac{\rho^2}{m^2} - \frac{\gamma 2m}{\hbar} \frac{\rho}{m} \mu = -\hbar (2\nabla R \nabla S) + R \nabla^2 S. \quad (\text{B.11})$$

Then, the imaginary part of the NLSE becomes:

$$\frac{\partial \rho}{\partial t} (1 + \gamma^2) - \gamma \hbar \sqrt{\frac{\rho}{m}} \nabla^2 \sqrt{\frac{\rho}{m}} + \frac{\gamma v^2 m^2}{\hbar} \frac{\rho}{m} + \frac{2\gamma g}{m \hbar} \rho^2 - \frac{2\gamma \rho}{\hbar} \mu + \nabla \cdot (\rho \mathbf{v}) = 0 \quad (\text{B.12})$$

and after rearranging, we obtain the final form of the imaginary part of the NLSE:

$$\frac{\partial \rho}{\partial t} (1 + \gamma^2) + \nabla \cdot (\rho \mathbf{v}) + \frac{2\gamma \rho}{\hbar} \left(\frac{mv^2}{2} + \frac{g\rho}{m} - \mu \right) - \gamma \hbar \sqrt{\frac{\rho}{m}} \frac{\partial^2 \sqrt{\frac{\rho}{m}}}{\partial x_j \partial x_j} = 0. \quad (\text{B.13})$$

This equation is a continuity equation modified by extra terms due to the dissipation γ .

Let us now continue our calculations with the real part of the NLSE, Eq.(B.5). Divide it, by mR and substitute R by ρ and ∇S by \mathbf{v} with the help of $\rho = mR^2$, $\mathbf{v} = (\hbar/m)\nabla S$ and $(\partial R/\partial t) = (1/2mR)(\partial \rho/\partial t)$.

We therefore obtain:

$$-\frac{\hbar}{mR} \left(R \frac{\partial S}{\partial t} + \gamma \frac{1}{2mR} \frac{\partial \rho}{\partial t} \right) = -\frac{\hbar^2}{2m^2 R} \left(\nabla^2 R - R \frac{v^2 m^2}{\hbar^2} \right) + gR^3 - \mu R, \quad (\text{B.14})$$

and

$$-\frac{\hbar}{m} \frac{\partial S}{\partial t} = \frac{\gamma \hbar m}{2m^2 \rho} \frac{\partial \rho}{\partial t} - \frac{\hbar^2}{2m^2} \sqrt{\frac{m}{\rho}} \nabla^2 \sqrt{\frac{\rho}{m}} + \frac{1}{2} v^2 + \frac{g}{m} \frac{\rho}{m} - \frac{\mu}{m}, \quad (\text{B.15})$$

or

$$-\frac{\hbar}{m} \frac{\partial S}{\partial t} = \frac{\gamma \hbar}{2m\rho} \frac{\partial \rho}{\partial t} - \frac{\hbar^2}{2m^2} \frac{m^{1/2}}{\rho^{1/2} m^{1/2}} \nabla^2 \rho^{1/2} + \frac{1}{2} v^2 + \frac{g\rho}{m^2} - \frac{\mu}{m}, \quad (\text{B.16})$$

$$-\frac{\hbar}{m} \frac{\partial S}{\partial t} = \frac{\gamma \hbar}{2m\rho} \frac{\partial \rho}{\partial t} - \frac{\hbar^2}{2m^2} \rho^{-1/2} \frac{\partial^2 \rho^{1/2}}{\partial x_j \partial x_j} + \frac{1}{2} v_j v_j + \frac{g\rho}{m^2} - \frac{\mu}{m}. \quad (\text{B.17})$$

Apply $\partial/\partial x_i$ to Eq.(B.17), so that:

$$-\frac{\hbar}{m} \frac{\partial}{\partial t} \frac{\partial S}{\partial x_i} = \frac{\gamma \hbar}{2m} \left(-\rho^{-2} \frac{\partial \rho}{\partial x_i} \frac{\partial \rho}{\partial t} + \rho^{-1} \frac{\partial^2 \rho}{\partial x_i \partial t} \right) - \frac{\hbar^2}{2m^2} \frac{\partial}{\partial x_i} \left(\rho^{-1/2} \frac{\partial^2 \rho^{1/2}}{\partial x_j \partial x_j} \right) + \frac{1}{2} \left(\frac{\partial v_j}{\partial x_i} v_j + v_j \frac{\partial v_j}{\partial x_i} \right) + \frac{g}{m^2} \frac{\partial \rho}{\partial x_i}. \quad (\text{B.18})$$

Then $\partial S/\partial x_i = (v_i m)/\hbar$, using $\mathbf{v} = (\hbar/m)\nabla S = (\hbar/m)\partial S/\partial x_i$ and so:

$$-\frac{\hbar}{m} \frac{\partial}{\partial t} \frac{v_i m}{\hbar} = -\frac{\gamma \hbar}{2m} \left(-\frac{1}{\rho^2} \frac{\partial \rho}{\partial x_i} \frac{\partial \rho}{\partial t} + \frac{1}{\rho} \frac{\partial^2 \rho}{\partial x_i \partial t} \right) - \frac{\hbar^2}{2m^2} \frac{\partial}{\partial x_i} \left(\rho^{-1/2} \frac{\partial^2 \rho^{1/2}}{\partial x_j \partial x_j} \right) + v_j \frac{\partial v_j}{\partial x_i} + \frac{g}{m^2} \frac{\partial \rho}{\partial x_i}. \quad (\text{B.19})$$

Multiply both parts by $-\rho$,

$$\rho \left(\frac{\partial v_i}{\partial t} + v_j \frac{\partial v_j}{\partial x_i} \right) = \frac{-g}{m^2} \rho \frac{\partial \rho}{\partial x_i} - \frac{\gamma \hbar}{2m} \left(-\frac{1}{\rho} \frac{\partial \rho}{\partial x_i} \frac{\partial \rho}{\partial t} + \frac{\partial^2 \rho}{\partial x_i \partial t} \right) + \frac{\hbar^2}{2m^2} \left[\rho^{1/2} \frac{\partial}{\partial x_i} \left(\frac{\partial^2 \rho^{1/2}}{\partial x_j \partial x_j} \right) - \frac{\partial \rho^{1/2}}{\partial x_i} \frac{\partial^2 \rho^{1/2}}{\partial x_j \partial x_j} \right]. \quad (\text{B.20})$$

Consider the final term in the [...] bracket, on the right hand side of Eq.(B.20):

$$\rho^{1/2} \frac{\partial}{\partial x_i} \left(\frac{\partial^2 \rho^{1/2}}{\partial x_j \partial x_j} \right) - \frac{\partial \rho^{1/2}}{\partial x_i} \frac{\partial^2 \rho^{1/2}}{\partial x_j \partial x_j}, \quad (\text{B.21})$$

and note that

$$\frac{\partial}{\partial x_j} \left[\rho^{1/2} \frac{\partial^2 \rho^{1/2}}{\partial x_i \partial x_j} - \frac{\partial \rho^{1/2}}{\partial x_i} \frac{\partial \rho^{1/2}}{\partial x_j} \right] = \rho^{1/2} \frac{\partial}{\partial x_i} \left(\frac{\partial^2 \rho^{1/2}}{\partial x_j \partial x_j} \right) - \frac{\partial \rho^{1/2}}{\partial x_i} \frac{\partial^2 \rho^{1/2}}{\partial x_j \partial x_j}, \quad (\text{B.22})$$

were, we have used $\rho^{1/2}(\partial/\partial x_j)(\partial^2 \rho^{1/2} \partial x_i \partial x_j) = \rho^{1/2}(\partial/\partial x_i)(\partial^2 \rho^{1/2} \partial x_j \partial x_j)$

Thus,

$$\rho \left(\frac{\partial v_i}{\partial t} + v_j \frac{\partial v_j}{\partial x_i} \right) = -\frac{g}{m^2} \rho \frac{\partial \rho}{\partial x_i} + \frac{\hbar^2}{2m^2} \frac{\partial}{\partial x_j} \left[\rho^{1/2} \frac{\partial^2 \rho^{1/2}}{\partial x_i \partial x_j} - \frac{\partial \rho^{1/2}}{\partial x_i} \frac{\partial \rho^{1/2}}{\partial x_j} \right] - \frac{\gamma \hbar}{2m} \left(-\frac{1}{\rho} \frac{\partial \rho}{\partial x_i} \frac{\partial \rho}{\partial t} + \frac{\partial^2 \rho}{\partial x_i \partial t} \right), \quad (\text{B.23})$$

where: $\rho(\partial \rho/\partial x_i) = (1/2)(\partial \rho^2/\partial x_i)$.

Define:

$$p = \frac{g\rho^2}{2m^2}, \quad \sigma_{ij} = \frac{\hbar^2}{2m^2} \left[\rho^{1/2} \frac{\partial^2 \rho^{1/2}}{\partial x_i \partial x_j} - \frac{\partial \rho^{1/2}}{\partial x_i} \frac{\partial \rho^{1/2}}{\partial x_j} \right], \quad (\text{B.24})$$

where p is a pressure and σ_{ij} are the quantum stresses, and note that:

$$\rho \frac{\partial^2}{\partial x_i \partial x_j} (\ln \rho^{1/2}) = \rho \frac{\partial}{\partial x_i} \left(\frac{1}{\rho^{1/2}} \frac{\partial \rho^{1/2}}{\partial x_j} \right) = -\frac{\partial \rho^{1/2}}{\partial x_i} \frac{\partial \rho^{1/2}}{\partial x_j} + \rho^{1/2} \frac{\partial^2 \rho^{1/2}}{\partial x_i \partial x_j}. \quad (\text{B.25})$$

Also, σ_{ij} finally become:

$$\sigma_{ij} = \frac{\hbar^2}{2m} \rho \left(\frac{\partial^2 \ln \rho^{1/2}}{\partial x_i \partial x_j} \right) = \frac{\hbar^2}{4m^2} \rho \frac{\partial^2 \ln \rho}{\partial x_i \partial x_j}. \quad (\text{B.26})$$

Thus, the real part of the NLSE has the form:

$$\rho \left(\frac{\partial v_i}{\partial t} + v_j \frac{\partial v_j}{\partial x_i} \right) = -\frac{\partial p}{\partial x_i} + \frac{\partial \sigma_{ij}}{\partial x_j} - \frac{\gamma \hbar}{2m} \left(-\frac{1}{\rho} \frac{\partial \rho}{\partial x_i} \frac{\partial \rho}{\partial t} + \frac{\partial^2 \rho}{\partial x_i \partial t} \right). \quad (\text{B.27})$$

Appendix C

Tables

C.1 Tables Relating Connections Between α , α' , γ , x_0 , ω , τ and the Exponential Constant of the Radial Position of the Vortex, Γ_1

See, Tables: C.1; C.2; C.3; C.4; C.5; C.6; C.7; C.8; C.9 and C.10.

C.2 Tables Relating Different Energies, L_z , the Initial Positions of Eight Vortex Pairs and the Decay Rate of the Number of Vortices

See, Tables: C.11; C.12; C.13; C.14; C.15; C.16 and C.17.

x_0	γ	α	α'
0.9	0.001	0.00477379	0.00219247
0.9	0.003	0.01518787	0.00292205
0.9	0.010	0.04895356	0.01398204
0.9	0.030	0.14171156	0.03371915
2.0	0.001	0.00454510	0.00135894
2.0	0.003	0.01449282	0.00187937
2.0	0.010	0.04747512	0.00498293
2.0	0.030	0.13704750	0.01673209

Table C.1: Friction coefficients, α and α' as a function of γ for initial positions: $(x_0, y_0) = 0.9$ and 2 .

γ	x_0	α	α'
0.003	0.7	0.01544760	0.00385565
0.003	0.9	0.01518787	0.00292205
0.003	1.1	0.01499830	0.00253312
0.003	2.0	0.01449282	0.00187938

Table C.2: Friction coefficients, α and α' as a function of initial position, $(x_0, 0)$ for a single vortex ($\gamma = 0.003$).

α	x_0
0.014493	0.6
0.014493	0.9
0.015884	1.2
0.015019	1.5
0.014740	1.8
0.014740	2.1
0.013906	2.4
0.014141	2.7
0.014462	3.0
0.013628	3.3
0.010445	3.6
0.012361	3.9
0.014141	4.2
0.011372	4.5
0.011496	4.8
0.010939	5.1
0.009827	5.4
0.009831	5.7

Table C.3: Friction coefficient α as a function of initial position $(x_0, 0)$ for a single vortex ($\gamma = 0.003$).

α'	ω	x_0
0.003956	0.1098	0.6
0.005737	0.1199	1.8
0.004203	0.1320	2.4
0.004821	0.1321	3.0
0.004079	0.2038	3.6
0.004149	0.2260	4.2
0.004493	0.2500	4.8
0.005074	0.2855	5.4

Table C.4: Friction coefficient α' as a function of ω and $(x_0, 0)$ for a single vortex ($\gamma = 0.003$).

τ	$\omega = \frac{2\pi}{\tau}$	x_0
58.3990	0.107591	0.3
56.8400	0.110542	0.6
55.7295	0.112744	0.9
54.0147	0.116324	1.2
53.8500	0.116679	1.5
52.9200	0.118729	1.8
51.4800	0.122051	2.1
49.9200	0.125865	2.4
48.3600	0.129925	2.7
47.6400	0.131889	3.0
45.2400	0.138885	3.3
42.9600	0.146256	3.6
40.9603	0.153397	3.9
38.8267	0.161826	4.2
36.8800	0.170368	4.5
33.2666	0.188873	4.8
30.4000	0.206683	5.1
26.4534	0.237519	5.4
22.5334	0.278838	5.7
19.0267	0.330229	6.0

Table C.5: Period τ and frequency ω of motion for a single vortex as a function of $(x_0, 0)$ ($\gamma = 0.003$).

γ	τ	$\omega = \frac{2\pi}{\tau}$
0.000	57.9040	0.108510
0.004	56.4643	0.111277
0.008	56.0934	0.112013
0.012	56.0534	0.112093
0.016	55.8667	0.112467
0.020	55.6200	0.112966
0.024	55.4266	0.113360
0.028	55.4040	0.113406
0.032	55.3400	0.113538
0.036	54.8320	0.114589
0.040	53.6640	0.117084
0.044	53.0933	0.118342
0.048	51.9360	0.120979
0.052	50.8320	0.123607
0.056	48.8960	0.128501
0.060	47.5307	0.132192
0.064	41.5707	0.151144

Table C.6: Period τ and frequency ω of motion for a single vortex as a function of γ for $(x_0, y_0) = (0.9, 0)$.

γ	τ	$\omega = \frac{2\pi}{\tau}$
0.000	54.8721	0.114506
0.004	54.6000	0.115076
0.008	53.7600	0.116875
0.012	53.4617	0.117527
0.016	53.0400	0.118461
0.020	51.8858	0.121096
0.024	51.6235	0.121712
0.028	51.2797	0.122527
0.032	49.9200	0.125865
0.036	48.9763	0.128290
0.040	45.5210	0.138028
0.044	44.9758	0.139701
0.048	43.3998	0.144774

Table C.7: Period, τ and frequency, ω of motion for one vortex as a function of γ for $(x_0, y_0) = (1.45, 0)$.

γ	Γ_1
0.004	0.00216
0.008	0.00434
0.016	0.00872
0.020	0.01084
0.024	0.01300
0.028	0.01510
0.032	0.01713
0.036	0.01918
0.044	0.02302
0.048	0.02482
0.052	0.02670
0.056	0.02851
0.060	0.03014
0.064	0.03187
0.068	0.03329
0.076	0.03647
0.080	0.03807

Table C.8: Exponential constant, Γ_1 of the radius of vortex trajectory as a function of γ for a single vortex with $(x_0, y_0) = (0.9, 0)$.

γ	Γ_1
0.004	0.002167
0.008	0.004385
0.012	0.006599
0.020	0.010957
0.028	0.015196
0.032	0.017208
0.036	0.019254
0.044	0.023206
0.052	0.027095
0.056	0.028609
0.060	0.030421
0.064	0.031647
0.068	0.033803
0.072	0.035269
0.076	0.036695
0.080	0.038559

Table C.9: Exponential constant, Γ_1 of the radius of vortex trajectory as a function of γ for a single vortex with $(x_0, y_0) = (1.45, 0)$.

x_0	Γ_1
0.3	0.001508
0.9	0.001616
1.2	0.001629
1.5	0.001644
2.7	0.001650
3.0	0.001653
3.6	0.001673
4.2	0.001691
4.8	0.001717
5.1	0.001753
5.4	0.001801
5.7	0.001948
6.0	0.003012

Table C.10: Exponential constant, Γ_1 of the radius of vortex trajectory as a function of x_0 for a single vortex with $\gamma = 0.003$.

Energies/Lz	Max value	Sat value	Difference
E_{tot}	21.947500	21.797700	0.1498000
E_{kin}	3.257800	3.177700	0.0801000
E_{trap}	12.381300	12.267600	0.1137000
E_{int}	6.294800	6.328200	-0.0334000
E_q	0.000054	0.000052	0.0000015
L_z	14.714500	14.526600	0.1879000

Table C.11: Maximum values, saturated values and difference between them for E_{tot} , E_{kin} , E_{trap} , E_{int} , E_q and L_z for an array of vortices with $\gamma = 0.03$ and $\Omega = 0.75$.

Energies/Lz	Max value	Sat value	Difference
E_{tot}	21.8639000	21.647200	0.2167000
E_{kin}	3.1772000	3.084700	0.0925000
E_{trap}	12.3721000	12.160700	0.2114000
E_{int}	6.3203000	6.378200	-0.0579000
E_q	0.0000526	0.000051	0.0000016
L_z	14.5624000	14.257900	0.3045000

Table C.12: Maximum values, saturated values and difference between them for E_{tot} , E_{kin} , E_{trap} , E_{int} , E_q and L_z for an array of vortices with $\gamma = 0.07$ and $\Omega = 0.75$.

γ	$\beta:E_{tot}$	$\beta:E_{kin}$	$\beta:E_{trap}$	$\beta:E_{int}$	$\beta:E_q$	$\beta:L_z$
0.003	0.001366	0.013760	0.001912	-0.002646	0.009497	0.009496
0.030	0.016962	0.179224	0.025185	-0.027926	0.126919	0.192771
0.070	0.047666	0.835296	0.060384	-0.051805	0.216713	0.825842

Table C.13: Increase rate of E_{tot} , E_{kin} , E_{trap} , E_{int} (decay rate), E_q and L_z (when the vortices come in in the condensate) as a function of $\gamma = 0.003$; 0.03 and 0.07 for $\Omega = 0.75$.

x_0	y_0	Sign
-5.6011	-5.7908	-1.0
-10.3988	-9.3938	1.0
0.1205	5.8287	-1.0
5.2207	8.9890	1.0
-5.5100	5.7926	-1.0
0.2419	7.4978	1.0
3.1515	-4.5491	-1.0
7.4946	-0.4094	1.0
-9.4201	7.1220	-1.0
-3.7025	5.3030	1.0
4.6748	-6.0519	-1.0
2.8308	-0.3423	1.0
7.2828	-9.3417	-1.0
5.7792	-3.5332	1.0
-7.9771	-1.7442	-1.0
-5.3021	3.6264	1.0

Table C.14: Initial positions of eight pairs of vortex - anti vortex (totally 16) with a proper sign.

γ	$\beta_{E_{tot}}$	$\beta_{E_{trap}}$	$\beta_{E_{int}}$	$\beta_{E_{quant}}$
0.028	-0.00003674	-0.00005850	0.00003614	-0.0013059
0.036	-0.00003296	-0.00005168	0.00003293	-0.0011646
0.040	-0.00003052	-0.00004775	0.00003053	-0.0010795
0.048	-0.00002705	-0.00004202	0.00002694	-0.0009597
0.056	-0.00002454	-0.00003782	0.00002428	-0.0008722
0.072	-0.00002119	-0.00003197	0.00002041	-0.0007512
0.076	-0.00002054	-0.00003081	0.00001961	-0.0007274
0.084	-0.00001931	-0.00002863	0.00001815	-0.0006860

Table C.15: Decay rate of total energy, trap energy and quantum energy and increase rate of internal energy for different γ 's.

γ	$\beta_{E_{kin}}$	β_{L_z}
0.020	-0.120567	-0.129676
0.028	-0.110014	-0.118706
0.030	-0.106843	-0.117571
0.032	-0.103876	-0.113986
0.036	-0.098008	-0.107535
0.040	-0.091974	-0.101411
0.048	-0.082159	-0.092014
0.056	-0.073988	-0.084387
0.070	-0.063253	-0.071122
0.072	-0.061965	-0.071133
0.076	-0.059595	-0.070027
0.084	-0.055184	-0.063537

Table C.16: Decay rate of kinetic energy and z -component of the angular momentum for different γ 's.

γ	β
0.003	-0.0089
0.048	-0.0837
0.070	-0.1437
0.100	-0.1840

Table C.17: Decay rate β of number of vortices and the corresponding γ when the random vortex - anti vortex pairs were placed in the condensate with $d_0 = 1.8$.

Appendix D

Parts of the Numerical Code

We have a main program and modules (global, solve, subs...), which are connected to the main program. For example, information about the vortex trajectory is included in subroutine: *get_trajectory* which is in module: subs. From the main program we can always call the trajectory.

After compiling the program in the *vortex_init.dat*, we choose the case of one vortex, vortex - anti vortex pair(s), vortex - vortex pair(s) and random vortex - anti vortex pairs. So, in *vortex_init.dat*, we choose the desired number with the proper signs and positions of the vortices.

2.....*sign*

-1.3..0.....1.

1.3.....0....-1.

Later, we use it in the vortex/vortices initial state(s). If the first number, which describe the number of vortices is a negative number, the program knows that we have chosen the *Random Method*. So,

```
!*****
```

```
module initial
```

```
private
```

```
real, allocatable :: vortex(:, :)
```

```
integer :: vortex_count
```

```
contains
```

```
subroutine vortex_init(psi, dx, dy)
```

```
use parameters
```

```
implicit none
```

```
!First, we define the variables complex, dimension(0 : nx, 0 : ny) :: psi
```

```
real, dimension(0 : nx, 0 : ny) :: density
```

```
complex :: psi_local, eye
```

```
real, intent(in) :: dx, dy
```

```
real, dimension(0 : nx) :: xp
```

```
real, dimension(0 : ny) :: yp
```

```

real :: c1 = -0.7, c2 = 1.15
real :: rr, amp, xpos, ypos, my_small_radius, v_sign, r_number, i_k, x_number, y_number
integer :: i, j, k
logical :: read_vortices, lrandom = .false., lcheck = .true.

```

```

my_small_radius = 1e - 3
eye = (0.0, 1.0)

```

!The code needs to know if the file 'vortex_init.dat' exists. So, if it does, we can use it to initialise the vortices.

```

    INQUIRE(FILE = 'vortex_init.dat', EXIST = read_vortices)
    k = 0
    !If 'read_vortices' is 'true'
    if(read_vortices) then
        !'vortex_init.dat' is opened
        open(81, file = 'vortex_init.dat')
        !The number of vortices is read
        read(81, fmt = '(i5)')vortex_count
        ! If the inserted number is negative, we have the random case.
        if(vortex_count < 0) then
            !We take its absolute value, so that this number is compatible with other cases.
            vortex_count = abs(vortex_count)
            ! Here, we decide to use the random case
            lrandom = .true.
        endif
        allocate(vortex(vortex_count, 3))
        !'lcheck' can be opened or not
        if(lcheck)open(85, file = 'locations.dat')
        !A do - loop, where 'vortex_count' is the total number of vortices.
        do k = 1, vortex_count
            ! Here, we define the sign of each vortex
            i_k = (-1.) ** k
            ! The random case
            if(lrandom) then
                ! The pair wise case
                if(lpairwise) then
                    ! For anti-vortices is valid
                    if(i_k < 0) then
                        !We call the first random number
                        call random_number(x - number)
                        !We call the second random number
                        call random_number(y - number)
                    endif
                endif
            endif
        enddo
    endif

```

```

!We create the first random number, which is compatible with the condensate size
x_number = ((x_number - 0.5) * 16)
!We create the second random number, which is compatible with the condensate size
y_number = ((y_number - 0.5) * 16)
!We call the third random number
call random_number(r_number)
!We form a random angle, in which direction the vortex/vortex-pair will move (in the beginning )

    r_number = r_number * 2 * pi
    print*, 'vortex trajectory angle', r_number * 360. / (2. * pi)
!The x-position of the anti-vortex
    vortex(k, 1) = x_number + r0 * cos(r_number - (0.5 * pi))
!The y-position of the anti-vortex
    vortex(k, 2) = y_number + r0 * sin(r_number - (0.5 * pi))
else
!The x-position of the vortex
    vortex(k, 1) = x_number + r0 * cos(r_number + (0.5 * pi))
!The y-position of the vortex
    vortex(k, 2) = y_number + r0 * sin(r_number + (0.5 * pi))
endif

else
! We call the first random number for the case of 'no' pair wise and form the x-position
call random_number(r_number)
    vortex(k, 1) = ((r_number - 0.5) * 16)
! We call the second random number for the case of 'no' pair wise and form the y-position
call random_number(r_number)
    vortex(k, 2) = ((r_number - 0.5) * 16) endif
!Here, we choose the sign for the vortices
    vortex(k, 3) = i_k
if(lcheck)write(85, *)vortex(k, 1), vortex(k, 2), vortex(k, 3)
else
! This is the case of 'no' randomly placed vortices, the program read the file 'vortex_init.dat'
read(81, *, end = 123)vortex(k, 1), vortex(k, 2), vortex(k, 3)
! We have on the screen: the number, the x-, the y-position(s) and the sign of the vortices
print*, 'vortex', k, ':', vortex(k, 1), vortex(k, 2), sign(1., vortex(k, 3))
endif
enddo
if(lcheck)close(85)
close(81)
do j = 0, Ny
!We form a square with y-coordinates
yp(j) = yl + j * dy

```

```

do i = 0, Nx
!We form a square with x-coordinates
xp(i) = xl + i * dx
! add the vortices
do k = 1, vortex_count
!Distance between the vortex and points on the x-directions xpos = xp(i) - vortex(k,1)
!Distance between the vortex and points on the y-directions ypos = yp(j) - vortex(k,2)
!The radius with the help of 'xpos' and 'ypos' ! We calculate the distance of the current point
from the last known vortex location.
rr = sqrt(xpos **2 + ypos **2)
! Here, we form the vortex/antivortex depending on the sign
psi_Local = xpos + eye * sign(1., vortex(k,3)) * ypos

if(rr > my_small_radius) then
! This is the final form of the vortex/vortices
psi(i,j) = psi(i,j) * psi_Local * (1.0 - exp(c1 * (rr **c2)))/rr
else
psi(i,j) = 0.
endif
end do
enddo
enddo
! otherwise there are no vortices
else
print*, 'no vortex_init.dat found!'
stop
end if
!the definition of the density
density = psi * conjg(psi) !the definition of the density
open(73, file = 'density_test.dat', form = 'unformatted')
write(73) density
close(73)

open(73, file = 'vortex_count.dat', form = 'unformatted')
!The number of vortices
write(73) vortex_count
write(73) vortex
close(73)
deallocate(vortex)
return
!not enough vortices to read
123 print*, 'end of vortex locations!'

```

```

print*, ' expected :', vortex_count
print*, ' found :', k - 1
print*, ' Please check vortex_init.dat or'
print*, ' change your initial condition.'
stop

end subroutine vortex_init
!*****

end module initial

!*****
!*****
!*****

module subs

private

interface get_trajectory
module procedure get_trajectory_1
module procedure get_trajectory_2
end interface

!*****

subroutine get_trajectory_1(density, t)
use parameters
use global
implicit none
!First, we define the variables integer :: i, j, k, i1, i2, i3, i4, j1, j2, j3, j4
integer, dimension(vortex_count) :: my_i, my_j

real :: density(0 : Nx, 0 : Ny)
real, dimension(vortex_count) :: dmin, xmin, ymin
real :: t, dx, dy, rr, ddd = 1e - 9
real :: d1, d2, d3, d0, x1, x2, x3, x0, a1, a2, a3, x4, d4
logical :: three_point
! update 'iwrite'
iwrite = iwrite + 1
! Here, we choose the three point case
three_point = .true.
!Here, we define the initial value of the density minimum
dmin = 9999.

```

```

!xmin become the vortex x-coordinate
xmin(:) = vortex(:,1)
!ymin become the vortex y-coordinate
ymin(:) = vortex(:,2)
! the size of the space step in the x direction
dx = (xr - xl)/Nx
! the size of the space step in the y direction
dy = (yr - yl)/Ny
!Initial conditions for 'my_i' and 'my_j'
my_i = 0
my_j = 0
!loop over all points in the box
do j = 0, ny
y(j) = yl + j * dy
do i = 0, nx
x(i) = xl + i * dx
do k = 1, vortex_count
! We define a radius in finding the trajectory with the last known position of the vortex
! We calculate the distance of the current point from the last known vortex location.
rr = (vortex(k,1) - x(i)) **2 + (vortex(k,2) - y(j)) **2
! We put a criterion for this radius
if(rr < 0.13) then
! We put a criterion for the density
! If we are within some distance of the previous vortex location, check the value of the density

    if(density(i,j) < dmin(k)) then
! If our if-criterion is true, the following definitions are valid, we update the minimum known
density and its location
dmin(k) = density(i,j)
xmin(k) = x(i)
ymin(k) = y(j)
my_i(k) = i
my_j(k) = j
endif
endif
enddo
enddo
enddo

! The density minimum is defined with the help of three points both in x- and y- directions.
! We construct the Lagrange's formula for polynomial interpolation. Through any three points
there is a unique quadratic. The interpolating polinomial of degree two through the three points is
given below. We have three terms, each of them are a polinomial of degree two and each are con-
```

structed to be zero at all of the x_i except one at which it is constructed to be y_i . !Here begin the three points definition and search for the vortex coordinates (three points with the corresponding densities.)

```

    if(three_point) then
k = 1
i = my_x(k); j = my_y(k)
x1 = x(i); x0 = x(i - 1); x2 = x(i + 1)
d1 = density(i, j); d0 = density(i - 1, j); d2 = density(i + 1, j)
xmin(k) = (-2 * d1 * (x0 + x2) + d0 * (x2 + x1) + d2 * (x1 + x0)) / (2 * d0 - 4 * d1 + 2 * d2)
x1 = y(j); x0 = y(j - 1); x2 = y(j + 1)
d1 = density(i, j); d0 = density(i, j - 1); d2 = density(i, j + 1)
ymin(k) = (-2 * d1 * (x0 + x2) + d0 * (x2 + x1) + d2 * (x1 + x0)) / (2 * d0 - 4 * d1 + 2 * d2)
    else
! We use every alternative of the points to calculate with the help of them 'xmin(k)' and 'ymin(k)'

k = 1
if(density(i + 1, j) > density(i - 1, j)) then
x2 = x(i - 1); d2 = density(i - 1, j)
x1 = x(i - 2); d1 = density(i - 2, j)
x3 = x(i); d3 = density(i, j)
x4 = x(i + 1); d4 = density(i + 1, j)
    else
x2 = x(i); d2 = density(i, j)
x1 = x(i - 1); d1 = density(i - 1, j)
x3 = x(i + 1); d3 = density(i + 1, j)
x4 = x(i + 2); d4 = density(i + 2, j)
    endif
a1 = d2 - d1
a2 = d4 - d3
a3 = d1 - d3
xmin(k) = (dx * a3 - x1 * a1 + x3 * a2) / (a2 - a1)
if(density(i, j + 1) > density(i, j - 1)) then
x2 = y(j - 1); d2 = density(i, j - 1)
x1 = y(j - 2); d1 = density(i, j - 2)
x3 = y(j); d3 = density(i, j)
x4 = y(j + 1); d4 = density(i, j + 1)
    else
x2 = y(j); d2 = density(i, j)
x1 = y(j - 1); d1 = density(i, j - 1)
x3 = y(j + 1); d3 = density(i, j + 1)
x4 = y(j + 2); d4 = density(i, j + 2)
    endif

```

```
a1 = d2 - d1
a2 = d4 - d3
a3 = d1 - d3
ymin(k) = (dy * a3 - x1 * a1 + x3 * a2)/(a2 - a1)
endif
! Here, we write the time, the x- and the y-coordinates of the vortices
if(mod(iwrite,8) == 0)write(18,*)t, xmin(1), ymin(1)
! We define the vortices x-, y-coordinates and the time
vortex(:,1) = xmin(:)
vortex(:,2) = ymin(:)
vortex(:,3) = t

end subroutine get_trajectory_1
|*****
end module subs
|*****
|*****
```

Bibliography

- ABO-SHAEER, J. R., RAMAN, C. & KETTERLE, W. 2002 *Phys. Rev. Lett.* **88**, 070409.
- ABO-SHAEER, J. R., RAMAN, C., VOGELS, J. M. & KETTERLE, W. 2001 *Science* **292**, 476.
- AFTALION, A. A. & JERRARD, R. L. 2002 *Phys. Rev. A* **66**, 023611.
- ANDERSON, B. P., HALJAN, P. C., REGAL, C. A., FEDER, D. L., COLLINS, L. A., CLARK, C. W. & CORNELL, E. A. 2001 *Phys. Rev. Lett.* **86**, 2926–2929.
- ANDERSON, B. P., HALJAN, P. C., WIEMAN, C. E. & CORNELL, E. A. 2000 *Phys. Rev. Lett.* **85**, 2857.
- ANDERSON, B. P. & KASEVICH, M. A. 2003 *Science* **282**, 1686.
- ANDERSON, M. H., ENSHER, J. R., MATTHEVS, M. R., WEIMAN, C. E. & CORNELL, E. A. 1995 *Science* **269**, 198.
- ARAKI, T., TSUBOTA, M. & BARENGHI, C. F. 2003 *Physica B* **329-333**, 226.
- ARAKI, T., TSUBOTA, M. & NEMIROVSKII, S. K. 2002 *PRL* **89**, 145301.
- BARENGHI, C. F., DONNELLY, R. J. & VINEN, W. F. 1983 *J. Low Temp. Phys.* **52**, 189.
- BARENGHI, C. F., DONNELLY, R. J. & VINEN, W. F. 2001 *Quantized Vortex Dynamics and Superfluid Turbulence*. Springer Verlag, Berlin.
- BAYM, G. & PETHICK, C. J. 1996 Ground-state properties of magnetically trapped bose-condensed rubidium gas. *Phys. Rev. Lett.* **76**, 6.
- BERLOFF, N. G. & YOUNG, A. J. 2007a *PRL* **99**, 145301.
- BERLOFF, N. G. & YOUNG, A. J. 2007b Dissipative dynamics of superfluid vortices at non-zero temperatures. *cond-mat* p. 0704.1971.
- BOSE, S. N. 1924 Plancks gesetz und lichtquanten-hypothese. *Z. Phys.* **26**, 178.
- BRADLEY, C. C., SACKETT, C. A., TOLLETT, J. J. & HULET, R. G. 1995 *Phys. Rev. Lett.* **75**, 1687.
- BRETIN, V., ROSENBUSCH, P., CHEVY, F., SHLYAPNIKOV, G. V. & DALIBARD, J. 2003 *Phys. Rev. Lett.* **90**, 100403.

- BURGER, S., BONGS, K., DETTMER, S., ERTMER, W., SENGSTOCK, K., SANPERA, A., SHLYAPNIKOV, G. V. & LEWENSTEIN, M. 1999 *PRL* **83**, 5198.
- CHEVY, F., BRETIN, V., ROSENBUSCH, P., MADISON, K. W. & DALIBARD, J. 2002 *PRL* **88**, 250402.
- CHOI, S., MORGAN, S. A. & BURNETT, K. 1998 *Phys. Rev. A* **57**, 4057 – 4060.
- CHU, S., COHEN-TANNOUJDI, C. & PHILLIPS, W. D. 2003 Nobel lectures in physics 1996-2000. *World Scientific, London* .
- CORNELL, E. A. & WIEMAN, C. E. 1995 *NIST News Releases Archives* **July 13**.
- CORNELL, E. A. & WIEMAN, C. E. 1998 *Scientific American* **278(3):40-45**, 26–31.
- DAVIS, K. B., MEWES, M. O., ANDREWS, M. R., VAN DRUTEN, N. J., DURFEE, D. S., KURN, D. M. & KETTERLE, W. 1995 *Phys. Rev. Lett.* **75**, 3969.
- DUINE, R. A., LEURS, B. W. A. & STOOF, H. T. C. 2004 *Phys. Rev. A* **69**, 053623.
- DUTTON, Z., BUDDE, M., SLOWE, C. & HAU, L. V. 2001 *Science* **293**, 663.
- EINSTEIN, A. 1925 Quantentheorie des einatomigen idealen gases. *Sitzber.Kgl.Preuss.Akad.Wiss.* .
- ENSHER, J. R., JIN, D. S., MATTHEWS, M. R., WIEMAN, C. E. & CORNELL, E. A. 1996 *Phys. Rev. Lett.* **77**, 4984.
- FEDICHEV, P. O. & SHLYAPNIKOV, G. V. 1999 Dissipative dynamics of a vortex state in a trapped bose-condensed gas. *Phys. Rev. A* **60**, R1779.
- FETTER, A. L. & SVIDZINSKY, A. A. 2001 *J. Phys* **13**, R135.
- FRIED, D. G. 1998 *Phys. Rev. Lett.* **81**, 3811.
- GARDINER, C. W., ANGLIN, J. R. & FUDGE, T. I. A. 2002 *J.Phys.B* **35**, 1555.
- GARDINER, C. W., ZOLLER, P., BALLAGH, R. J. & DAVIS, M. J. 1997 *Phys. Rev. Lett.* **79**, 1793.
- GINZBURG, V. L. & PITAEVSKII, L. P. 1958 *Sov. Phys. JETP* **7**, 858.
- GROSS, E. P. 1957 Unified theory of interacting bosons. *Phys. Rev.* **106**, 161.
- HAGLEY, E. 1999 *Science* **283**, 1706.
- HALJAN, P. C., CODDINGTON, I., ENGELS, P. & CORNELL, E. A. 2001 *Phys. Rev. Lett.* **87**, 210403.
- HALL, H. E. & VINEN, W. F. 1956 *Proc. R. Soc. A* **238**, 204.
- HANSCH, I. B. T. W. & ESSLINGER, T. 1999 *Phys. Rev. Lett.* **82**, 3008.
- HANSEL, W., HOMMELHOFF, P., HANSCH, T. W. & REICHEL, J. 2001 *Nature* **413**, 498.

- HESS, H. F. 1986 *Phys. Rev. B* **34**, 3476.
- HODBY, E., HOPKINS, S. A., HECHENBLAIKNER, G., SMITH, N. L. & FOOT, C. J. 2003 *Phys. Rev. Lett.* **91**, 090403.
- HOLLAND, M., BURNETT, K., GARDINER, C., CIRAC, J. I. & ZOLLER, P. 1996 *Phys. Rev. A* **54**, R1757.
- JACKSON, B. 1999 Vortices in trapped bose-einstein condensates. *thesis* .
- JACKSON, B., BARENGHI, C. F. & PROUKAKIS, N. P. 2007 *J. Low Temp. Phys.* **148**, 387–391.
- JACKSON, B., MCCANN, J. F. & ADAMS, C. S. 2000 *Phys. Rev. A* **61**, 013604.
- JACKSON, B., PROUKAKIS, N., BARENGHI, C. F. & ZAREMBA, E. 2008 *in preparation* .
- JIN, D. S., MATTHEWS, M. R., ENSHER, J. R., WIEMAN, C. E. & CORNELL, E. A. 1997 *PRL* **78**, 764.
- JONES, C. A. & ROBERTS, P. H. 1982 *J.Phys.A: Math.Gen* **15**, 2599–2619.
- KOBAYASHI, M. & TSUBOTA, M. 2005 *Phys. Rev. Lett.* **94**, 065302.
- LANDAU, L. 1941 *J. Phys. (USSR)* **5**, 71.
- LEADBEATER, M., WINIECKI, T., SAMUELS, D. C., BARENGHI, C. F. & ADAMS, C. S. 2001 *Phys. Rev. Lett.* **86**, 1410.
- LEANHARDT, A. E. 2002 *Phys. Rev. Lett.* **89**, 190403.
- LONDON, F. 1938 *Nature* **141**, 643.
- LUNDH, E. & AO, P. 2000 *Phys. Rev. A* **61**, 063612.
- MADARASSY, E. J. M. & BARENGHI, C. F. 2008a accepted. *JLTP* .
- MADARASSY, E. J. M. & BARENGHI, C. F. 2008b submitted. *Geophysical and Astrophysical Fluid Dynamics* .
- MADISON, K. W., CHEVY, F., V.BRETIN & DALIBARD, J. 2001 *Phys. Rev. Lett.* **86**, 4443.
- MADISON, K. W., CHEVY, F., WOHLLEBEN, W. & DALIBARD, J. 2000 *Phys. Rev. Lett.* **84**, 806.
- MAMAIEV, A. V., SAFFMAN, M. & ZOZULYA, A. A. 1996 *Phys. Rev. Lett.* **76**, 2262.
- MATTHEWS, M. R. 1999 *Phys. Rev. Lett.* **83**, 2498.
- MAURER, J. & TABELING, P. 1998 , vol. 43.
- MEWES, M. O., ANDREWS, M. R., VAN DRUTEN, N. J., KURN, D. M., DURFEE, D. S., TOWNSEND, C. G. & KETTERLE, W. 1996 *Phys. Rev. Lett.* **77**, 988.
- MODUGNO, G. 2001 *Science* **294**, 1320.

- NORE, C., ABID, M. & BRACHET, M. E. 1997 *Phys. Rev. Lett.* **78**, 3896.
- OGAWA, S., TSUBOTA, M. & HATTORI, Y. 2001 *Journ. of the Phys. Soc. of Japan* **71**, 813–821.
- OTT, H., FORTAGH, J., SCHLOTTERBECK, G., GROSSMANN, A. & ZIMMERMANN, C. 2001 *Phys. Rev. Lett.* **87**, 230401.
- PARKER, N. G. & ADAMS, C. S. 2005 *Phys. Rev. Lett.* **95**, 145301.
- PENCKWITT, A. A., BALLAGH, R. J. & GARDINER, C. W. 2002 *Phys. Rev. Lett.* **89**, 260402–1.
- PITAEVSKII, L. P. 1958 *Zh. Eksp. Teor. Fiz.* **35**, 408.
- PITAEVSKII, L. P. 1959 *Sov. Phys. JETP* **35**, 282.
- PROUKAKIS, N. P. 2007 Beyond gross-pitaevskii mean field theory. *cond-mat* p. 0706.3541v1.
- ROKHSAR, D. S. 1997 *Phys. Rev. Lett.* **79**, 2164.
- ROSENBUSCH, P., BRETIN, V. & DALIBARD, J. 2002 *Phys. Rev. Lett.* **89**, 200403.
- RUPRECHT, P. A., HOLLAND, M. J., BURNETT, K. & EDWARDS, M. 1995 *Phys. Rev. A* **51**, 4704.
- SANTOS, F. P. D. 2001 *Phys. Rev. Lett.* **86**, 3459.
- SCHWARZ, K. W. 1982 Dissipative dynamics of a vortex state in a trapped bose-condensed gas. *Phys. Rev. Lett.* **49**, 283.
- SCHWARZ, K. W. 1988 Dissipative dynamics of a vortex state in a trapped bose-condensed gas. *Phys. Rev. B* **38**, 2398.
- SHIN, Y. 2004 *cond-mat* p. 0407045.
- SMITH, M. R., DONNELLY, R. J., GOLDENFELD, N. & VINEN, W. 1993 *Phys. Rev. Lett.* **71**, 2583.
- SVIDZINSKY, A. A. & FETTER, A. L. 2000a *Phys. Rev. Lett.* **84**, 5919.
- SVIDZINSKY, A. A. & FETTER, A. L. 2000b *Phys. Rev. A* **62**, 063617.
- TAKASU, Y. 2003 *Phys. Rev. Lett.* **91**, 040404.
- TISZA, L. 1938 *Nature* **141**, 913.
- TSUBOTA, M., ARAKI, T. & NEMIROWSKII, S. K. 2000 *PRB* **62**, 11751.
- TSUBOTA, M., BARENGHI, C. F., ARAKI, T. & MITANI, A. 2004 *PRB* **69**, 134515.
- TSUBOTA, M., KASAMATSU, K. & UEDA, M. 2002 *Phys. Rev. A* **65**, 023603.
- VINEN, W. F. 2001 *Phys. Rev. B* **64**, 134520.
- WEBER, T., HERBIG, J., MARK, M., NAGERL, H. & GRIMM, R. 2003 *Science* **299**, 232.
- ZAREMBA, E., NIKUNI, T. & GRIFFIN, A. 1999 *J. Low Temp. Phys.* **116**, 277.